OL. 15 NO. 1 SEPTEMBER 1967
BLISHED MONTHLY

JOURNAL OF ELECTROANALYTICAL CHEMISTRY

AND INTERFACIAL ELECTROCHEMISTRY

International Journal devoted to all Aspects of Electroanalytical Chemistry, Double Layer Studies, Electrokinetics, Colloid Stability, and Electrode Kinetics.

ELSEVIER

GENERAL INFORMATION

See also Suggestions and Instructions to Authors which will be sent free, on request to the Publishers.

Types of contributions

(a) Original research work not previously published in other periodicals.
(b) Reviews on recent developments in various fields.
(c) Short communications.
(d) Bibliographical notes and book reviews.

Languages

Papers will be published in English, French or German.

Submission of papers

Papers should be sent to one of the following Editors:
Professor J. O'M. Bockris, John Harrison Laboratory of Chemistry, University of Pennsylvania, Philadelphia 4, Pa. 19104, U.S.A.
Dr. R. H. Ottewill, Department of Chemistry, The University, Bristol 8, England.
Dr. R. Parsons, Department of Chemistry, The University, Bristol 8, England.
Professor C. N. Reilley, Department of Chemistry, University of North Carolina, Chapel Hill, N.C. 27515, U.S.A.

Authors should preferably submit two copies in double-spaced typing on pages of uniform size. Legends for figures should be typed on a separate page. The figures should be in a form suitable for reproduction, drawn in Indian ink on drawing paper or tracing paper, with lettering etc. in thin pencil. The sheets of drawing or tracing paper should preferably be of the same dimensions as those on which the article is typed. Photographs should be submitted as clear black and white prints on glossy paper. Standard symbols should be used in line drawings, the following are available to the printers:

All references should be given at the end of the paper. They should be numbered and the numbers should appear in the text at the appropriate places.
A summary of 50 to 200 words should be included.

Reprints

Fifty reprints will be supplied free of charge. Additional reprints (minimum 100) can be ordered at quoted prices. They must be ordered on order forms which are sent together with the proofs.

Publication

The *Journal of Electroanalytical Chemistry and Interfacial Electrochemistry* appears monthly and has four issues per volume and three volumes per year.

Subscription price: £ 18.18.0 or $ 52.50 or Dfl. 189.00 per year; £ 6.6.0 or $ 17.50 or Dfl. 63.00 per volume; plus postage. Additional cost for copies by air mail available on request. For advertising rates apply to the publishers.

Subscriptions

Subscriptions should be sent to:

ELSEVIER PUBLISHING COMPANY, P.O. Box 211, Amsterdam, The Netherlands.

JOURNAL OF ELECTROANALYTICAL CHEMISTRY AND INTERFACIAL ELECTROCHEMISTRY

VOL. 15 (1967)

JOURNAL
of
ELECTROANALYTICAL CHEMISTRY
and
INTERFACIAL ELECTROCHEMISTRY

AN INTERNATIONAL JOURNAL DEVOTED TO ALL ASPECTS OF ELECTROANALYTICAL CHEMISTRY, DOUBLE LAYER STUDIES, ELECTROKINETICS, COLLOID STABILITY AND ELECTRODE KINETICS

Vol. 15 1967

ELSEVIER PUBLISHING COMPANY
AMSTERDAM

PRINTED IN THE NETHERLANDS

ELECTROANALYTICAL CHEMISTRY AND INTERFACIAL ELECTROCHEMISTRY
Elsevier Publishing Company, Amsterdam – Printed in The Netherlands

DETERMINATION OF THE ADSORPTION COEFFICIENTS $\frac{\partial q^1}{\partial q}$ AND $\frac{\partial \ln \beta}{\partial q}$ WHEN THE STANDARD FREE ENERGY OF ADSORPTION IS LINEARLY DEPENDENT ON SURFACE CHARGE OF AN ELECTRODE

EDWARD DUTKIEWICZ
Department of Physical Chemistry, A. Mickiewicz University, Poznań (Poland)
(Received October 10th, 1966)

1. INTRODUCTION

The standard free energy of adsorption ($\Delta\bar{G}^0$) of ions (or molecules) at an electrode depends strongly on the electrical state of the electrical double layer at an interface, *i.e.*, on the electrostatic field (X) across the double layer. Generally, this might be represented by the following function[1]:

$$-\ln \beta = \Delta\bar{G}^0/kT = \Delta G^0/kT + aX + bX^2 + cX^3 + \ldots \qquad 1(1)$$

where β is the adsorption coefficient.

Equation 1(1) may also be expressed using the surface charge density on the metal as electrical variable:

$$-\ln \beta = \Delta\bar{G}^0/kT = \Delta G^0/kT + a'q + b'q^2 + c'q^3 + \ldots \qquad 1(2)$$

In many cases, the standard free energy of adsorption is represented by a linear function of charge[2-6]. Thus eqn. 1(2) becomes:

$$-\ln \beta = \Delta G^0/kT + a'q \qquad 1(3)$$

The determination of the coefficient $(\partial \ln \beta/\partial q)_q = -a'$, is carried out, according to the method of PARSONS[2], graphically. The change in $\ln \beta$ with charge is found from the shift of the isotherm or surface pressure curve required to superpose it with the curve at $q = 0$. The slope of this shift when plotted against change of charge then gives the coefficient, a'.

In this paper, an attempt has been made to develop a method of determination of $(\partial \ln \beta/\partial q)_q$ more directly from experimental data.

2. THEORETICAL RELATIONS

It has already been shown[3], by thermodynamic arguments, that if an isotherm has the form:

$$\Gamma = \Gamma(\beta a) \qquad 2(1),$$

where Γ is the surface excess of adsorbate, a the bulk activity and β is defined as

above, providing that the other isotherm parameters are independent of q, then the changes in the electrode potential (ΔE) and in the measured reciprocal capacity (ΔC^{-1}) at constant charge (q) due to the adsorption process, are given by the following equations:

$$(\Delta E)_q = (E - E^b)_q = -kT \left(\frac{\partial \ln \beta}{\partial q}\right) \cdot \Gamma \qquad 2(2)$$

and

$$\Delta\left(\frac{1}{C}\right)_q = \left(\frac{1}{C} - \frac{1}{C^b}\right)_q = -kT \left\{\left(\frac{\partial^2 \ln \beta}{\partial q^2}\right) \cdot \Gamma + \left(\frac{\partial \ln \beta}{\partial q}\right)^2 \left(\frac{\partial \Gamma}{\partial \ln \beta}\right)\right\} \qquad 2(3)$$

where E = potential difference across the cell;
E^b = potential difference across the cell, when $\Gamma = 0$;
C = differential capacity of the electrical double layer;
C^b = differential capacity of the electrical double layer, when $\Gamma = 0$.

If the free energy of adsorption is a precisely linear function of charge, then $\partial^2 \ln \beta / \partial q^2 = 0$ and eqn. 2(3) may be written:

$$\Delta\left(\frac{1}{C}\right)_q = -kT \left(\frac{\partial \Gamma}{\partial \ln \beta}\right) \cdot \left(\frac{\partial \ln \beta}{\partial q}\right)^2 \qquad 2(4).$$

Now, if we divide eqn. 2(4) by eqn. 2(2), we get:

$$\left(\frac{\Delta C^{-1}}{\Delta E}\right)_q = \left(\frac{\partial \Gamma}{\partial \ln \beta}\right) \cdot \left(\frac{\partial \ln \beta}{\partial q}\right) \cdot \frac{1}{\Gamma} \qquad 2(5)$$

If the charge due to specifically adsorbed ions is put as q^1 instead of Γ, ($q^1 = ze\Gamma$) then eqn. 2(5) may be presented as:

$$\left(\frac{\Delta C^{-1}}{\Delta E}\right)_q = \left(\frac{\partial q^1}{\partial \ln \beta}\right) \cdot \left(\frac{\partial \ln \beta}{\partial q}\right) \cdot \frac{1}{q^1} \qquad 2(6)$$

or

$$\left(\frac{\Delta C^{-1}}{\Delta E}\right)_q = \left(\frac{\partial q^1}{\partial q}\right) \cdot \frac{1}{q^1} \qquad 2(7)$$

From eqn. 2(7) it follows that a plot of the ratio $(\Delta C^{-1}/\Delta E)_q$ *vs.* $1/q^1$ at constant charge, has a slope of $\partial q^1/\partial q$. This coefficient, as we know[7], is characteristic of the adsorption isotherm.

We may have another limiting case, when the adsorbed layer is so dilute that it obeys Henry's law, then eqn. 2(1) may be expressed as:

$$\partial \Gamma / \partial \ln \beta = \Gamma \qquad 2(8)$$

or

$$\partial q^1 / \partial \ln \beta = q^1 \qquad 2(9)$$

and eqn. 2(6) becomes:

$$\left(\frac{\Delta C^{-1}}{\Delta E}\right)_q = q^1 \cdot \left(\frac{\partial \ln \beta}{\partial q}\right) \cdot \frac{1}{q^1} \qquad 2(10)$$

Hence, it follows that for very dilute solution, the ratio $\left(\frac{\Delta C^{-1}}{\Delta E}\right)_q$ is directly equal to $\partial \ln \beta / \partial q$

$$\left(\frac{\Delta C^{-1}}{\Delta E}\right)_q = \frac{\partial \ln \beta}{\partial q} \qquad 2(11)$$

It is clear from eqn. 2(11), that a plot of ΔC^{-1} *vs.* ΔE at constant charge for very dilute concentrations should be a straight line of slope $\partial \ln \beta/\partial q$. This is a more general conclusion than equation 2(7), since the assumption of Henry's law (which must hold for sufficiently low surface concentration) necessarily involves the assumption of an isotherm of form 2(1) as there are no isotherm parameters other than β.

3. INTERPRETATION OF EXPERIMENTAL RESULTS WITH THEORETICAL RELATIONS

Equations 2(7) and 2(11) derived above were tested for the system, mercury in contact with formamide solutions of potassium iodide + potassium fluoride, at constant ionic strength. Experimental data were obtained by measuring the differential capacity of the electrical double layer in contact with solutions of xM KI + $(1-x)$ M KF in formamide[8] at 25°.

Figure 1 shows a plot of $\Delta C^{-1}/\Delta E$ *vs.* reciprocal charge due to iodide ion adsorption from potassium fluoride solution in formamide on a mercury electrode.

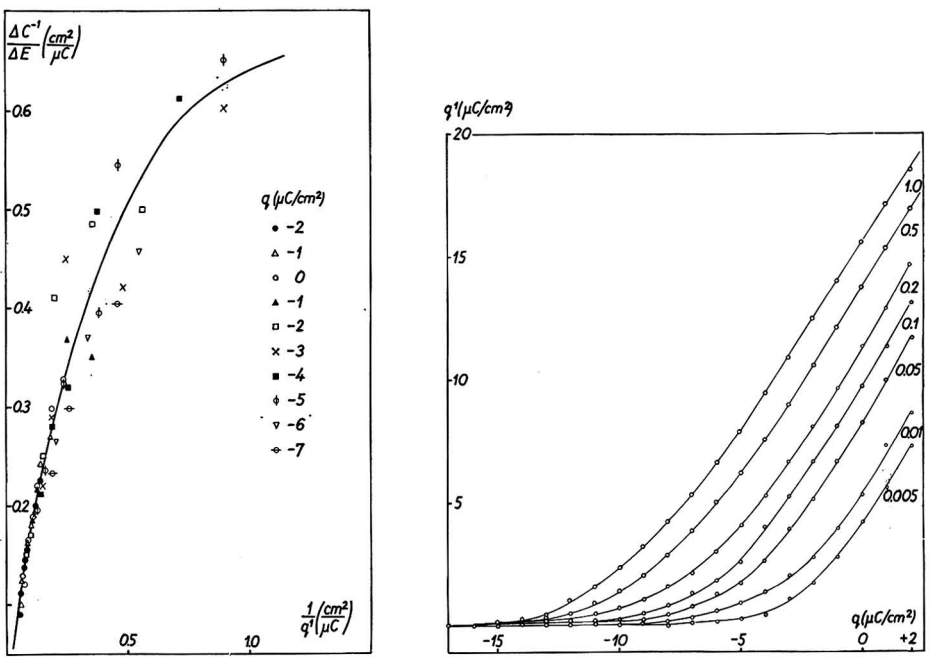

Fig. 1. Ratio of change in the capacity and in the potential of an electrode at constant charge, $(\Delta C^{-1}/\Delta E)_q$ ($cm^2\mu C^{-1}$), plotted against reciprocal specifically adsorbed charge $1/q^1$ ($cm^2\mu C^{-1}$), due to iodide ions adsorption on mercury from xM KI + $(1-x)M$ KF in formamide at 25°. The values of q^1 were calcd. by the usual thermodynamic method.

Fig. 2. Charge due to specifically adsorbed iodide ions, q^1 (μCcm^{-2}), as a function of surface charge density, q (μCcm^{-2}), at constant concn. of iodide ions, adsorbed on mercury from xM KI + $(1-x)M$ KF in formamide at 25°. The values of q and q^1 were calcd. by the usual thermodynamic method. The value of iodide concn., x (M), is indicated by each line.

It may be seen from this figure, that the experimental points lie on a common curve. The scatter for more dilute solutions and small values of specifically adsorbed charge, q^1, is certainly due to experimental error. The curve presented in Fig. 1 should have a slope, according to eqn. 2(7), of $\partial q^1/\partial q$. The value of this slope is equal to 1.5. This is in good agreement with a slope of plot q^1 *vs.* q at constant bulk concentration of iodide ions[8]. This plot is shown in Fig. 2, where q^1 has been calculated by the usual thermodynamic route from the interfacial tension/log activity relation. Of course, this is valid for higher concentrations of KI and more positive surface charge of the electrode.

The slope for dilute concentration and more negative charge becomes lower because the isotherm begins to approach Henry's law behaviour and $\partial q^1/\partial q$ becomes smaller while eqn. 2(7) transforms into eqn. 2(11); then the slope should be equal to $\partial \ln \beta/\partial q$. In order to estimate the coefficient $\partial \ln \beta/\partial q$, it is better to plot the experimental values of ΔC^{-1} against ΔE at constant charge. This plot is presented in Fig. 3.

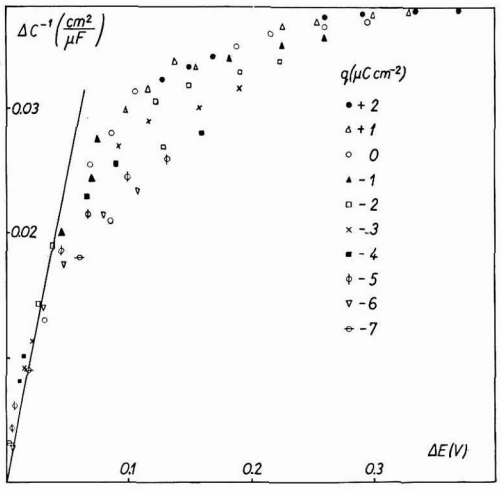

Fig. 3. Change of reciprocal capacity, ΔC^{-1} ($cm^2\mu F^{-1}$), plotted against the shift of potential, ΔE (V), as the KI concn. in the bulk is increased. Same system as in Figs. 1 and 2.

The slope in the region of very small values of ΔE, found from Fig. 3 was 0.50. This slope $\Delta C^{-1}/\Delta E$, which should be equal to $\partial \ln \beta/\partial q$, according to eqn. 2(11), may be calculated directly from the experimental data, provided ΔC^{-1} and ΔE are less than 0.02 $cm^2\mu F^{-1}$ and 0.05 V, respectively and correspond to low concentration of the bulk solution and negative charge of the electrode. The resulting value of $\Delta C^{-1}/\Delta E = \partial \ln \beta/\partial q$ calculated in this way from experimental data is equal to 0.493; this is in satisfactory agreement with the value, 0.508, found using PARSONS' method of analysis[2].

The part of the curve in Fig. 3 for more positive charges and larger values of ΔE, is described by eqn. 2(7) since Henry's law is not valid here. So, if we know q^1 for this region, we can also calculate the coefficient $\partial q^1/\partial q$ from this plot.

In conclusion, it can be said that a plot of $\Delta C^{-1}/\Delta E$ *vs.* $1/q^1$ at constant charge of the electrode provides a possibility of estimating the adsorption coefficient,

$\partial q^1/\partial q$, and the relation of ΔC^{-1} as a function of ΔE (also at constant charge) enables us to obtain $\partial \ln \beta/\partial q$ directly from the experimental data.

Once $\partial \ln \beta/\partial q$ is known, the surface excess (Γ) of adsorbed species may be obtained from eqn. 2(2)[6] because all factors are accessible from experiment:

$$\Gamma = -\frac{\Delta E}{kT} \cdot \left(\frac{\partial \ln \beta}{\partial q}\right)^{-1} \qquad 3(1)$$

It must be emphasized, that in order to obtain reasonable results from eqns. 2(7) and 2(11), the experimental data must be highly accurate and also, in the case of eqns. 2(7) and 3(1) (but not of 2(11)), the isotherm parameters must be independent of charge. Nevertheless, the good agreement between the results obtained in two different ways supports the suggestion that it is possible to determine the adsorption coefficients, $\partial q^1/\partial q$ and $\partial \ln \beta/\partial q$, in the manner shown above.

SUMMARY

The relations between the change in the electrode capacity and in the electrode potential resulting from the adsorption process at constant charge, have been presented. It may be possible using this information, to estimate the adsorption coefficient, $\partial q^1/\partial q$, and the coefficient $\partial \ln \beta/\partial q$, relating the standard free energy of adsorption to the charge when the former is linearly dependent on the charge on the electrode. This has been tested by the interpretation of some experimental results.

ACKNOWLEDGEMENT

I wish to thank Dr. ROGER PARSONS for reading and discussing this paper.

REFERENCES

1 R. PARSONS, *J. Electroanal. Chem.*, 5 (1963) 397.
2 R. PARSONS, *Proc. Roy. Soc. (London)*, A261 (1961) 79.
3 R. PARSONS, *Trans. Faraday Soc.*, 55 (1959) 999.
4 R. PAYNE, *J. Chem. Phys.*, 42, No. 10 (1965) 3371.
5 R. PAYNE, *J. Phys. Chem.*, 69 (1965) 4113.
6 E. DUTKIEWICZ AND R. PARSONS, *J. Electroanal. Chem.*, 11 (1966) 100.
7 R. PARSONS, *Proceedings of the Second International Congress on Surface Activity*, Vol. III, Butterworth's Scientific Publications, London, 1957, p. 38.
8 E. DUTKIEWICZ, to be published.

ELECTROANALYTICAL CHEMISTRY AND INTERFACIAL ELECTROCHEMISTRY
Elsevier Publishing Company, Amsterdam – Printed in The Netherlands

NEW TECHNIQUE FOR ELECTROCAPILLARY MEASUREMENTS USING THE LIPPMANN ELECTROMETER

B. E. CONWAY AND L. G. M. GORDON
Department of Chemistry, University of Ottawa, Ottawa (Canada)
(Received December 27th, 1966)

INTRODUCTION

For studies of equilibrium electrochemical adsorption at mercury by surface tension measurements, the use of the Lippmann electrometer is preferable to the use of drop-weight techniques, particularly when slow adsorption processes, *e.g.*, in the case of organic adsorbates, are involved. The technique of capillary electrometer measurements hitherto developed, normally involves, however, rather tedious observations of (a) the position of a fine thread of mercury in a capillary as it is brought to a fiducial mark (*e.g.*, cross-wires in a viewing microscope) near the end of the capillary, and (b) the height of mercury in a manometer when the mercury in the capillary has been brought to the fiducial mark. The latter measurement must usually be made with an accuracy of 0.003 cm using a cathetometer. In the present paper, we describe a technique which materially simplifies both these measurements and eliminates some of the tedium attached to these two aspects of the determination of an electrocapillary curve, which for proper definition, requires some thirty points to be determined for any given temperature and concentration of adsorbate and electrolyte, if precise data on the thermodynamics of adsorption are to be deduced.

EXPERIMENTAL PROCEDURES

1. Location of the meniscus in the capillary

In earlier attempts to improve the facility of electrocapillary measurements, we considered the use of a photoelectric optical device for sensing the position of the mercury thread, or an electrical contact system using an extremely fine wire in the capillary terminating at the desired level of the "fiducial mark" near the lower end of the capillary. Neither of these methods could be made to operate satisfactorily nor was reasonably practical.

(a) Resistance indicator. A new approach, based on the measurement of the resistance of the column of supporting electrolyte solution *below* the descending column of mercury in the capillary, has been developed successfully.

The lower meniscus of a column of mercury supported in the fine capillary is adjusted in the usual way[1–3] to a fiducial position (see below) by means of pressure from a gas line containing a reservoir bulb and communicating to the upper meniscus of the column of mercury (Fig. 1) and to one side of a 1-in. diameter U-tube manometer. Fine adjustment is made according to the procedure of PARSONS AND JOSHI[3]

by manipulating a screw-operated copper bellows connected by glass–metal seals to the gas line. In the optical measurements which were carried out as a control procedure to test the reliability of the new method, the position of the mercury thread in the capillary was viewed by means of a binocular stereo-zoom microscope (5–50 × magnification). Such a microscope has a good depth of focus and the mercury thread can be

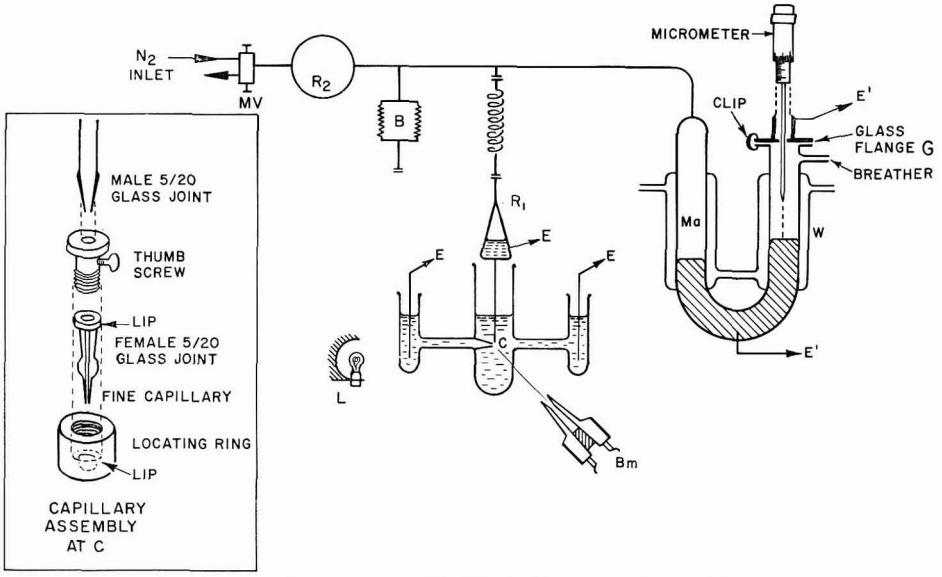

Fig. 1. Schematic diagram of apparatus: (E), Electrode connections; (E'), electrical contacts; (W), water jacket; (Ma), manometer; (Bm.), binocular microscope; (C), capillary (see inset); (L), lamp; (B), bellows; (R_2), bulb; (R_1), reservoir.

easily seen. Viewing of the thread is made more facile by arranging illumination of the capillary in the electrochemical cell by means of a lamp situated at the *side* (see Fig. 1) rather than the rear of the cell; the mercury thread then appears as a thin bright line and its position can be seen very easily.

The circuit shown in Fig. 2 was set up and comprises the usual d.c. polarisation arrangement using helipot potential dividers (or a potentiostat) and a Radiometer pH-millivoltmeter for measurement of the potential of the mercury electrode with respect to that of a standard reference electrode in a third compartment of the cell. The circuit differs from those conventionally used in previous work by inclusion of a shielded 1:4 transformer (T_2) (of the type used for conductance bridges) through which a low level a.c. signal of magnitude ΔV, can be injected from an oscillator (O) (Fig. 2) into the d.c. polarising circuit between the counter electrode and the capillary electrode (W) of mercury. The a.c. current passing in the capillary electrode part of the circuit will be determined mainly by the impedance, Z, offered to the current by the very thin column of electrolyte solution* (ohmic resistance, R) below the mercury meniscus in

* Direct measurement of the resistance of this column of electrolyte by means of an impedance or Wheatstone bridge is not possible owing to the low resistance solution paths which are provided in parallel through the reference and counter electrodes when the electrocapillary measurements are in progress.

the capillary, in combination with the double-layer capacitance of the very small area of the meniscus in the capillary. These impedance contributions may be written Z_R (for the electrolyte column) and Z_c for the double-layer and are obviously in a series relation. Under "ideal polarisation"[4] conditions, any reaction resistance impedance

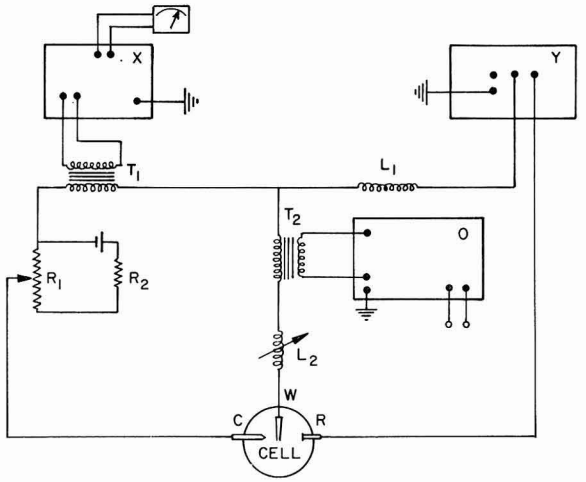

Fig. 2. Electrical circuit for indication of the position of the mercury meniscus in the capillary. (W), Working electrode — Hg capillary; (R), reference electrode, 0.1 *N* calomel; (C), counter electrode, 0.1 *N* calomel or Pt; (X), tuned amplifier and Null detector, General Radio Co., Type 1232-A, Ser. No. 1281; (Y), Radiometer, Type PHM4C No. 46833, Copenhagen; (O), wide band oscillator, Model 200CD, Tektronix; (T_1), transformer, Gen. Rad. Co., Type 578-B (step-down); (L_1), large inductance (35 H) or a.c. filter; (L_2), two variable inductances (1 H) in series, Gen. Rad. Co., Type 107N, Ser. No. 9463; (R_1), helipot (20 Ω).

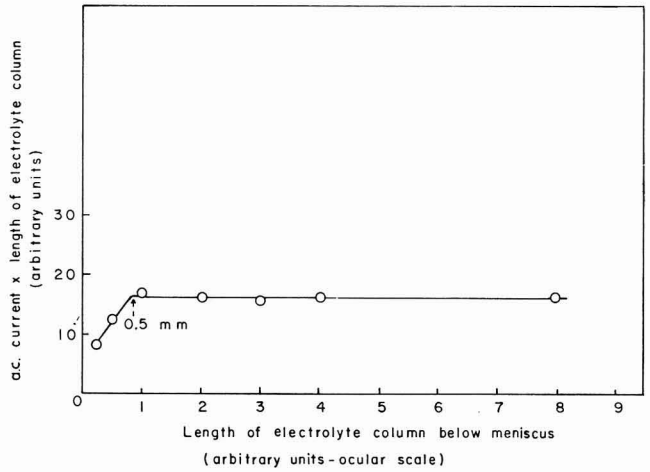

Fig. 3. Test of linearity of resistance response in relation to a.c. passing in detector circuit.

contribution at the interface is infinite and being in parallel with the double-layer capacitance will not influence Z. For a given double-layer capacitance, the position of the mercury in the capillary will directly determine Z_R ($=R$), and hence the a.c. current flowing in the circuit, since other resistances in the circuit are orders of mag-

nitude smaller. Since the a.c. current, i, and the resistance, R (proportional to the length of electrolyte column below the mercury meniscus) are hyperbolically related, *viz.*

$$iR = V_{\text{a.c.}} \tag{1}$$

where $V_{\text{a.c.}}$ is the constant a.c. potential operating, the detection of the current flowing for a given $V_{\text{a.c.}}$ provides a very sensitive method for following the position of the mercury thread, since as the latter approaches the end of the capillary, the current i rapidly rises reciprocally in R. The results shown in Fig. 3 demonstrate the reciprocal relation between i and R except very near the end of the capillary where R becomes so small that C presumably determines the impedance appreciably, and end-effects become significant.

The a.c. current flowing in the polarisation circuit is passed through another step-down transformer, T_1, and the current in the secondary of this transformer is fed to a tuned General Radio Null Detector X operating on the same frequency as the input a.c. The rectified current displayed by means of a microammeter is a function of the distance the mercury thread has advanced down the capillary. For a given a.c. input voltage, the deflection can, with suitable adjustments (see below), be reproducibly and precisely related to the position of the mercury meniscus.

Since the resistance of each solution used in a series of runs will vary from run to run, a single optical "calibration" must be made once for each electrocapillary curve by noting the meter deflection when the mercury meniscus, for the given solution is brought to the same fiducial mark (as determined by optical viewing). The fiducial mark itself can be taken as one "optical scale division" in a ruled ocular above a ruling adjusted to be coincident with the bottom of the capillary. Alternatively, a more permanent fiducial mark may be made by winding a very fine platinum or tungsten wire around the capillary and bending it back so that its end points to a position near the bottom of the capillary which can be seen by the viewing microscope.

Introduction of the small a.c. voltage in the working electrode circuit had no detectable effect on the level of the meniscus at a given d.c. polarisation potential.

(b) Capacitance effects. For a given d.c. voltage level at the mercury meniscus, microscopic changes of position of the mercury thread could be made to correspond to large (up to 30% full-scale) deflections at the detector meter. In test runs with 1 N aq. KCl, however, changes of d.c. polarisation potential produced a small but significant difference of the meter deflection for the same absolute position of the mercury in the capillary (determined by the conventional optical viewing method). Since the effect was dependent on the a.c. frequency, it was considered likely that the normal changes which the double-layer capacity undergoes with potential were responsible for causing significant changes of impedance of the column of electrolyte in series combination with the interfacial double-layer capacitance, C, at the meniscus. The impedance offered by the transformers is also frequency-dependent. Since Z is determined by

$$Z = (R^2 + Z_c^2)^{\frac{1}{2}}, \tag{2}$$

and Z_c evidently causes in part the variation of Z with frequency and d.c. polarisation potential, an attempt was made to eliminate the latter effects by introduction of a variable inductance L_2 (0–1 H) in series with the capillary electrode so that the resulting impedance of the circuit would be

$$Z = (R^2 + (Z_c - Z_L)^2)^{\frac{1}{2}}, \tag{3}$$

where L in Z_L is the total inductance of the a.c. circuit including any contributions from the transformers, and the current in the detector for any position of the mercury meniscus and any d.c. potential could be maximized (Z minimized) by adjustment of L_2. The variable inductance, L_2, then compensates for variations of Z_c, through changes of C with potential. In practice, L_2 is chosen sufficiently large that the variation of Z with d.c. potential (with the meniscus at a given position) is made negligible. This approach gave a very satisfactory solution to the problem that the meter needle deflection, as a function of position of the meniscus, was affected by the d.c. potential of the electrode. The second fixed inductance, L_1, screens the potentiometer, Y, from any residual a.c. signal from W through R (Fig. 2).

(c) Frequency effect. The circuit designed had an impedance which varied with a.c. frequency, presumably due to the presence of the inductance and transformers in series with the double-layer capacity of the mercury meniscus and the resistance of the electrolyte column. The frequency chosen for the measurements was that for which the circuit was observed to have maximum admittance (7–8 kHz) and the resulting sensitivity for the location of the meniscus was highest. All measurements were made at 7 kHz.

2. Excess pressure measurements

The second type of improvement introduced in the measurement technique was development of a direct reading micrometer manometer. A U-tube manometer, with 1-in. diameter columns of mercury on each side, was provided with thermostat water jackets, W, on each side and a $2\frac{1}{2}$ in. glass flange (Fig. 1) at one of the ends. The other side of the manometer was connected in the usual manner to the gas pressure and metal bellows assembly, and to the upper end of the capillary electrode by means of a flange seal joined to a glass–metal seal. The flange, G, was connected with metal clamps to a brass head in which was fixed a single-ended micrometer capable of measuring a displacement of 0.001 cm, with a 5-cm traverse. This allowed total pressure changes of up to 10 cm to be measured from a previously fixed level. The shaft of the micrometer was securely connected to a $\frac{1}{4}$-in. diameter stainless steel rod machined to a sharp 60°-bevel at the end. Adjustment of the micrometer allowed the point of the bevel to be brought into contact with the mercury meniscus in the manometer tube, a condition which could be exactly indicated by completion of an electrical circuit through the mercury, the micrometer and its shaft, and a 1.2-V battery operating through a 100-kΩ resistance. Contact was shown by the sudden deflection of a microammeter included in this circuit. Figure 5 shows that reproducibility of excess pressure measurement was at least as good as that attained by direct observations with a vernier cathetometer.

Since the micrometric pressure measurements are made with reference to only one side of the manometer, it is important to have the manometer tubes of exactly the same diameter and of uniform bore. This was tested by making cathetometer measurements on both sides, together with the micrometer measurements, and showing that the mean of the heights on each side was equal (within 0.003 cm) to the stationary level when no excess pressure was applied.

The combination of the direct reading manometer (the difference of levels of the upper and lower menisci of mercury in the capillary electrode must be separately measured but does not change significantly during the course of measurements on a

single electrocapillary curve if a suitable mercury reservoir is used) and the mercury meniscus position detector, enables electrocapillary measurements to be carried out with much greater facility than is possible with the usual techniques. Coupling of the micrometer with a 100-turn helipot would allow the possibility of direct recording of the excess pressure, through a divided reference voltage arrangement.

3. Capillary design

In order to facilitate interchange of capillaries when necessary, a modification to the conventional arrangement was made. The capillary was constructed from a short piece of glass which could be attached to the main column and reservoir by means of a glass joint. The latter was held in position as shown in the inset in Fig. 1 by means of a Teflon sleeve and collar provided with a screw thread to maintain a tight seal.

The upper end of the capillary assembly was provided with a 50-ml reservoir for mercury in the form of a small conical flask sealed to the column tube below and to a flange above through a glass–metal seal. The whole column tube and reservoir could be raised or lowered in the cell through a sliding glass sleeve constructed of ground Tru-bore tubing. An optimum level for optical viewing through a plane glass plate window in the cell could therefore be chosen by appropriate adjustments.

RESULTS

Some typical results for surface tension measurements in 0.001 N and 0.002 N aq. KCl are shown in Fig. 4, together with results for a solution of an organic electrolyte, N-methylpyridinium iodide. The central solid dots are the measurements obtained by the electrical system, and the circumscribing circles the points obtained by optical measurements on the same solution at the same potentials; they are indistinguishable. Since the differences are not sufficiently large to be represented on the

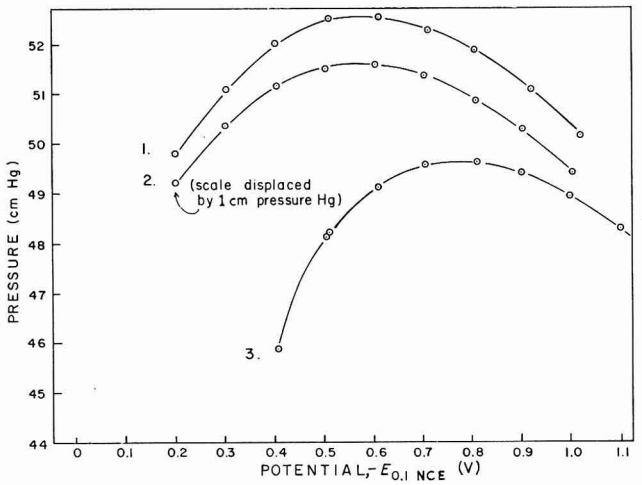

Fig. 4. Comparison of electrocapillary curves determined for aq. KCl soln. and N-methylpyridinium iodide by the electrical (○) and optical detection (·) procedures. (1), 0.001 N aq. KCl; (2), 0.002 N aq. KCl; (3), 0.01 N aq. KCl + 0.1 N N-methylpyridinium iodide.

usual scale of graphs for surface tension, or corresponding excess pressure as a function of electrode potential, a special plot of these differences, ΔP in pressure (determined by cathetometry) and $\Delta\gamma$ in surface tension, is shown in Fig. 5 for various solutions and electrode potentials. The differences, ΔP, in Fig. 5 correspond to mean $\Delta\gamma$ of

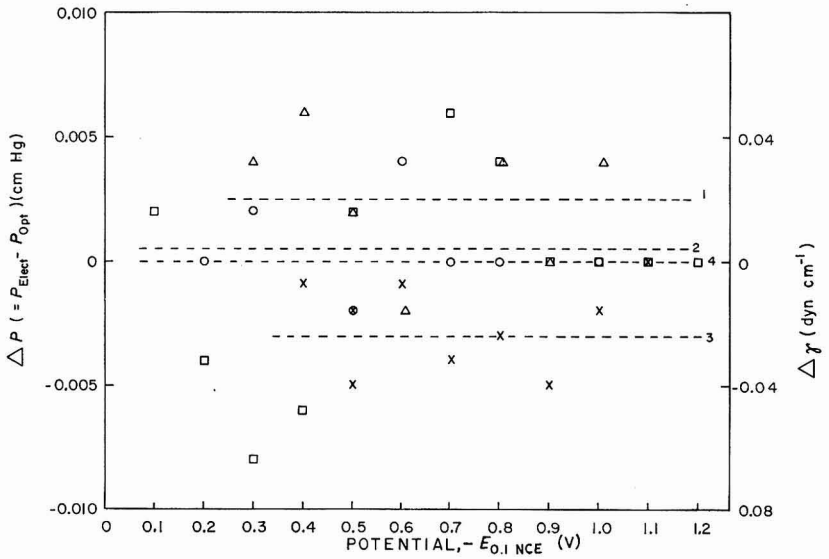

Fig. 5. Large-scale representation of differences, ΔP of the excess pressure, and $\Delta\gamma$ of surface tension, for various electrocapillary measurements determined by the optical and electrical methods as a function of electrode potential and for various sols. (P-values by cathetometry). (1), (△), 0.005 N KCl; (2), (○), 0.01 N KCl; (3), (×), 0.01 N KCl + 0.1 N N-methylpyridinium iodide; (4), (□), 0.1 N KCl.

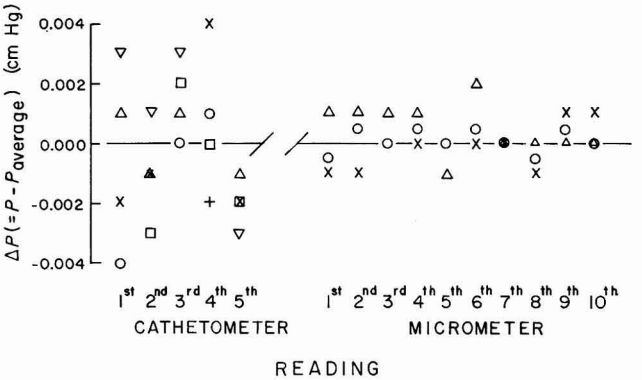

Fig. 6. Reproducibility of excess pressure measurements by optical cathetometry and by direct micrometer measurements. Various symbols represent values of ΔP obtained for several settings of Hg level by three observers.

only 0.03 dyn cm^{-1}, which is well within the accuracy of conventional previous techniques. The reproducibilities of the excess pressure measurements determined by cathetometry and by the micrometer method are compared in Fig. 6. It is seen that use of the micrometer method improves reproducibility of ΔP substantially, and this

is an important factor in the improvement of the overall reproducibility of the γ-measurements.

ACKNOWLEDGEMENTS

Grateful acknowledgement is made to the National Research Council, Canada, for support of this work.

SUMMARY

A new method for capillary electrometer measurements has been developed and is based on an electrical procedure for location of the mercury meniscus in the capillary of the apparatus. In combination with a direct-reading micrometer manometer, results at least as reproducible and precise as those obtained by conventional optical procedures are obtained, but much less laboriously. Tests on several solutions have been carried out. The procedures described allow the possibility of further development towards a partially automated system for electrocapillary measurements.

REFERENCES

1 R. PARSONS AND M. A. V. DEVANATHAN, *Trans. Faraday Soc.*, 49 (1953) 673.
2 R. G. BARRADAS AND B. E. CONWAY, *Electrochim. Acta*, 5 (1961) 319, 349; see also *Collection Czech. Chem. Commun.*, (1967) in press.
3 R. PARSONS AND K. M. JOSHI, *Electrochim. Acta*, 4 (1961) 129.
4 D. C. GRAHAME, *Chem. Rev.*, 41 (1947) 441.

ELECTROANALYTICAL CHEMISTRY AND INTERFACIAL ELECTROCHEMISTRY
Elsevier Publishing Company, Amsterdam – Printed in The Netherlands

ESTIMATION OF ADSORBED ANION CHARGE DENSITY FROM THE ELECTRODE CHARGE–POTENTIAL RELATIONSHIP

LOWELL R. McCOY AND HARRY B. MARK, JR.
Department of Chemistry, University of Michigan, Ann Arbor, Mich. 48104 (U.S.A.)
(Received June 24th, 1966; in revised form December 30th, 1966)

INTRODUCTION

GIERST[1] and FRUMKIN[2,3] have shown that valuable information concerning the nature of electrode mechanisms can be obtained if the potential of the outer Helmholtz plane, ψ°, is known as a function of electrode potential. In cases where these studies involve electrode potentials relatively negative to the electrocapillary maximum, and a low concentration of electrolyte, ψ° can be calculated from data obtained by GRAHAME[4] for sodium fluoride solutions. Such calculations have been made by RUSSELL[5] who has listed corresponding values of the electrode potential*, charge, and ψ° in tabular form for a number of concentrations of sodium fluoride. In more concentrated solutions and at potentials in the vicinity of, or positive to, the electrocapillary maximum, serious deviations from RUSSELL's values can arise from the adsorption of anions. If the degree of the adsorption is known, corrections can be made for this effect. However, there is little data available in the literature relating the adsorbed anion charge density to electrode potential. It was noted when collecting such data (see acknowledgement) for other studies, that an apparent relationship existed between that degree of anion adsorption for a given electrolyte and the position of its electrode charge–potential curve with respect to a semi-hypothetical curve representing no anion adsorption. Although the correlation developed on this basis is quite approximate it may offer a basis for estimation of the adsorbed anion charge density in a single experiment to establish the electrode charge–potential curve. The charge–potential curve can be obtained from electrocapillary curves[6], differential capacity measurements[6] or by the potential step method[7]. The correlation also indicates that a substantial degree of adsorption of fluoride may exist at sufficiently positive potentials.

CORRELATION OF ANION ADSORPTION DATA

Calculation of ψ°-potentials in the presence of adsorbed anions requires that both the electrode charge and the adsorbed ion charge densities be known. The charge in the diffuse zone, q^{d}, is obtained from the difference, and the ψ°-value can then be calculated from the Gouy–Chapman equation. The procedures and equations employed in these calculations as well as those used in the determination of the adsorbed ion charge have been well summarized by others[6,8,9] and, thus, will not be discussed

* Shown incorrectly as S.C.E.; should refer to N.C.E.

here. Figures 1 and 2 illustrate the electrode charge–potential curves for a number of electrolytes* at 0.1 and 1.0 N concentrations, respectively. On each curve has been placed small index lines indicating the adsorbed anion charge density, q^i, for that electrolyte corresponding to a specific electrode charge value. These are shown in 5-μC/cm^2 intervals, the positions having been obtained by interpolation of graphs in which q^i was plotted as a function of electrode charge using the original data. Inspection of Figs. 1 and 2 shows that rather smooth curves may be drawn through the index lines representing the same values for q^i for the various electrolytes and that these curves tend to parallel the curve for potassium or sodium fluoride at electrode potentials negative to -0.4 V (N.C.E.). At electrode potentials positive to the latter

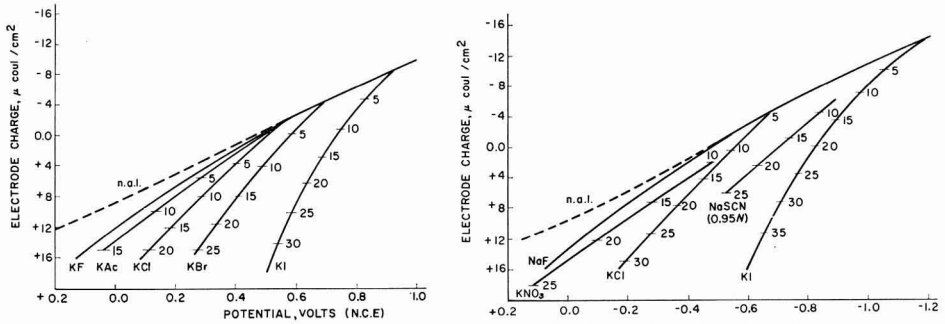

Figs. 1-2. Electrode charge–potential curves for: (1) 0.1 N solns; (2) 1.0 N solns. Adsorbed charge in μC cm^{-2}.

value, the extrapolated *equal adsorbed charge lines* cross the curve for the fluoride ion suggesting that adsorption of the fluoride ion may be occurring in this more positive potential region. A hypothetical *non-adsorption line* (n.a.l.) was therefore constructed for each concentration, making the positive charge–potential relationship symmetrical at the E.C.M. to the negative charge–potential curves for the fluoride ion. The n.a.l. for potentials positive to the E.C.M. appears as a dotted line in Figs. 1 and 2. In the case of 0.1 N potassium fluoride, the curve was constructed employing the data obtained by GRAHAME[4]. As data for 1.0 N potassium fluoride was not available, however, it was necessary to use RUSSELL'S[5] extrapolated values for 1.0 N sodium fluoride. The actual corresponding charge–potential values used in constructing the line representing no adsorption over the entire potential range appear in Table 1. Again, inspection of Figs. 1 and 2 suggests that the lines connecting the same values of q^i for the various electrolytes at either concentration tend to follow the dotted n.a.l. in the more positive potential region.

The relationship described above can be viewed more clearly in Figs. 3 and 4. The quantity, Δq, appearing as the ordinate in these graphs, represents the difference between the electrode charge corresponding to a pair of q^i and electrode potential values for a given electrolyte, and the electrode charge taken from the n.a.l. at the same potential. Plotted in this manner, the values of q^i for the various electrolytes

* Unpublished data for KNO_3 and mixtures of NH_4NO_3 and NH_4F were supplied by R. PAYNE. Unpublished data for NaSCN was furnished by R. PARSONS who also supplied unpublished data for KCl obtained by D. GRAHAME. Data relevant to other salts at 0.1 N concn. can be found in ref. 11.

tend to fall along lines which appear to converge at some positive potential. While the data for potassium nitrate shows a rather poor agreement, the other data presented in Figs. 3 and 4 exhibit a pattern which is remarkably independent of the size and charge of the anions. This correlation is put to a more severe test in Figs. 5 and 6, in which data for the sodium salts of CN^-, CNS^-, ClO_4^-, ClO_3^- and BrO_3^- obtained by WROBLOWA *et al.*[10] have been positioned upon the *grid* tentatively established in

TABLE 1

CHARGE–POTENTIAL VALUES EMPLOYED TO PREPARE THE "NON-ADSORPTION LINE"

0.1 N KF		*0.1 N KF*		*0.1 N KF*	
$-E$*	q	$-E$*	q	$-E$*	q
1.40	−16.45	0.60	−2.62	0.144	6.51
1.30	−14.79	0.50	−0.59	0.094	7.40
1.20	−13.17	0.472	0.00	0.044	8.24
1.10	−11.57	0.394	1.61	−0.006	9.12
1.00	−9.95	0.344	2.62	−0.056	9.95
0.90	−8.28	0.294	3.63	−0.106	10.77
0.80	−6.51	0.244	4.61		
0.70	−4.61	0.194	5.58		

1.0 N NaF		*1.0 N NaF*		*1.0 N NaF*	
$-E$	q	$-E$	q	$-E$	q
1.416	−16.00†	0.650	−4.21	0.094	8.08
1.295	−14.00†	0.550	−1.95	−0.006	9.78
1.170	−12.00†	0.472	0.00	−0.104	11.40
0.950	−9.78	0.394	1.95	−0.204	13.00
0.850	−8.08	0.294	4.21		
0.750	−6.24	0.194	6.24		

* *vs.* N.C.E. † Unpublished data from R. PARSONS for 1.0 *N* KCl, balance of column from RUSSELL's values for NaF[5].

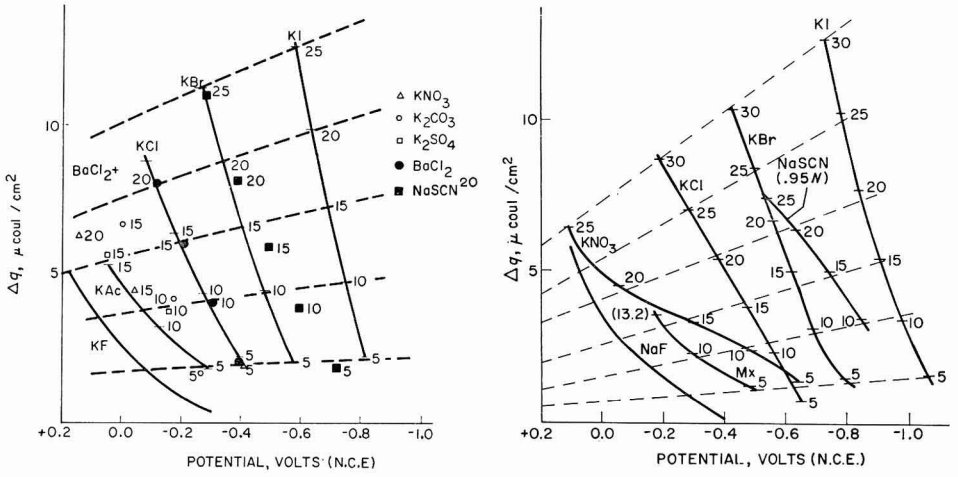

Figs. 3-4. Correlation diagram for: (3) 0.1 *N* solns.; (4) 1.0 *N* solns.; using data obtained by GRAHAME[4,8,9,11] and PAYNE[12,13]. Adsorbed charge in μC cm^{-2}. Mx = 0.1 *N* NH_4NO_3 + 0.9 *N* NH_4F.

Figs. 3 and 4. These anions are of particular interest because, by their size and complexity, their adsorption characteristics may be expected to differ significantly from those of the halogen ions. It is evident that the correlation obtained with these more complex ions is rather poor. It should be noted in this connection, however, that the data presented in Figs. 5 and 6 were obtained from interfacial tension

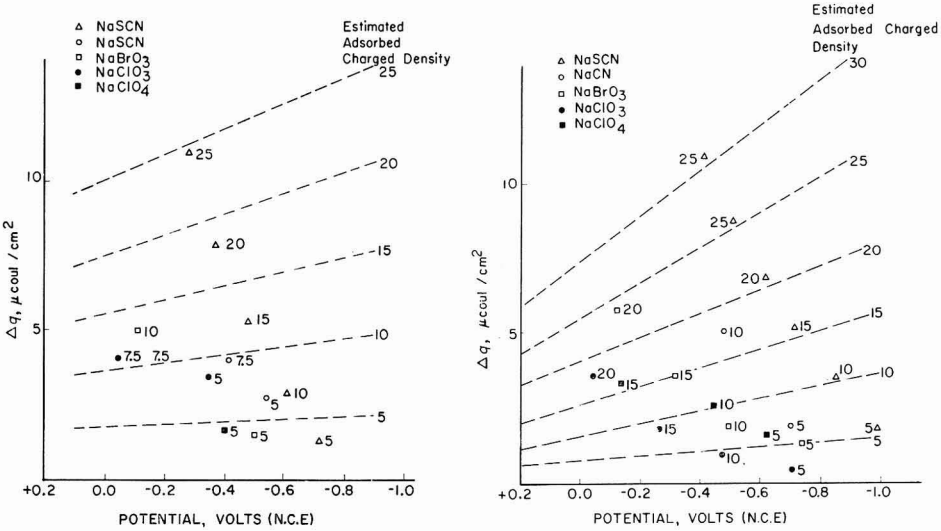

Figs. 5-6. Correlation diagram for: (5) 0.1 *N* solns.; (6) 1.0 *N* solns.; using data obtained by WROBLOWA *et al.*[10].

measurements and that the *scatter* of the electrode charge–potential data at the more negative electrode potentials (where the curves for all of the salts should coincide in the relative absence of anion adsorption) is considerably greater than that observed in the data shown in Figs. 1 and 2 (where the values were established from differential capacitance measurements). The charge–potential curve for 0.1 *N* NaSCN is particularly disturbing in this respect as the cathodic branch of the curve relative to the E.C.M. differs greatly from that of the other salts in this region. The potential of the E.C.M. of about −0.605 V (corrected to N.C.E.) found by WROBLOWA *et al.*[10] for NaSCN differs significantly from the value of −0.628 V found by GRAHAME AND SODERBERG[11] for KSCN. In this potential range, little difference would be expected between the values for the sodium and potassium salts. At least part, though certainly not all, of the instances of poor correlation observed in Figs. 5 and 6 may therefore result from a shift of the charge–potential curves along the potential axis. As noted above, however, the large scatter of the data at more negative potentials precludes any attempts at re-positioning the curves along the potential scale. There is reason to question, therefore, whether at least part of the lack of correlation observed in Figs. 5 and 6 in contrast to Figs. 3 and 4 may lie in the lack of precision in the data obtained by WROBLOWA *et al.*[10].

Inspection of Figs. 3 and 4 indicates that adsorption of fluoride ion may occur to a substantial degree at sufficiently positive potentials (or electrode charge). While this possibility has been discussed by a number of authors[4,12–16], generally

accepted values of adsorbed charge densities of this ion as a function of electrode potential or charge are wholly lacking. PAYNE[12,13] has examined this subject in detail with regard to his data for mixed systems of the nitrate or perchlorate ions and the fluoride ion and has considered the possibility of competitive adsorption. Figure 4 would indicate that such a competition would be expected.

DISCUSSION

In view of the very approximate nature of the correlation presented in Figs. 3–6, any attempt to present a theoretical basis for its existence would be at best premature and none will be attempted here. Some commentary upon the implications of the method itself may, however, be made. It appears preferable to conduct this, or any other attempt at a correlation, using solutions at the same activity rather than at the same concentration, but it was felt that there was insufficient published data to warrant this effort. The assumption of a symmetrial "non-adsorption line" has considerable theoretical significance. As noted above, this line was chosen as an extension of the cathodic portion of the charge–potential curve for the fluoride ion for the simple reason that lines connecting equal adsorbed charges appeared to parallel such an extension. On the other hand, the absence of a precise correlation of data at more cathodic potentials prevented any attempt to describe this course as truly symmetrical. MOHILNER[17] has pointed out that, if symmetry were assumed, this would require also that, in the absence of adsorbed ions, the differential inner capacitance be a symmetric even function of the charge upon the electrode; a situation contrary to that found by GRAHAME in his calculations of the sodium fluoride data. However, the inner capacitance values were calculated by GRAHAME[4] with the assumption that adsorption of the fluoride ion was absent, and agreement between the theoretical and experimental capacitance values calculated on this basis was not too satisfactory at more positive electrode charge values. This point has also been discussed critically by PARSONS[18] in connection with an earlier treatment of inner capacitance as a function of electrode charge by MACDONALD[19], which assumed such a symmetrical relationship. A simple test may be applied by observing that, if adsorption of fluoride ion were actually present and if a symmetrical charge–potential

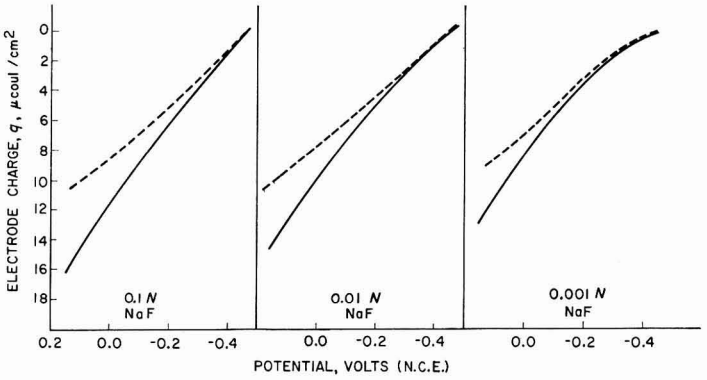

Fig. 7. Symmetry of electrode charge–potential curves at the E.C.M. as a function of the concn. of NaF. (—) Experimental $+q$–V curve; (--) symmetrical extension of $-q$–V curve.

relationship should in fact exist in the absence of adsorption, the hypothetical anodic extension of the charge–potential relationship symmetrical at the E.C.M. with respect to the experimental cathodic portion of the curve should exhibit a greater coincidence with the experimental cathodic portion of the curve as the concentration of sodium fluoride decreases. Figure 7 prepared from RUSSELL's[5] tables indicates that such a trend is observed.

SUMMARY

A correlation, based upon available data for a number of electrolytes at 0.1 and 1.0 *N* concentrations, may permit adsorbed anion charge densities to be estimated as a function of electrode potential by comparing the experimentally-determined charge–potential relationship for a previously uninvestigated electrolyte with a semi-hypothetical curve representing no anion adsorption. The results are believed sufficiently precise to permit the calculation of approximate ψ°-potentials for use in kinetic studies. The correlation indicates that the adsorption of fluoride ion may be substantial at sufficiently positive potentials.

ACKNOWLEDGEMENTS

The authors are indebted to Dr. ROGER PARSONS for much of the data included in this study, to Dr. RICHARD PAYNE for data relating to potassium nitrate and ammonium nitrate–fluoride mixtures and to the Department of Chemistry, Amherst College, which supplied copies of a number of the Technical Reports to the Office of Naval Research prepared by Dr. DAVID GRAHAME and his co-workers. This research was supported in part by a grant from the U.S. Army Research Office, Durham, Contract No. Da-31-124-ARO-D-284.

REFERENCES

1 L. GIERST, *Trans. Symp. Electrode Processes, Philadelphia, Pa., 1959*, p. 109.
2 A. FRUMKIN, *ibid.*, p. 1.
3 A. FRUMKIN, *Advan. Electrochem. Electrochem. Eng.*, 1 (1961) 65.
4 D. C. GRAHAME, *J. Am. Chem. Soc.*, 76 (1954) 4819.
5 C. D. RUSSELL, *J. Electroanal. Chem.*, 6 (1963) 486.
6 P. DELAHAY, *Double Layer and Electrode Kinetics*, Interscience Publishers, Inc., New York, 1965, chaps. 2–5.
7 R. A. OSTERYOUNG, private communication, 1966.
8 D. C. GRAHAME AND B. A. SODERBERG, *J. Chem. Phys.*, 22 (1954) 449.
9 D. C. GRAHAME, *Chem. Rev.*, 41 (1947) 441.
10 H. WROBLOWA, Z. KOVAC AND J. O'M. BOCKRIS, *Trans. Faraday Soc.*, 61 (1965) 1523.
11 D. C. GRAHAME AND B. A. SODERBERG, Technical Report No. 14 to the Office of Naval Research, Feb. 18, 1954.
12 R. PAYNE, *J. Phys. Chem.*, 69 (1965) 4113.
13 R. PAYNE, *ibid.*, 70 (1966) 204.
14 J.O'M. BOCKRIS, M.A.V. DEVANATHAN AND K. MÜLLER, *Proc. Roy. Soc. (London)*, A274 (1963) 55.
15 M. A. V. DEVANATHAN, *Trans. Faraday Soc.*, 50 (1954) 373.
16 J. R. MACDONALD AND C. A. BARLOW, JR., *J. Chem. Phys.*, 36 (1962) 3026.
17 D. M. MOHILNER, private communication, 1966.
18 R. PARSONS, *Advan. Electrochem. Electrochem. Eng.*, 1 (1961) 6.
19 J. R. MACDONALD, *J. Chem. Phys.*, 22 (1954) 4857.
20 R. PARSONS AND P. C. SYMONS, private communication, 1966.
21 R. PARSONS, R. PAYNE AND J. LAWRENCE, private communication, 1966.

ELECTROANALYTICAL CHEMISTRY AND INTERFACIAL ELECTROCHEMISTRY
Elsevier Publishing Company, Amsterdam – Printed in The Netherlands

EFFECT OF AMALGAM FORMATION ON THE POTENTIAL OF MERCURY-BASED REFERENCE ELECTRODES
II. THE Hg/Hg_2SO_4 AND Hg/HgO ELECTRODES

A. M. SHAMS EL DIN, L. A. KAMEL AND F. M. ABD EL WAHAB
Laboratory of Electrochemistry and Corrosion, National Research Centre, Dokki, Cairo (U.A.R.)
(Received November 17th, 1966; in revised form January 30th, 1967)

INTRODUCTION

In a recent publication we reported on the effect of small amounts of metallic impurities in mercury, on the potential of the saturated calomel electrode[1]. These electrodes were found to give rise to initial potentials very near to the normal metal/metal ion potential of the impurity concerned. After a certain time, depending on the type and concentration of impurity, surface area, and temperature, the potential changed suddenly to establish the value of the $Hg/Hg_2Cl_2/Cl^-$ system. The experimental results were quantitatively explained on the basis of diffusion of the metal atom to the electrode/electrolyte interface.

In the present communication, the work is extended to two other commonly used mercury-based reference electrodes, *viz.*, the $Hg/Hg_2SO_4/SO_4^{2-}$ and $Hg/HgO/OH^-$ electrodes. Investigations on these electrodes from the present stand-point have not hitherto been reported. The discharge of metal impurities in the two electrodes is expected to differ. Thus, whereas the dissolution reaction in the sulphate electrode will lead — as is the case with the chloride electrode — to the formation of simple *(aquo)* metal ions, the same reaction in the oxide electrode is governed to a large extent by the physical and/or chemical properties of the impurity oxide (hydroxide). It was also of interest to establish whether such electrodes would establish the thermodynamically-reversible $Hg/HgO/OH^-$ potential.

EXPERIMENTAL

Liquid Zn-, Cd-, Sn-, Pb-, and Cu-amalgams of different concentrations were prepared electrolytically *in situ* as previously described[1]. A volume of 1.5 ml of mercury was used as cathode. The prepared electrodes were thoroughly washed with distilled water and dried with narrow strips of filter paper. Reference electrodes were prepared by covering the amalgams with layers of Hg_2SO_4 or HgO, *ca.* 1 mm thick, followed by the corresponding electrolyte. The moment of addition of the paste was considered as the zero time of preparation of the electrode. In order to prevent chemical dissolution of the amalgams, neutral sulphate electrodes were usually employed for the experiments. Unless otherwise stated, the electrolyte was 0.1 *M* K_2SO_4. Similarly, the main work with the HgO electrode was carried out with 0.5 *N* NaOH. Potentials were measured on a Pye precision potentiometer and, in experiments lasting for long

times, on a pen recording potentiometer (Speedomax Type G, Leeds and Northrup). Potentials were measured relative to pure, calibrated sulphate or oxide electrodes of doubly-distilled mercury equilibrated for 4 weeks. Measurements were carried out at a room temperature of 24–26°.

RESULTS AND DISCUSSION

(i) The $Hg/Hg_2SO_4/SO_4^{2-}$ electrode

The behaviour of mercurous sulphate electrodes in which the mercury is contaminated with metallic impurities is virtually identical with that of calomel electrodes under similar conditions[1]. Thus, the time–potential curves of these electrodes showed initial potentials very near to the corresponding standard metal/metal ion values. In analogy to the chloride electrode, displacement of the metallic impurity is assumed to take place according to the general reaction:

$$M(Hg) + Hg_2SO_4 \rightarrow M^{2+} + SO_4^{2-} + 2\ Hg \qquad (1)$$

These initial potentials did not persist, however, but changed rapidly to the Hg/Hg_2SO_4 value under the experimental conditions used. The application of the theory of voltammetry at constant currents[2] to the experimental results supported the conclusion that the discharge of metallic impurities was governed by the rate of diffusion of the metal atoms to the amalgam/electrolyte interface.

During equilibration of mercurous sulphate electrodes in which the mercury was contaminated with tin, an interesting observation was made. Shortly after its preparation, the electrode developed a potential of *ca.* −850 mV, due to the dissolution of Sn^{2+}. At the transition time, the potential did not tend directly to zero value but became irregular over a considerable length of time, depending on the tin content of the amalgam. This was related to the ease of hydrolysis of the Sn^{2+} ion in neutral sulphate solutions. Support for this conclusion came from experiments with 0.10, 0.50 and 1.00 *M* H_2SO_4 electrodes. With the 0.10 *M* electrode, the oscillations in potential were replaced by a clear step extending over a relatively long period. This step became shorter in 0.50 *M* H_2SO_4, and disappeared completely in 1.00 *M* H_2SO_4 where hydrolysis was totally suppressed.

Electrodes with binary amalgams were also investigated. Their time–potential curves showed a discharge step for each of the amalgamated metals at its respective potential. The discharge times of the less noble metal were equal to, or slightly shorter than, those for single amalgams of equal concentration. Those for the second component were, however, much longer. Similar results were also obtained in the case of the calomel electrode and were explained on the basis of a displacement reaction between the noble-metal ion in solution and the active metal atom at the amalgam interface.

(ii) The $Hg/HgO/OH^-$ electrode

Traces of metal impurities in mercury affect also the potential of the $Hg/HgO/OH^-$ reference electrode. The effect is again due to the reducting property of the amalgam which, according to the overall reaction:

$$M(Hg) + HgO \rightarrow MO + Hg \qquad (2,a)$$

or

$$M(Hg) + HgO + H_2O \rightarrow M(OH)_2 + Hg \qquad (2,b)$$

leads to the discharge of the metal impurity. The displacement reaction takes place even in cases where the impurity oxide is less soluble than HgO (*e.g.*, SnO). The standard free energy changes of reaction (2,a) for Zn, Sn, Cd, Pb and Cu are, respectively[3], −62.06, −47.51, −39.80, −31.26 and −21.00 kcal/mole. The corresponding figures for reaction (2,b) for the first four metals are −61.92, −46.92, −41.78 and −29.92 kcal/mole. The difference between the two sets of figures is apparently the free energy of dehydration of the hydroxide which, except in the case of cadmium, is in favour of oxide formation.

Depending on the chemical and/or physical properties of the metal oxide formed, the contaminated mercury oxide electrode, in contrast to the chloride and sulphate electrodes, may not establish its expected, thermodynamically-reversible potential. For the same reason, the way in which an impure electrode reaches steady-state potentials (whether these are the normal values or not) depends upon both the type of impurity in the mercury and the concentration of the alkali of the electrolyte. These potentials are normally established — except for the case of the copper amalgam — after considerable periods as compared with the chloride or sulphate electrodes of equal impurity content.

The variation with time of the potential of mercury oxide electrodes in which the mercury was contaminated with increasing amounts of lead is depicted in the curves of Fig. 1. Zero-potentials are approached from negative values and at the bottom of the curves a potential of *ca.* −550 mV is measured. This is close to that of the reaction:

$$Pb + 2\ OH^- \rightleftharpoons PbO + H_2O + 2\ e \qquad (3)$$

under the prevailing conditions of Pb^0 and OH^- activities. The times for the establishment of zero-potentials were roughly proportional to the lead content of the

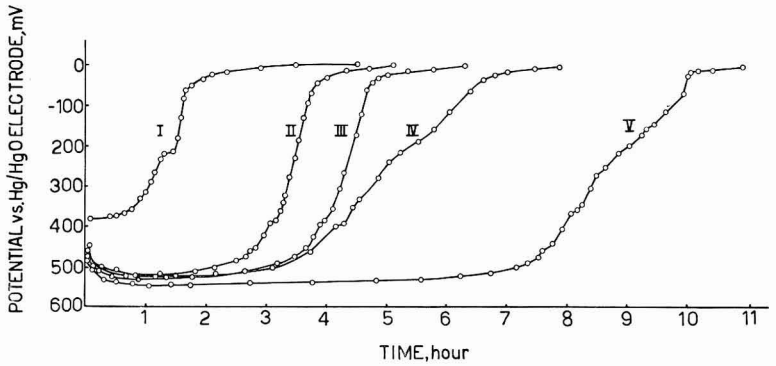

Fig. 1. Time–potential curves for HgO electrode of Pb-amalgam: (I) 2.40; (II), 3.60; (III), 4.80; (IV), 5.40; (V), $6.00 \cdot 10^{-3}$ wt.% Pb-amalgam.

amalgam. Copper in mercury gave rise to similar curves, but zero-potentials were reached more readily. Starting potentials of *ca.* −100 mV correspond to the reaction:

$$2\ Cu + 2\ OH^- \rightleftharpoons Cu_2O + H_2O + 2\ e \qquad (4)$$

When the mercury of the electrode contained cadmium, starting potentials very near to that of the pure reference were measured. These drifted, however, with

time, first slowly and almost linearly, and later more rapidly, towards more negative values (Fig. 2). The time of the linear potential drift was longer the higher the cadmium content of the amalgam. For relatively concentrated amalgams, a potential arrest at about -600 mV was recorded; this extended over a period of several hours. The potential then dropped once again to *ca.* -760 mV, and remained constant for as long as 8 days (end of experiment). This last potential is close to that of the Cd/CdO system under the prevailing conditions of metal atom and electrolyte activities. The

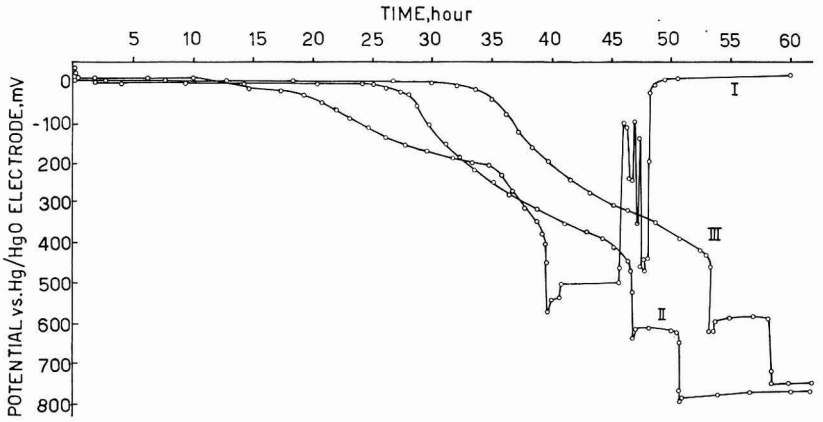

Fig. 2. Time–potential curves for HgO electrodes of Cd-amalgam: (I), 1.12; (II), 1.68; (III), $2.24 \cdot 10^{-1}$ wt-% Cd-amalgam.

behaviour of cadmium-contaminated electrodes seems, therefore, to be governed by the rate at which CdO forms on their surface. Once this film is complete, it isolates the mercury completely from the electrolyte and the electrode functions as a Cd/CdO electrode. Accordingly, cadmium is one of the most harmful contaminations in mercury, not only because it develops a compact oxide film which obstructs the regular discharge of the metal, but also because such an effect appears only after relatively long times (subsequent to the preparation of the electrode) during which it would be assumed that the electrode is functioning properly as a Hg/HgO electrode. This last effect is more pronounced the higher the cadmium content of the amalgam.

When mercury contains little cadmium, the behaviour is as described above, except that the potential of the electrode, after reaching the arrest at -600 mV, does not drop further to the more negative value of -760 mV, but changes again to approach the potential of the Hg/HgO electrode (curve 1, Fig. 2). It is reasonable to assume, therefore, that the reaction taking place at -600 mV determines whether the electrode will or will not regain the zero-potential. This reaction is, however, not completely understood. Its potential does not correspond to any of the known equilibrium values of cadmium in alkaline solutions[4]. It is of interest to note, however, that the oxidation curves of massive cadmium electrodes in alkaline solutions obtained under certain specified galvanostatic conditions exhibit an arrest at potentials positive to the Cd/CdO value[5]. The cause and characteristics of this particular step are now being investigated.

The behaviour of mercury oxide electrodes containing zinc is of particular interest. In 1 and 2 *M* NaOH, clear discharge steps were recorded at *ca.* -1300 mV

(curves 2 and 3, Fig. 3). The length of these steps increased with increase in the zinc content of the amalgam. From the measured potentials it is difficult to decide with certainty to which of the two reactions:

$$Zn(Hg) + HgO + H_2O \rightarrow Zn(OH)_2 + Hg \quad (5)$$

or

$$Zn(Hg) + HgO + 2OH^- \rightarrow ZnO_2^{2-} + H_2O + Hg \quad (6)$$

the discharge step corresponds. The difference between the standard potentials of these two systems amounts to only 29 mV.

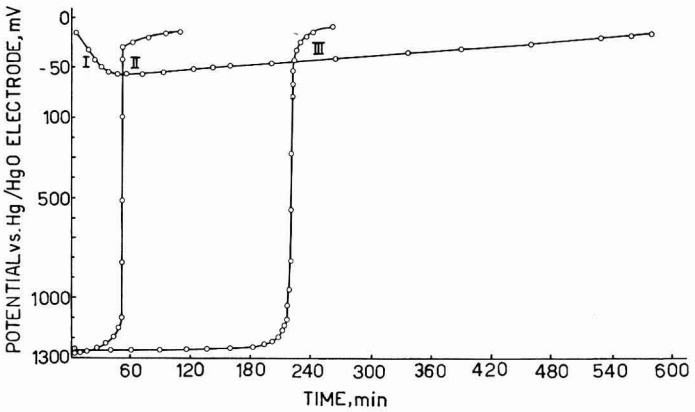

Fig. 3. Time–potential curves for HgO electrodes of $6.44 \cdot 10^{-2}$ wt-% Zn-amalgam in: (I), 0.5; (II), 1.0; (III), 2 *M* NaOH.

Zinc-contaminated electrodes with less concentrated electrolytes behave in a different manner. Thus in 0.5 *M* NaOH, starting potentials of *ca.* −45 mV relative to the pure electrode, were measured. These changed, however, with time to more negative values and then levelled up again, producing a minimum in the potential–time curves (curve 1, Fig. 3). The potential dip was larger the more concentrated the amalgam. The potentials bear no relation to equilibrium values involving zinc in alkaline media. It is probable that in this particular electrolyte the discharge of the zinc amalgam leads to the formation of an oxide which is less compact than the one formed in concentrated solutions and which readily diffuses away from the electrode surface so that neither $Zn/Zn(OH)_2$ nor Zn/ZnO_2^{2-} potentials are measured. In 0.1 *M* NaOH, on the other hand, the starting potentials varied between −300 and −700 mV, depending on the zinc content of the amalgam. The potential then changed very quickly towards zero-values without developing a discharge step.

Mercuric oxide electrodes prepared with tin amalgams behave in a manner which is also not completely understood. In 0.5 *M* NaOH, the potential measured directly after the preparation of the electrode was + 10 mV with respect to the pure electrode. It decreased, however, with time, first slowly and then more quickly, to give a potential valley before finally levelling up again (Fig. 4). Thereafter, the potential remained constant for periods extending to 30 h (end of experiment). These final potentials depended primarily on the tin content of the amalgam, being more negative the higher the concentration. For any one tin content, the rate of potential

decrease was faster, and the potential minimum occurred at more negative values, the more concentrated the electrolyte (Fig. 5). In these concentrated solutions a new phenomenon was also recorded. Thus, after the minimum the potential levelled up to a constant value depending on the electrolyte concentration. Suddenly the potential

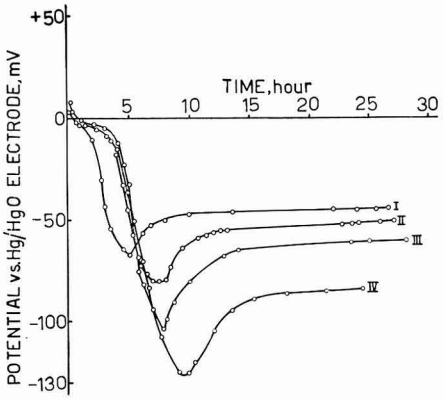

Fig. 4. Time–potential curves for HgO electrodes of Sn-amalgam: (I), 0.58; (II), 1.60; (III), 1.74; (IV), $2.32 \cdot 10^{-1}$ wt-% Sn-amalgam.

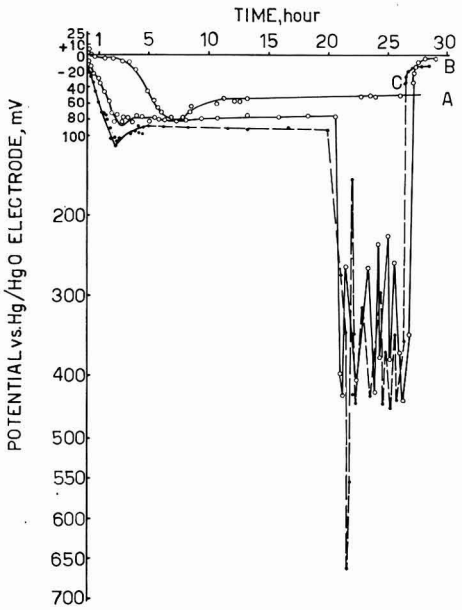

Fig. 5. Time–potential curves for HgO electrodes of $1.61 \cdot 10^{-1}$ wt-% Sn-amalgam in; (A), 0.5; (B), 1.0; (C), 2.0 *M* NaOH.

changed to a more negative value and oscillations were recorded over a range of ~200 mV for a period of several hours. The potential then changed once again to a more positive value and thereafter remained constant (curves B and C, Fig. 5). The oscillations in potential are most probably the result of alternate formation and dissolution of an $Sn(OH)_2$ film formed on the surface of the electrode. The potential

range over which this process occurs, as well as the starting or final potentials, do not conform with any of the known redox systems involving tin in alkaline solutions[6]. Similarly, none of these values corresponds to the oxidation steps of the same amalgams in alkaline solutions obtained under galvanostatic conditions[7]. Like cadmium, tin impurities in a mercuric oxide electrode are harmful since the electrode does not regain its reversible potential even after long standing.

SUMMARY

Mercury-based reference electrodes in which mercury is contaminated with metallic impurities give rise to initial and/or final potentials far removed from the thermodynamically-reversible Hg/Hg_2^{2+} (Hg^{2+}) potentials. Where simple *(aquo)* metal ions can form (*e.g.*, in the Cl^- or SO_4^{2-} electrodes) the electrode potential tends ultimately to the reversible values.

The chemical and/or physical nature of the impurity oxide (hydroxide) determine whether or not a mercury oxide reference electrode regains its reversible potential. Cadmium and tin are harmful contaminations in mercury.

As a rule, mercury-based reference electrodes, before use should be allowed ample time to discharge their impurities and establish the expected potentials. It is also recommended that they should be calibrated frequently to confirm the absence of impurities the effect of which only appears a long time after their preparation.

REFERENCES

1 A. M. Shams El Din and L. A. Kamel, *J. Electroanal. Chem.*, 11 (1966) 111.
2 P. Delahay, *New Instrumental Methods in Electrochemistry*, Interscience Publishers Inc., New York, 1954, p. 179.
3 W. M. Latimer, *Oxidation Potentials*, Prentice Hall, Englewood Cliffs, 1953, pp. 148, 150, 168, 172, 175 and 183.
4 Ref. 3, p. 172.
5 I. Sanghi, S. Visvanathan and S. Ananthanarayanan, *Electrochim. Acta*, 3 (1960) 65.
6 A. M. Shams El Din and F. M. Abd El Wahab, *Electrochim. Acta*, 9 (1964) 883.
7 L. A. Kamel, Ph.D. thesis, University of Cairo, 1966.

ELECTROANALYTICAL CHEMISTRY AND INTERFACIAL ELECTROCHEMISTRY
Elsevier Publishing Company, Amsterdam – Printed in The Netherlands

PRETREATMENT OF Pt–Au AND Pd–Au ALLOY ELECTRODES IN THE STUDY OF OXYGEN REDUCTION

A. DAMJANOVIC AND V. BRUSIĆ
The Electrochemistry Laboratory, The University of Pennsylvania, Philadelphia, Pa. (U.S.A.)
(Received December 6th, 1966)

For the analysis of factors that affect the rate and mechanism of a given electrode reaction, alloys (binary alloys as a complete series of solid solutions) have been used as working electrodes[1]. The pretreatment such an alloy electrode may undergo before being used for electrochemical measurements raises a problem, however. The pretreatment must not alter the electrode surface so that it is no longer representative of the bulk of the alloy phase; otherwise, the experimental results may not correspond to the original alloy system and this may obscure the factors affecting the catalysis. The manner in which the electrode pretreatment may alter the behavior of an alloy electrode was recently demonstrated for the H^+/H_2 reaction at Au–Pt alloy electrodes[2]. An alloy electrode rich in Au that was subjected to repeated anodic and then cathodic pulses became more *active* ($\sim$10 times) than the electrodes treated either chemically or thermally (see below). Meaningful results in the study of the kinetics and catalysis of reaction are, apparently, only obtained at electrodes pretreated either chemically or thermally.

The problem of the pretreatment of alloy electrodes arose in a study of the kinetics of O_2-reduction at various alloys. It is discussed here for the case of Pt–Au and Pd–Au alloys.

Pt–Au and Pd–Au electrodes in the form of wires were either sealed at one end into a glass tube which served as an electrode holder, or were threaded through a hole in a small Teflon cylinder which fitted inside a true bore tube. These electrodes were treated in one of the following three ways:

(*i*) *Chemically*. An electrode was first degreased with organic solvents and then treated with conc. HCl, and washed with conductivity water. Subsequently, it was placed into the test compartment of a cell* which was filled with oxygen-saturated 0.1 *N* $HClO_4$ solution. Finally, the electrode was subjected to a short ($\sim$5 sec) cathodic pulse at 0.3 V *versus* the reversible hydrogen electrode in the same solution.

(*ii*) *Electrochemically*. After an electrode had been degreased and washed with conductivity water, it was subjected to an anodic pulse (at 1.7 V, for $\sim$5 sec) and then to a cathodic pulse (at 0.3 V, for $\sim$10 sec). Pulses are sometimes repeated.

(*iii*) *Thermally*. After the electrode had been degreased and washed with conductivity water, it was placed into a furnace situated above the cell[4]. The electrode was then heated at 300 or 650°, in either case in a stream of H_2 (for $\sim$5 min) and then in N_2 (for 10–60 min). In some experiments the treatment in H_2 was omitted.

* Details of the cell are given elsewhere[3].

The electrode was cooled inside the furnace and then lowered into the test compartment of the cell without being exposed to the atmosphere.

Potential–log (cathodic) current density relationships were determined by both decreasing and increasing current.

An electrode of Pt-rich Pt–Au alloy (5% Au), which is treated either chemically or thermally at 300°, shows the same V–log i relationships for O_2-reduction (a, Fig. 1). The same electrode treated electrochemically shows, however, a somewhat higher activity for the reduction (b, Fig. 1). The slopes of the V–log i lines remain similar to that for a Pt electrode[4] (Pt, Fig. 1). There is, however, a tendency for a steeper slope to appear at high current densities in the case of thermally and chemically treated electrodes.

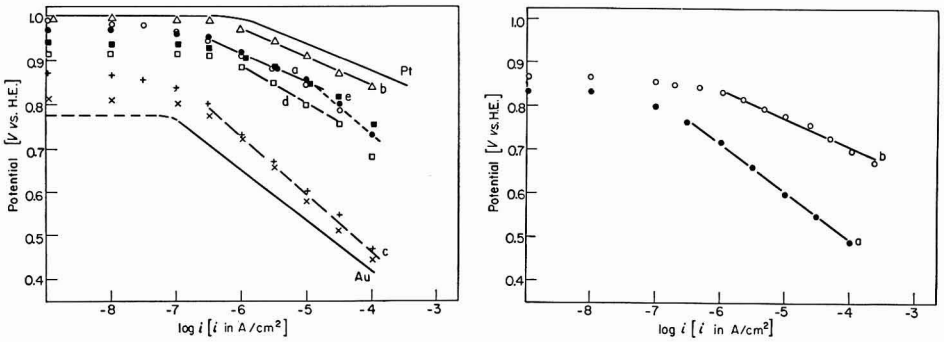

Fig. 1. Effect of electrode pretreatment on O_2-reduction at Pt–Au alloy electrodes. Pt–5% Au alloy electrode: (a), chemically (●) and thermally (○) treated; (b), electrochemically (△) treated electrodes. Pt–80% Au alloy electrode: (c), chemically (×) and thermally (+) treated; (d), electrochemically (□) treated; (e), electrochemically treated electrode after repeated anodic and cathodic pulsing (■). (Thermal pretreatment refers to 300°).

Fig. 2. Effect of electrode pretreatment on O_2-reduction at a Pd–75% Au alloy electrode. (a), chemically treated; (b), electrochemically treated electrode.

A Pt–Au electrode *rich in Au* (80% Au) is more affected by different electrode pretreatments than the Pt-rich alloy. Again, the activity of the electrode is nearly the same for the thermally (at 300°) and chemically treated electrodes (c, Fig. 1). The electrochemically treated electrode, however, shows a markedly different behavior (d, Fig. 1). Its activity at about 0.8 V (*vs.* H.E.) is nearly 10^2 higher than that for the thermally or chemically treated electrodes. This activity of the electrode of Au-rich alloy increases even further when anodic and cathodic pulsing is repeated (e, Fig. 1). Thus, with repeated anodic and cathodic pulses, the V–log i relationship for the electrochemically treated alloy electrodes (80% Au) approaches the relationship for a Pt electrode (Pt, Fig. 1). In addition to the changes in activity, the slope $(\partial V/\partial \ln i)$, for the electrochemically treated electrodes is different from those for the chemically or thermally treated electrodes. The slope for electrochemically treated electrodes is close to that for an oxide-free Pt electrode[4] ($\sim -RT/F$), while the slopes for the chemically or thermally treated electrodes are nearly the same as for an Au electrode ($\sim -2RT/F$). This indicates that the mechanism of O_2-reduction at an electrochemically treated Pt–Au alloy electrode, *which is rich in gold*, is the same as found for a Pt electrode, while the mechanism at chemically or thermally

treated electrodes is the same as for a Au electrode. If anodic and cathodic pulses are applied to an electrode that was initially pretreated either thermally or chemically, the behavior of this electrode also approaches that of a Pt electrode.

Similar effects of electrode pretreatments are observed with Au–Pd alloy electrodes. For instance, an electrochemically treated Au-rich electrode (75% Au) shows a marked increase in activity over that of a chemically treated electrode (Fig. 2). At the same time, the $\partial V/\partial \ln i$ slope changes from about $-2RT/F$ (the same slope as for an Au electrode) to about $-RT/F$. The latter slope corresponds to a palladium electrode.

It has been observed that thermal treatment also affects the kinetics of the reaction. When a platinum-rich (95%) Pt–Au alloy electrode is thermally treated at 300° for 5 min in H_2 and then for 10 min in N_2 atmosphere, the V–log i relationship is as shown in Fig. 3, line a. If, however, the temperature is raised to 650°, for the same time of treatment the activity of the electrode decreases with respect to that of the electrode heated at 300° (b, Fig. 3). With the increasing time of thermal treatment, the activity decreases still further, while there is a tendency for the $|\partial V/\partial \ln i|$ slope to increase (c, Fig. 3).

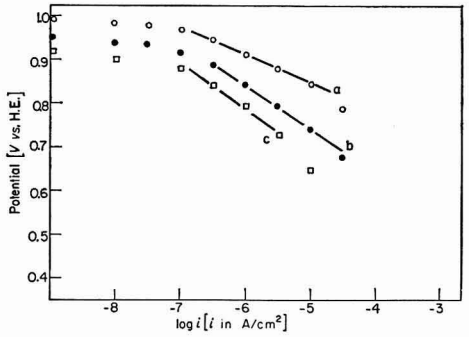

Fig. 3. Effect of thermal pretreatment on O_2-reduction at a Pt–5% Au alloy electrode. (a), at 300° for 5 min in H_2 and 10 min in N_2; (b), at 650° for 5 min in H_2 and 10 min in N_2; (c), at 650° for 5 min in H_2 and 30 min in N_2.

Pt–Au alloys rich in gold, or Pd–Au alloys, are less affected by the temperature or the time of the thermal treatment than Pt–Au alloys rich in Pt. Thus, only a slight decrease in the activity of a Pd–Au alloy (rich in Pd) is observed even after 60 min at 650°.

The above observations may be rationalised in the following way. When a noble-metal electrode is brought to a high anodic potential (>1.5 V *vs.* H.E.), oxides form at the surface[5,6]. Similarly, oxides will form at the surface of an alloy electrode. An oxide during the cathodic pulse (at 0.3 V *vs.* H.E.) reduces, but metal ions which composed the oxide phase may either re-enter the parent lattice, or nucleate new crystals at the surface. Some ions would undoubtedly go to the solution as cations, though not necessarily in the proportion corresponding to the alloy composition[7]. In either case, it is possible that on applying an anodic and then a cathodic pulse to an alloy electrode, the alloy components separate and small patches of crystals form at the electrode surface. These crystals may have a different composition from the bulk of the alloy itself.

Justification for such a situation can be found in experiments with Cu–Au alloys. When such an alloy is made an anode, Au crystals appear at the surface, while Cu is dissolving preferentially[7,8]. Here, the more noble component has crystallized at the electrode surface. In the case of Pt–Au or Pd–Au alloys, it is possible that during the process of applying an anodic and then a cathodic pulse, both components in each alloy crystallize as individual phases* in small patches at the electrode surface, rather than as one phase of the same composition as the bulk of the given alloy.

For example, if only 10% of the surface of an electrochemically treated Pt–Au alloy rich in Au is covered with Pt, or Pt-rich crystals, the overall rate of O_2-reduction will be determined by the rate at these crystals. This is because the rate at Au, or at Pt–Au electrodes rich in gold, is far less (at 0.8 V by about 4 orders of magnitude) than at Pt electrodes. With repeated anodic and cathodic pulses, more of these crystals may appear at the surface, and the activity further increases. Hence, an electrode of a Pt–Au alloy rich in gold behaves as if it were a Pt electrode. This is also true for a Pd–Au alloy.

The change in the activity and mechanism for O_2-reduction at a Pt–Au alloy electrode rich in Pt with the thermal treatment at high temperature and long times, is indicative of a change of the electrode surface, which now appears as if enriched in gold. It is suggested that this enrichment by gold in the surface layers of the electrode originates in the tendency to reduce the surface energy. Platinum, with a much higher heat of sublimation, is expected, according to the relationship arising from the Stefan's ratio[9], to have a higher surface tension than Au. Similarly, it may be expected that a Pt-rich Au–Pt alloy has a higher surface tension than Au or a Au-rich Pt–Au alloy. With increased temperature and time of thermal treatment, diffusion of atoms becomes possible and they can rearrange in the surface layer in such a way that the surface energy is reduced. According to this model, the less pronounced effect of temperature and time observed at Pd–Au alloys is due to smaller differences in surface energies between these two metals.

The above examples of the effect of electrode pretreatments on the activity and mechanism for O_2-reduction at different alloy electrodes are intended to illustrate how profoundly various electrode pretreatments may affect the behavior of the electrodes and how carefully the pretreatment of electrodes should be selected. This should not be confined only to the oxygen reaction or to alloys of noble metals, but should also have bearing on other electrode reactions and other alloys.

In a study of the kinetics and the catalytic properties of an alloy electrode, attention should be paid to the type of the electrode pretreatment that will result in a clean electrode surface reflecting the properties of the bulk of the alloy. The electrochemical treatments involving anodic and subsequent cathodic pulses, which are often used to *activate* an electrode, although possibly suitable for metal electrodes, should be used only with caution, particularly if in this process oxides form and reduce, or preferential dissolution of one alloy component occurs. Prolonged thermal treatment of alloy electrodes at higher temperatures may also prove to be unsuitable in a number of electrochemical studies. The chemical and thermal treatments at lower temperatures for short times appear to be suitable methods for preparing alloy electrodes.

* Possibly with some solution of one component into the phase of the other.

ACKNOWLEDGEMENTS

We wish to thank the U.S. Army Electronics Material Laboratory, Fort Monmouth, N. J. (Contract No. Da-36-039-Sc88921) for financial support. We thank also Professor J. O'M. BOCKRIS for valuable discussions, and Mr. DARKO SEPA for his help in some experiments.

REFERENCES

1 J. J. MCDONALD AND B. E. CONWAY, *Proc. Roy. Soc. London*, A269, (1962) 419; B. E. CONWAY, E. M. BEATTY AND P. A. D. DEMAINE, *Electrochim. Acta*, 7 (1962) 39; J. P. HOARE AND S. SCHULDINER, *J. Phys. Chem.*, 62 (1958) 229; S. SCHULDINER AND J. P. HOARE, *J. Phys. Chem.*, 61 (1957) 705.
2 R. JAHAN-MANNAN, private communication.
3 W. VISSCHER AND M. A. V. DEVANATHAN, *J. Electroanal. Chem.*, 8 (1964) 127.
4 A. DAMJANOVIC AND V. BRUSIĆ, to be published.
5 W. M. LATIMER, *Oxidation Potentials*, Prentice Hall Inc., Englewood Cliffs, N.J., 1964.
6 A. K. N. REDDY, M. GENSHAW AND J. O'M. BOCKRIS, *J. Electroanal. Chem.*, 8 (1964) 406.
7 B. T. RUBIN, private communication.
8 H. GERISCHER AND H. RICKERT, *Z. Metallk.*, 46 (1955) 681.
9 E. A. MOELWYN-HUGHES, *Physical Chemistry*, Pergamon Press, New York, 1961.

ELECTROANALYTICAL CHEMISTRY AND INTERFACIAL ELECTROCHEMISTRY
Elsevier Publishing Company, Amsterdam – Printed in The Netherlands

ANODIC OXIDATION OF CHLORIDES, BROMIDES AND IODIDES ON A PLATINUM MICROELECTRODE WITH PERIODICAL RENEWAL OF THE DIFFUSION LAYER

GIORGIO RASPI, FRANCESCO PERGOLA AND DANILO COZZI*
Istituto di Chimica Analitica, Università di Pisa (Italy)

(Received November 30th, 1966)

In a previous paper[1] the results of the investigation of the behaviour of a new platinum microelectrode with periodical renewal of the diffusion layer were reported. In particular, it was established that the mean diffusion currents obtained at constant electrode potential are in good agreement with those calculated using a simple expression containing the time during which the diffusion layer is being renewed (generally less than 25 msec) and the time during which the electrode is stationary (generally greater than 2 sec).

To investigate further the characteristics of the platinum electrode (platinized or not) with periodical renewal of the diffusion layer, we have initiated a study of the relations between the electrode potential and the current. We have used the redox systems of the halogens (alone or in a mixture) since they are of interest and many of them are reversible.

The direct polarographic study of the systems:

$$Cl_2 + 2\,e \rightleftarrows 2\,Cl^- \qquad E^{\circ\prime} = +1.390\ V\ (NHE)^{**}$$

$$Br_2 + 2\,e \rightleftarrows 2\,Br^- \qquad E^{\circ\prime} = +1.112\ V\ (NHE)^{**}$$

$$I_2 + 2\,e \rightleftarrows 2\,I^- \qquad E^{\circ\prime} = +0.627\ V\ (NHE)^{**}$$

with the dropping mercury electrode is not possible because of their high potentials and also because of the formation, at the electrode surface, of mercurous compounds of low solubility and low dissociation.

Laitinen and Kolthoff[2] suggested the use of the rotating platinum electrode for the amperometric determination of bromine, since with this electrode there is a proportionality between diffusion-current and concentration, at constant ionic strength. El Wakkad *et al.*[3] report a single wave, corresponding to the oxidation process: $2\,Br^- \rightarrow Br_2 + 2\,e$, obtained with a stationary platinum-leaf electrode in bromide solution.

Voltammetric curves of mixtures of I^-, I_2 and IO_3^- were studied by Brunner[4] with a plane platinum electrode. Kolthoff and Harris[5] used the rotating platinum

* Present address: Istituto di Chimica Analitica, Università di Firenze (Italy).

** Value calculated using the equation: $E = E^{\circ} - 0.0295 \log S$, where S = solubility of the halogen in water.

electrode for micro-iodometric titrations for which Harris and Lindsey[6] recommend the vibrating platinum electrode. Kolthoff and Jordan[7] found that, under certain conditions, and with a rotating platinum electrode, iodide ions give two anodic waves: the first wave corresponds to the formation of I_2 and the second wave to the oxidation of I_2 to I^+. El Wakkad *et al.*[3] using a stationary plane platinum electrode, with iodide solutions obtained two waves, the first corresponding to the reversible system I_2/I^- and the second to the irreversible formation of HIO_2. Gokhshtein[8] studied the anodic oxidation of concentrated solutions of iodides at a platinum microelectrode.

PROCEDURE AND APPARATUS

The platinum electrode with periodical renewal of the diffusion layer can be used either smooth or platinized. The platinization, when necessary, was carried out in the following way: the electrode was cleaned with nitric acid, then hydrogen was allowed to develop at its surface by polarizing it as a cathode in a dilute solution of sulfuric acid for about 1 min. Finally it was platinized for 4 sec with a current density of 1.2 A cm^{-2} in a 3% solution of chloroplatinic acid containing (1/40)% of lead acetate. The electrode was washed with distilled water after each step of the treatment. Each series of polarograms was carried out with a freshly platinized electrode, the previous platinization having been removed by treatment with boiling, dilute *aqua regia*.

Oxygen was removed from the solutions, when necessary, by passing pure nitrogen through them. A saturated mercurous sulfate electrode was used as a reference electrode and was connected with the cell through an ammonium nitrate bridge gelified with agar-agar. The potentials reported in the present paper are referred to the SCE.

Measurements were carried out with a "Polarecord" E 261 Metrohm, modified to give a slow variation of the applied potential (0.5 mV sec^{-1}). The temperature was maintained at $25 \pm 0.1°$.

RESULTS

Cl_2/Cl^-, Br_2/Br^- and I_2/I^- systems

An anodic wave of limited amplitude and with small oscillations is obtained by applying an increasing positive potential to a smooth electrode in a 10^{-3} *M* Cl^- solution with 1 *N* $HClO_4$. This wave does not appear if the scanning is carried out in the reverse direction, *i.e.*, with a decreasing positive potential. The reaction, $2\,Cl^- \rightarrow Cl_2 + 2\,e$, is influenced by the presence (or not) of platinum oxides on the smooth platinum electrode and is therefore subject to an appreciable overvoltage. It is, on the contrary, reversible on a platinized electrode (Fig. 1, curve (a)) and gives then a well-shaped wave, in both senses of changing potential, with a chloride ion concentration of $2 \cdot 10^{-4}$ *M*. Since the redox potential of Cl_2/Cl^- is rather high and the oxygen discharge may mask the oxidation wave of chloride ion to chlorine, it is preferable to work in a strongly acid solution. In 3 *N* $HClO_4$, the proportionality between the mean limiting current and the chloride ion concentration is verified down to a concentration of $5 \cdot 10^{-5}$ *M*.

A single anodic wave corresponding to the process, $2\,Br^- \rightarrow Br_2 + 2\,e$, is obtained by applying an increasing positive potential to a smooth platinum electrode in a $5 \cdot 10^{-4}$ *M* bromide solution in 1 *M* $HClO_4$. Its half-wave potential is +0.970 V and is independent of the pH of the solution at constant Br^- concentration; therefore,

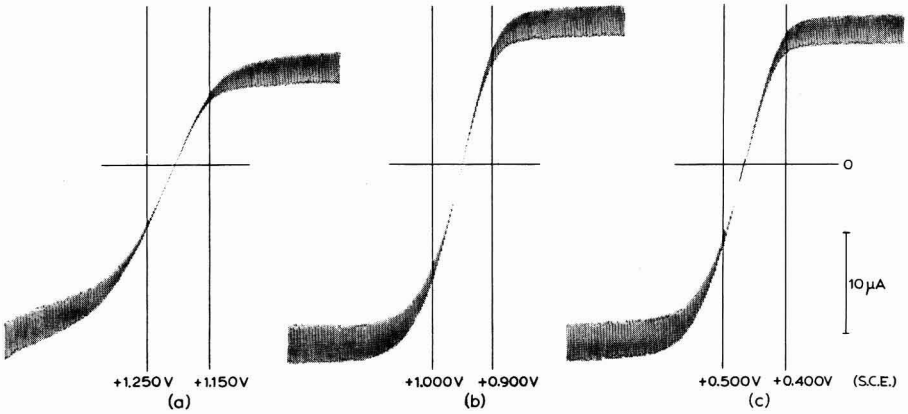

Fig. 1. Cathanodic waves obtained with 1 *N* $HClO_4$ in presence of: (a), $7 \cdot 10^{-4}$ *M* Cl^- and $3 \cdot 10^{-4}$ *M* Cl_2; (b), $1 \cdot 10^{-3}$ *M* Br^- and $5 \cdot 10^{-4}$ *M* Br_2; (c), $1 \cdot 10^{-3}$ *M* I^- and $5 \cdot 10^{-4}$ *M* I_2.

a decrease in the pH of the solution may cause the oxidation wave of bromide to bromine to overlap the oxygen discharge wave. At bromide concentrations of $5 \cdot 10^{-4}$ *M*, the masking of the former wave by the latter takes place at pH-values greater than 8. The process appears to be completely reversible in 1 *N* $HClO_4$ independent of the state of the electrode (Fig. 1, curve (b)); the mean diffusion limiting current is proportional to the bromide (ion) concentration. Ill-shaped, poorly reproducible waves are obtained using 1 *N* $NaNO_3$ as base electrolyte (the bromide concentration being constant). This can be attributed to the state of the electrode surface, as in the case of the Cl_2/Cl^- system. A platinized electrode again gives very good results.

Two distinct anodic waves were obtained by applying an increasingly positive potential to a smooth platinum electrode in a $5 \cdot 10^{-4}$ *M* solution of I^- ions in 1 *N* $HClO_4$ (Fig. 2). The first wave, with a half-wave potential of +0.488 V was well-shaped and essentially diffusion-controlled. It is caused by the oxidation of iodide ion to iodine. The second wave, which is characterized by a fall in the current, corresponds to the oxidation of iodine to iodate.

The oxidation of iodide ions to iodine is completely reversible (Fig. 1, curve (c)) on both smooth and platinized-platinum electrodes and does not depend on the condition of the electrode surface. The half-wave potential does not change with change in the pH of the solution, provided that the concentration of the electroactive species is unchanged. The mean limiting diffusion currents are well-defined and are constant in the pH range 0–8, at constant concentration and ionic strength, in perchloric, nitric and sulfuric media.

The shape of the iodide wave depends on whether it is obtained with increasing or decreasing positive potential: in the former case a completely anodic wave appears, whereas in the latter the wave is partially cathodic (Fig. 3, curves (a) and (a')). The

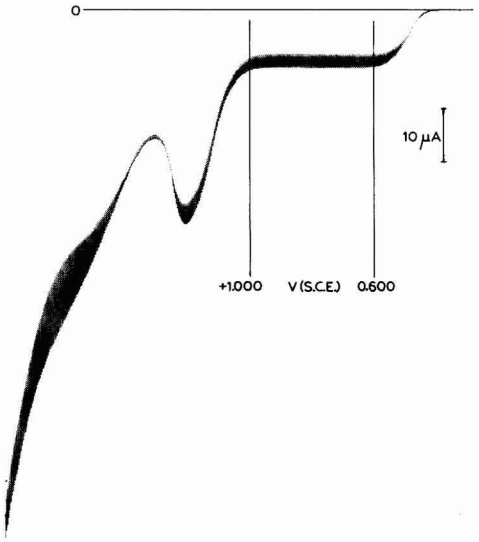

Fig. 2. Voltammetric curve of $5 \cdot 10^{-4}$ *M* iodide ion in 1 *N* $HClO_4$.

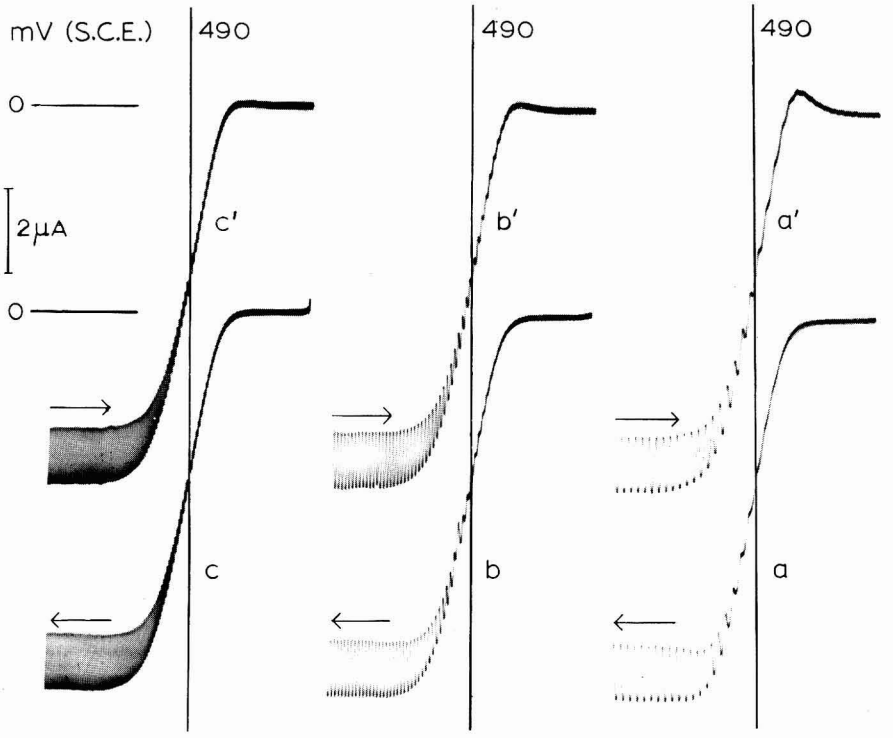

Fig. 3. Oxidation waves of iodide ion ($5 \cdot 10^{-4}$ *M* in 1 *N* $HClO_4$) obtained with: (a, b, c), increasing positive potential; (a′, b′, c′), decreasing positive potential. Recording speeds: (a, a′), 150; (b, b′), 100; (c, c′), 50 mV/min.

whereas in the latter the wave is partially cathodic (Fig. 3, curves (a) and (a′). The cathodic contribution is due to the reduction of some iodine, which had been adsorbed on the electrode surface during the previous oxidation of the I^- ion at a more positive potential. This phenomenon is more apparent with a platinized electrode since a larger quantity of iodine is adsorbed at the much larger electrode surface: the amplitude of the cathodic portion increases. On the other hand, the cathodic contribution decreases when the rate of change of potential decreases (Fig. 3, curves (b′) and (c′)).

In the three instances, the proportionality between diffusion current and the halogen ion and free halogen concentration has been verified; it has also been verified that the mean limiting diffusion current[1] follows the equation:

$$\bar{i} = K_X C$$

where:

$$K_X = \frac{nFAD_X}{r} + \frac{nFAD_X^{\frac{1}{2}}}{\pi^{\frac{1}{2}} t_{tot}} (2t_{tot}^{\frac{1}{2}} - 1.5t_p^{\frac{1}{2}}) \qquad (1)$$

and:

$\bar{i}$ = current (μA);
C = concentration of electro-oxidable or reducible electrolyte (M);
n = number of Faradays/mole required by the reaction at the electrode;
F = Faraday constant;
A = effective electrode surface (0.0675 cm^2);
D_X = diffusion coefficient;
r = radius of the platinum sphere (0.0937 cm);
t_{tot} = pulse period (4 sec);
t_p = electrode washing period (0.025 sec).

The relation between the current and the electrode potential at each point of the cathanodic wave, when both species are present without interacting (the contribution of the chemical equilibrium $I^- + I_2 \rightleftarrows I_3^-$ to the electrode process is negligible at the concentrations employed[12]), is easily obtained by considering that the halogen ion concentration at the electrode surface is as follows:

$$C_{X^-}^{\circ} = C_{X^-} + \frac{i}{K_{X^-}} = \frac{(-i_d)_a + i}{K_{X^-}}$$

assuming a negative sign for anodic currents, whereas the halogen concentration is

$$C_{X_2}^{\circ} = \{(i_d)_c - i\}/K_{X_2}$$

$(i_d)_c$ being the cathodic mean limiting diffusion current. Introducing these relations into the Nernst equation gives the general expression:

$$E = E_{X_2/X^-}^{\circ'} + 0.0295 \log \frac{f_{X_2} K_{X^-}^2}{f_{X^-}^2 K_{X_2}} + 0.0295 \log \frac{(i_d)_c - i}{[-(i_d)_a + i]^2}$$

from which, by equating $(i_d)_c$ and $(-i_d)_a$ to zero, respectively, the following equations are derived:

$$E = E_{X_2/X^-}^{\circ'} + 0.0295 \log \frac{f_{X_2} K_{X^-}^2}{f_{X^-}^2 K_{X_2}} + 0.0295 \log \frac{-i}{(-i_d + i)^2} \qquad (2)$$

$$E = E^{\circ'}_{X_2/X^-} + 0.0295 \log \frac{f_{X_2} K^2_{X^-}}{f^2_{X^-} K_{X_2}} + 0.0295 \log \frac{i_d - i}{i^2} \quad (3)$$

where:

f_{X_2} = activity coefficient of the halogen (= 1);

f_{X^-} = mean activity coefficient of HX at unit activity (= 0.809 for HCl; 0.871 for HBr; 0.963 for HI);

K_{X^-}, K_{X_2} = proportionality constants, respectively equal to $(-i_d)_{X^-}/C_{X^-}$ and $(i_d)_{X_2}/C_{X_2}$, the values of which depend on the characteristics of the electrode, the diffusion coefficients of the electroactive species, D_{X^-} and D_{X_2}, and the times, t_p and t_{tot}.

Experimental K_X-values are constant (Table 1) for I^-, Br^-, I_2 and Br_2 and in very good agreement with the values calculated by means of eqn. (1). The K_X-values have not been calculated for Cl^- and Cl_2 because of the uncertainty of the effective area of the platinized electrode.

In particular, the half-wave potential of the oxidation wave is given by the equation:

$$E_{\frac{1}{2}} = E^{\circ'}_{X_2/X^-} + 0.0295 \log \frac{f_{X_2} K^2_{X^-}}{f^2_{X^-} K_{X_2}} + 0.0295 \log \frac{2}{-i_d} \quad (4)$$

or also, since $-i_d = K_{X^-} C_{X^-}$:

$$E_{\frac{1}{2}} = E^{\circ'}_{X_2/X^-} + 0.0295 \log \frac{f_{X_2} K^2_{X^-}}{K_{X_2}} + 0.0295 \log \frac{2}{f^2_{X^-} C_{X^-}} \quad (5)$$

TABLE 1

Electroactive species	*Concn.* ($M \cdot 10^4$)	i_d (μA)	K_{X^-} (10^3 $\mu A\ mole^{-1}\ l$)		*Electroactive species*	*Concn.* ($M \cdot 10^4$)	i_d (μA)	K_{X_2} (10^3 $\mu A\ mole^{-1}\ l$)	
			(*exptl.*)	(*calc.*)				(*exptl.*)	(*calc.*)
Cl^-	2	4.10	20.5		Cl_2	2	5.84	29.2	
	4	8.12	20.3			4	11.80	29.5	
	6	12.36	20.6			6	17.58	29.3	
	8	16.32	20.4			8	23.52	29.4	
	10	20.70	20.7			10	29.60	29.6	
		average:	20.5	—			average:	29.4	—
Br^-	0.5	0.84	16.8		Br_2	0.5	1.21	24.2	
	1	1.71	17.1			1	2.46	24.6	
	2	3.46	17.2			2	4.88	24.4	
	4	6.92	17.3			4	9.92	24.8	
	8	13.68	17.1			8	19.60	24.5	
		average:	17.1	17.14			average:	24.5	24.65
I^-	0.5	0.84	16.8		I_2	0.5	1.22	24.4	
	1	1.73	17.3			1	2.47	24.7	
	2.5	4.30	17.2			2	4.88	24.4	
	5	8.50	17.0			3	7.44	24.8	
	10	17.20	17.2			5	12.10	24.2	
		average:	17.1	17.07			average:	24.5	24.54

From eqn. (2), the electrode potential when $\log \{-i/(-i_d+i)^2\} = 0$ is:

$$E' = E^{\circ'}_{X_2/X^-} + 0.0295 \log \frac{f_{X_2} K^2_{X^-}}{f^2_{X^-} K_{X_2}} \quad (6)$$

independent of the concentration of the electro-oxidable species. The calculated and experimental values (Fig. 4) of E' are in good agreement. By substituting the E'-value into eqn. (4), E' is found to be identical with $E_{\frac{1}{2}}$ when $i_d = 2\ \mu A$, or when $C_{X^-} = 2/K_{X^-}$,

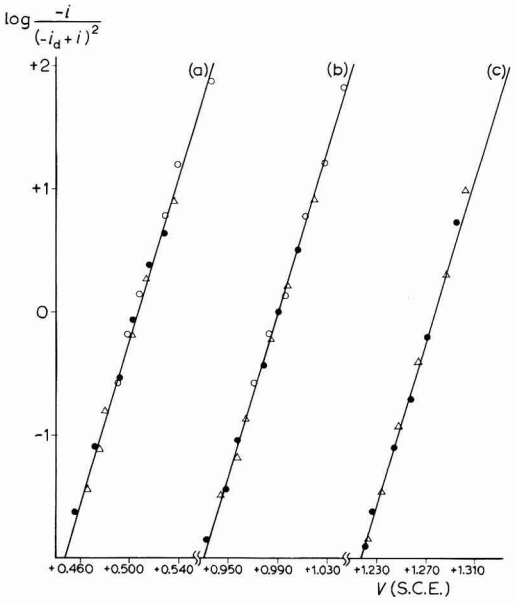

Fig. 4. Test of eqn. (2) for oxidation of: (a), chloride ion; (b), bromide ion; (c), iodide ion. Concns.: (○), $5 \cdot 10^{-5}$ M; (△), $5 \cdot 10^{-4}$ M; (●), $1 \cdot 10^{-3}$ M.

obtained by equating the two right-hand sides of eqns. (5) and (6). In our case, introducing the values of K_{X^-} and K_{X_2} previously reported, such a condition would be realized with a concentration of 9.8×10^{-5} M for chloride ion and 1.17×10^{-4} M for bromide and iodide ions. Table 2 which contains the calculated and experimental values of $E_{\frac{1}{2}}$ and values of i_d at various concentrations of chloride, bromide and iodide ions, shows that such conditions are actually verified.

Anodic waves of iodides in the presence of chlorides

The voltammetric curve obtained with electrode potentials between +0.250 and +1.00 V in a $5 \cdot 10^{-4}$ M solution of iodide ion, plus 0.5 M HCl and 0.5 M $HClO_4$, shows two well-defined anodic waves (Fig. 5) independent of the sense of recording. The first step corresponds to the reaction, $2\ I^- \rightarrow I_2 + 2\ e$, and corresponds with the first oxidation wave of iodide ion in the absence of chlorides. The second anodic wave ($E_{\frac{1}{2}} = +0.682$ V) corresponds to the oxidation reaction, $I_2 + 4\ Cl^- \rightarrow 2\ ICl_2^- + 2\ e$. This last process is reversible at the electrode, as shown by the mathematical analysis of the wave, which gives a value of 30 mV for the ratio $\Delta E/\Delta \log \{(-i)^2/(-i_d+i)\}$.

TABLE 2

Electroactive species	*Concn.* $(M \cdot 10^4)$	E' *(mV)*		$E_{\frac{1}{2}}$ *(mV)*		i_d *(μA)*
		calc.	*exptl.*	*exptl.*	*calc.*	
Cl^-	2	1277	1269	1267	1268	4.10
	4	1277	1273	1261	1259	8.12
	6	1277	1273	1256	1254	12.36
	8	1277	1279	1251	1250	16.32
	10	1277	1276	1250	1247.5	20.70
	20	1277	1279	1245	1238.5	41.20
Br^-	0.5	990	992	1001	1001	0.84
	1	990	991	992	992	1.71
	2	990	989	985	983	3.46
	4	990	996	977	974	6.92
	8	990	995	968	964	13.68
	20	990	988	959	953.5	34.50
I^-	0.5	507	502	520	518	0.84
	1	507	505	509	509	1.73
	2.5	507	508	495	497	4.30
	5	507	503	485	488	8.50
	8	507	508	484	481	13.80
	10	507	506	478	479.5	17.20

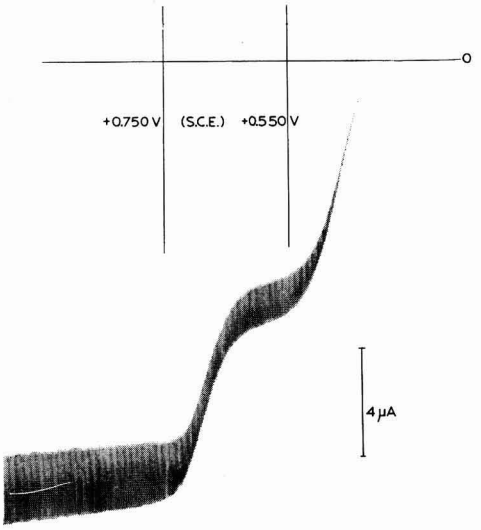

Fig. 5. Anodic wave of $5 \cdot 10^{-4}$ *M* iodide ion in 0.5 *N* $HClO_4$ and 0.5 *N* HCl.

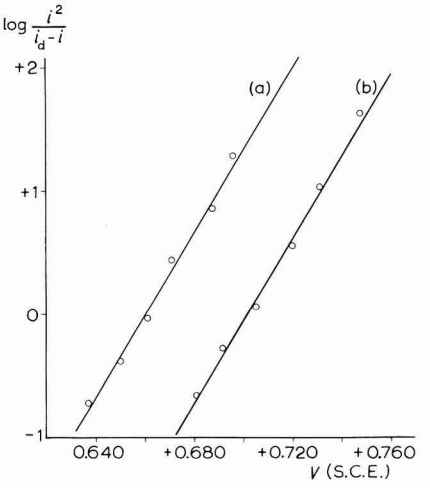

Fig. 6. Test of eqn. (14) for oxidation of iodine to: (a), ICl_2^- in 0.5 *N* $HClO_4$ and 0.5 *N* HCl; (b), IBr_2^- in 1 *N* $HClO_4$ and $5 \cdot 10^{-3}$ *N* HBr. Concn. iodide ion: $5 \cdot 10^{-4}$ *M*.

A $5 \cdot 10^{-4}$ *M* solution of iodine chloride in 0.5 *M* HCl and 0.5 *M* $HClO_4$ gives rise to two cathodic waves (Fig. 7 (a)) going towards less positive potentials; the first wave corresponds to the reduction: $2\ ICl_2^- + 2\ e \rightarrow I_2 + 4\ Cl^-$, and has the same

half-wave potential as the 2nd anodic wave (Fig. 5), the 2nd wave corresponds to the reduction of iodine to iodide ion. If an amount of iodide ion equal to one-half of the iodine chloride already present is added to this solution, a cathanodic wave arises and the height of the second reduction wave increases (Fig. 7 (b)). The anodic portion of the cathanodic wave corresponds to the oxidation of the iodine previously formed from the partial reduction of the iodine chloride operated by the iodine added; the cathodic portion (of the wave) corresponds to the reduction of the excess iodine chloride still present in the solution. The increase in height of the second reduction wave, which corresponds to the reaction, $I_2+2\ e\rightarrow 2\ I^-$, is due to the formation of I_2.

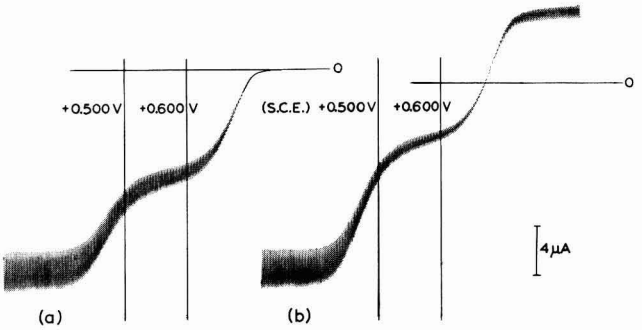

Fig. 7. (a), Voltammetric curve of $5\cdot 10^{-4}$ *M* iodine chloride in 0.5 *N* $HClO_4$ and 0.5 *N* HCl; (b), as (a) after iodide ion addition.

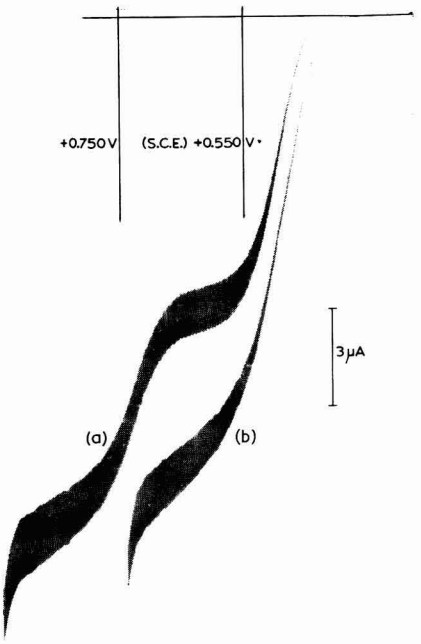

Fig. 8. Oxidation waves of $5\cdot 10^{-4}$ *M* iodide ion in: (a), 1 *N* $HClO_4$ and $5\cdot 10^{-3}$ *M* HBr; (b), 0.5 *N* $HClO_4$ and 0.5 *N* HBr.

If the chloride ion activity in the $5 \cdot 10^{-4}$ M solution of iodide is decreased, the ionic strength of the solution (equal to 1) and the iodide ion activity being kept constant, the half-wave potential of the first wave does not change, whereas that of the second wave shifts toward more positive values.

Anodic waves of iodides in the presence of bromides

The voltammetric curve obtained with electrode potentials between +0.25 and +0.90 V in a $5 \cdot 10^{-4}$ M solution of iodide ion and 1 N $HClO_4$ shows two well-defined anodic waves (Fig. 8, curve (a)) independent of recording direction. The first wave corresponds to the reaction, $2\,I^- \rightarrow I_2 + 2\,e$, the second to the oxidation, $I_2 + 4\,Br^- \rightarrow 2\,IBr_2^-$. The analysis of this second wave shows that the ratio $\Delta E/\Delta \log \{(-i)^2/(-i_d+i)\}$ is equal to 30 mV. By varying the activity of the bromide ion (at fixed unit ionic strength and iodide ion concentration, $5 \cdot 10^{-4}$ M), the half-wave potential of the second wave is shifted whereas that of the first wave remains practically constant. Increasing the bromide concentration causes the second wave to shift toward the first, and eventually there is a complete overlap to form a single anodic wave (Fig. 8, curve (b)), corresponding to the oxidation:

$$I^- + 2\,Br^- \rightarrow IBr_2^- + 2\,e.$$

DISCUSSION

It is known that chlorides and bromides stabilize the +1 oxidation state of iodine. The following process of oxidation of iodine ions at the electrode in the presence of chlorides and bromides may be supposed:

$$\begin{aligned} 2\,I^- &\rightarrow I_2 + 2\,e \quad \text{(a)} \\ I_2 + 2\,X^- &\rightarrow 2\,IX + 2\,e \quad \text{(b)} \end{aligned} \tag{7}$$

$$\begin{aligned} 2\,I^- &\rightarrow I_2 + 2\,e \quad \text{(a)} \\ I_2 + 4\,X^- &\rightarrow 2\,IX_2^- + 2\,e \quad \text{(b)} \end{aligned} \tag{8}$$

$$I^- + 2\,X^- \rightarrow IX_2^- + 2\,e \tag{9}$$

Reactions (7) and (8) would cause two anodic waves, corresponding to the oxidation of iodide ion to iodine and eventually to I (+1) complex (Fig. 5, Fig. 8, curve (a)). Reaction (9) causes a single anodic wave corresponding to the direct reversible oxidation of iodide ion to IX_2^- at the electrode (Fig. 8, curve (b)). In Fig. 9, line (a) shows the half-wave potentials of the oxidation wave of iodide ion to iodine, calculated by eqn. (5) for $pa_{I^-} = 3.32$, 4.32 and 5.32, respectively. The equations of the waves and of the half-wave potentials corresponding to processes (7b), (8b) and (9), where I (+1) is formed, are reported below.

Reaction (7b)

The potential along the polarographic wave is given by:

$$E = E^{\circ}_{IX/I_2(aq)} + 0.0295 \log \frac{f_{IX}^2 K_{I_2}}{f_{I_2} K_{IX}^2} - 0.0295 \log a_{X^-}^2 + 0.0295 \log \frac{(-i)^2}{-i_d + i} \tag{10}$$

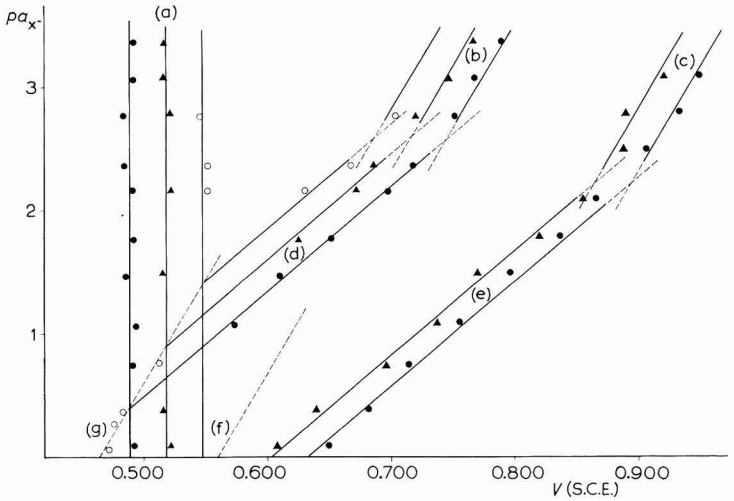

Fig. 9. Changes of $E_{\frac{1}{4}}$ of the oxidation waves to I(+1) complex as a function of the activity of X^- ($=Cl^-$ or Br^-). (a), $E_{\frac{1}{4}}$-values calc. by eqn. (5) for the oxidation of I^- to I_2; (b) and (c), calc. by eqn. (13) for the systems IBr/I_2 and ICl/I_2, respectively; (f) and (g), calc. by eqn. (18) for ICl_2^-/I^- and IBr_2^-/I^-, respectively. Exptl. values measured with solns. having pa_{I^-}: (●), 3.32; (▲), 4.32; (○), 5.32.

where:

$E^{\circ}_{IX/I_2(aq)} = E^{\circ}_{IX/I_2(sol)} + 0.0295 \log S$, S being the solubility of iodine ($133 \cdot 10^{-5}$ M)

$E^{\circ}_{ICl/I_2(aq)} = (1.19–0.085)$ V (NHE), $+0.864$ V (SCE)[9,10];

$E^{\circ}_{IBr/I_2(aq)} = (1.02–0.085)$ V (NHE), $+0.694$ V (SCE)[10];

f_{IX} = activity coefficient of IX ($=1$);

K_{IX} = proportionality constant between $(i_d)_{IX}$ and C_{IX}, dependent on the electrode characteristic and on the diffusion coefficient of IX. Under the conditions of our experiments at $t_{tot}=4$ sec, $K_{IX} = 171 \cdot 10^{-4}$ μA mole^{-1}l (see Table 3);

a_{X^-} = activity of the complexing ion (Cl^- or Br^-).

TABLE 3

Electroactive species	*Concn.* ($M \cdot 10^5$)	i_d (μA)	K_{IX} (10^3 μA *mole*$^{-1}$ *l*)	*Electroactive species*	*Concn.* ($M \cdot 10^4$)	i_d (μA)	$K_{IX_2^-}$ (10^3 μA *mole*$^{-1}$ *l*)
ICl	1	0.17	17.0	ICl_2^-	0.5	0.84	16.8
in 2 mM HCl	2.5	0.43	17.2	in 0.1 M HCl	0.75	1.27	16.9
	5	0.84	16.8		1	1.73	17.3
	7.5	1.29	17.2		2.5	4.30	17.2
	10	1.73	17.3		5	8.65	17.3
		average:	17.1			average:	17.1
IBr	1	0.17	17.0	IBr_2^-	0.5	0.86	17.2
in 1 mM HBr	2.5	0.42	16.8	in 0.1 M HBr	0.75	1.27	17.0
	5	0.87	17.4		1	1.69	16.8
	7.5	1.27	17.0		2.5	4.33	17.3
	10	1.72	17.2		5	8.60	17.2
		average:	17.1			average:	17.1

The half-wave potential is given by:

$$E_{\frac{1}{2}} = E^{\circ}_{IX/I_2(aq)} + 0.0295 \log \frac{f^2_{IX} K_{I_2}}{f_{I_2} K^2_{IX}} - 0.0295 \log a^2_{X^-} + 0.0295 \log \frac{-i_d}{2} \quad (11)$$

or, since $-i_d = K_{I^-} C_{I^-}$:

$$E_{\frac{1}{2}} = E^{\circ}_{IX/I_2(aq)} + 0.0295 \log \frac{f^2_{IX} K_{I_2}}{f_{I_2} K^2_{IX}} - 0.0295 \log a^2_{X^-} + 0.0295 \log \frac{f_{I^-} C_I}{2} \quad (12)$$

In Fig. 9 the straight lines (b) and (c) show the shift of the half-wave potential calculated by means of eqn. (12) as a function of the activity of the complexing agent (respectively, Br^- and Cl^-), at fixed iodide ion activity and unit ionic strength of the solution. A unit increase of pa_{I^-} causes a shift of the half-wave potential of 29.5 mV towards less positive values. Experimental values obtained at pa_{I^-} equal to 5.32, 4.32 and 3.32, respectively, are shown in the figure. They are in good agreement with the calculated values.

Reaction (8b)

The potential along the wave is given by:

$$E = E^{\circ}_{IX_2^-/I_2(aq)} + 0.0295 \log \frac{f^2_{IX_2^-} K_{I_2}}{f_{I_2} K^2_{IX_2^-}} - 0.0295 \log a^4_{X^-} + 0.0295 \log \frac{(-i)^2}{-i_d + i} \quad (13)$$

where:

$E^{\circ}_{IX_2^-/I_2(aq)} = E^{\circ}_{IX/I_2(aq)} - 0.0295 \log K^2$, K being the partial stability constant of the complex IX_2^-. For the complex ICl_2^-, $\log K = 2.22$[11], from which $E^{\circ}_{ICl_2^-/I_2(aq)} = +0.733$ V. For the complex IBr_2^-, $\log K = 2.57$[11], from which $E^{\circ}_{IBr_2^-/I_2(aq)} = +0.543$ V.

$f_{IX_2^-}$ = activity coefficient of IX_2^- (equal to 0.99, calculated by means of the equation: $-\log_{IX_2^-} = 0.511\, I^{\frac{1}{2}}/(1 + 1.5\, I^{\frac{1}{2}}) - 0.2\, I^{\frac{1}{2}}$ where I is the ionic strength, in this case equal to 1.

$K_{IX_2^-}$ = proportionality constant between $(i_d)_{IX_2^-}$ and $C_{IX_2^-}$, dependent on the electrode characteristics and on the diffusion coefficient of IX_2^-. Under the conditions of our experiments at $t_{tot} = 4$ sec, $K_{IX_2^-} = 171 \cdot 10^{-4}$ μA mole^{-1} l (Table 3).

The half-wave potential is given by:

$$E_{\frac{1}{2}} = E^{\circ}_{IX_2^-/I_2(aq)} + 0.0295 \log \frac{f^2_{IX_2^-} K_{I_2}}{f_{I_2} K^2_{IX_2^-}} - 0.0295 \log a^4_{X^-} + 0.0295 \log \frac{-i_d}{2} \quad (14)$$

or, since $-i_d = K_{I^-} C_{I^-}$:

$$E_{\frac{1}{2}} = E^{\circ}_{IX_2^-/I_2(aq)} + 0.0295 \log \frac{f^2_{IX_2^-} K_{I_2}}{f_{I_2} K^2_{IX_2^-}} - 0.0295 \log a^4_{X^-} + 0.0295 \log \frac{f_{I^-} C_{I^-}}{2} \quad (15)$$

In Fig. 9, the straight lines (d) and (e) reproduce the shifts of the half-wave potential calculated by means of eqn. (15) as a function of the activity of the complexing agent (Br^- and Cl^-, respectively) at constant activity of the iodide ion and unit ionic strength of the solution. A unit increase of pa_{I^-} causes a shift of the half-wave potential of 29.5 mV toward less positive values. The experimental values obtained for pa_{I^-} equal

to 5.32, 4.32 and 3.32, respectively, are shown in the figure. They are in good agreement with the calculated values.

The electrode potential at $\log\{(-i)^2/(-i_d+i)\}=0$, is independent of the iodide ion concentration and is given by the following equation:

$$E' = E^{\circ}_{IX_2^-/I_{2(aq)}} + 0.0295 \log \frac{f^2_{IX_2^-} K_{I_2}}{f_{I_2} K^2_{IX_2^-}} - 0.0295 \log a^4_{X^-} \quad (16)$$

The calculated and experimental values for E' in the presence of chlorides and bromides (Fig. 6, lines (a) and (b)) are in good agreement.

Reaction (9)

The potential along the polarographic wave is:

$$E = E^{\circ}_{IX_2^-/I^-} + 0.0295 \log \frac{f_{IX_2^-} K_{I^-}}{f_{I^-} K_{IX_2^-}} - 0.0295 \log a^2_{X^-} + 0.0295 \log \frac{-i}{-i_d+i} \quad (17)$$

where $E^{\circ}_{IX_2^-/I^-}$, which is obtained from the relation: $\frac{1}{2}(E^{\circ}_{IX_2^-/I_{2(aq)}} + E^{\circ}_{I_{2(aq)}/I^-})$, is:

$E^{\circ}_{ICl_2^-/I^-} = +0.559$ V

$E^{\circ}_{IBr_2^-/I^-} = +0.465$ V

The half-wave potential is:

$$E_{\frac{1}{2}} = E_{IX_2^-/I^-} + 0.0295 \log \frac{f_{IX_2^-} K_{I^-}}{f_{I^-} K_{IX_2^-}} - 0.0295 \log a^2_{X^-} \quad (18)$$

In Fig. 9, the straight lines (f) and (g) show the shift of the half-wave potentials, calculated by means of eqn. (18), as a function of the activity of the chloride and bromide ion respectively, at fixed (unit) ionic strength of the solution. It can be seen that, in the presence of $5 \cdot 10^{-4}$ *M*, iodide ion reaction (9) will take place at the electrode only if the chloride ion activity is high ($\log a_{Cl^-} > 1$), whereas the direct oxidation of I^- to IBr_2^- should be possible at a pa_{Br^-} value of 0.4. At this value, in fact, the two lines (a) and (d) corresponding to $pa_{I^-} = 3.32$, cross each other, *i.e.*, the waves corresponding to the reactions, $2\,I^- \rightarrow I_2 + 2\,e$ and $I_2 + 4\,Br^- \rightarrow 2\,IBr_2^- + 2\,e$, merge into a single wave corresponding to the reaction $I^- + 2\,Br^- \rightarrow IBr_2^- + 2\,e$.

The straight lines (d) and (e), corresponding to $pa_{I^-} = 4.32$ and 5.32 show that the values of pa_{Br^-} and pa_{Cl^-} at which complete overlapping of the anodic waves takes place, increase when the iodide ion activity in the solution decreases, thus making possible the reaction $I^- + 2\,Cl^- \rightarrow ICl_2^- + 2\,e$ for $pa_{Cl^-} = 0$ and $pa_{I^-} = 5.71$. The experimental values relative to the reaction $I^- + 2\,Br^- \rightarrow IBr_2^- + 2\,e$ are reported in Fig. 9 and are in good agreement with the calculated values.

CONCLUSION

It is evident that the currents obtainable with the electrode with periodical renewal of the diffusion layer, are strictly related to the applied potentials by means of expressions derived from theoretical principles. It has already been shown, that the mean limiting currents obtained with this electrode are independent (within relatively large limits) of the conditions in which the electrode is operating and are calculable

with precision, hence we may conclude that the electrode with periodical renewal of the diffusion layer is well suited to the study of redox processes, particularly at high potentials.

ACKNOWLEDGEMENT

The authors are grateful to the "Consiglio Nazionale delle Ricerche" of Italy for financial support.

SUMMARY

The redox process, $Cl_2+2\,e\rightarrow 2\,Cl^-$, occurs reversibly on a platinized-platinum microelectrode with periodical renewal of the diffusion layer. The processes, $Br_2+2\,e\rightarrow 2\,Br^-$ and $I_2+2\,e\rightarrow 2\,I^-$ occur reversibly in 1 *N* $HClO_4$ either on a smooth or platinized electrode. In 1 *N* $NaNO_3$ the first of these reactions occurs only on a smooth electrode. The voltammetric curves obtained with a $5\cdot10^{-4}$ *M* iodide solution in HCl at a concentration between 1 and 10^{-3} *N* (the ionic strength being kept constant by the addition of $HClO_4$) show two anodic waves of about the same height. The first wave is due to the oxidation of iodide ion to iodine, the second to the reaction $I_2+4\,Cl^-\rightarrow 2\,ICl_2^-+2\,e$ or $I_2+2\,Cl^-\rightarrow ICl^-+2\,e$, according to the activity of the chloride ion in the solution. The voltammetric curves obtained with $5\cdot10^{-4}$ *M* iodide ion in HBr at a concentration between 1 and 0.28 *N* show a single anodic wave corresponding to the oxidation, $I^-+2\,Br^-\rightarrow IBr_2^-+2\,e$. Decreasing the bromide ion concentration below 0.28 *N* causes a distortion of the wave and finally a splitting: the two waves thus obtained correspond to the oxidation reactions of iodide ion to iodine and of this iodine to IBr_2^- or to IBr. The reversibility of the various oxidation–reduction systems and also the $E_{\frac{1}{2}}$-values of the corresponding waves as functions of the concentrations of halide ions, have been verified. A strict relation between the $E_{\frac{1}{2}}$-potentials and the electrode characteristics has been established. The results are in very good agreement with the values calculated on the basis of the equation valid for spherical diffusion.

REFERENCES

1 D. Cozzi, G. Raspi and L. Nucci, *J. Electroanal. Chem.*, 12 (1966) 36–44.
2 H. A. Laitinen and I. M. Kolthoff, *J. Phys. Chem.*, 45 (1941) 1079.
3 S. E. S. El Wakkad, S. E. Khalafalla and A. M. Shams El Din, *Rec. Trav. Chim.*, 76 (1957) 789.
4 E. Brunner, *Z. Physik. Chem.*, 56 (1906) 321.
5 I. M. Kolthoff and W. E. Harris, *Anal. Chem.*, 21 (1947) 963.
6 E. D. Harris and A. J. Lindsey, *Analyst*, 76 (1951) 647.
7 I. M. Kolthoff and J. Jordan, *J. Am. Chem. Soc.*, 75 (1953) 1571.
8 A. Ya. Gokhshtein, *Soviet Electrochemistry*, 1 (1965) 809.
9 M. Bourstyn, *Bull. Soc. Chim. France*, 8 (1941) 533.
10 W. M. Latimer, *Oxidation Potentials*, Prentice-Hall, New York.
11 J. H. Faull, Jr., *J. Am. Chem. Soc.*, 56 (1934) 522.
12 R. Guidelli and G. Piccardi, *Electrochim. Acta*, in press.

ELECTROANALYTICAL CHEMISTRY AND INTERFACIAL ELECTROCHEMISTRY
Elsevier Publishing Company, Amsterdam – Printed in The Netherlands

PROBLEMS IN THE POLAROGRAPHY OF CHROMATE

I. R. MILLER
Polymer Department, Weizmann Institute of Science, Rehovot (Israel)
(Received November 14th, 1966)

INTRODUCTION

The first systematic studies of the polarography of chromate as a function of pH were made by LINGANE AND KOLTHOFF[1]. They found four distinct waves with half-waves in the potential regions: I—0.35 V; II—1.0 V; III—1.5 V; IV—1.7 V relative to the normal calomel electrode (NCE), at pH = 7. In region IV, the chromate is reduced by six electrons to metallic chromium, whereas in regions II and III, three and four electrons, respectively, take part in reducing the chromate to the trivalent or bivalent chromium ion. As regards region I, where the diffusion current is not proportional to the chromate concentration, these authors assumed the formation of insoluble layers of chromium hydroxide which impede the current, and discarded previous assumptions of the possibility of intermediate degrees of reduction. Their results were in accordance with the theoretical linear increase in diffusion current as a function of concentration in the presence of 0.1 and 1.0 *N* NaOH at potentials above −0.8 and −0.7 V relative to NCE, respectively. They assumed that the reduction product under these conditions is the more soluble anionic form of trivalent chromium, CrO_2^-.

The conclusions of KOLTHOFF AND LINGANE were criticized by GIERST *et al.*[2,3] on three main grounds.

1. These authors claimed that the theoretical diffusion current cannot be achieved even at extremely low chromate concentration. If an insoluble product were responsible for the reduction in the diffusion current, such a result would however be expected.

2. The reduction in diffusion current is even more pronounced at alkaline pH than it is in neutral solution, if the ionic strength is sufficiently low. The increase in NaOH concentration is equivalent to an increase in the ionic strength; both shift the *principal wave*, the term coined by GIERST *et al.* for wave II, toward more positive potentials.

3. The existence of an insulating layer on the mercury surface is not indicated by typical irregularities in current oscillations, as is usually observed in similar cases.

The first claim is substantiated only in the case of strongly alkaline solution. At pH 7, as will be shown later (Fig. 2), the current in region I becomes equal to that in region II at a chromate concentration of $2 \cdot 10^{-5}$ *M* or lower. In the presence of 0.01 *N* Na_2CO_3 + 0.1 *N* $NaNO_3$, the current in region I does not reach the theoretical value even when the chromate concentration is as low as 0.2×10^{-5} *M*; the ratio of current to concentration, however, increases with decreasing chromate concentration.

The second argument is essentially correct. The estimate of the potential ψ_δ neglecting any possible adsorption of chromium in any form, in the Frumkin relation[4,5]

$$k = k_0 \exp(\alpha n F/RT)[-\phi-(Z_A/n-1)\psi_\delta] \quad (1)$$

is, however, questionable. In this relation:

k is the rate constant of the electrode process;
k_0 is the rate constant when the value of the exponent is zero;
α is the transfer coefficient;
n is the number of electrons participating in the rate-controlling step;
ϕ is the polarization potential of the electrode (referred to, for convenience, as the potential difference from the electrocapillary maximum);
Z_A is the charge of the depolarizer;
ψ_δ is the potential prevailing at a distance, δ, from the surface at which the electroreduction occurs.

The third argument which refers to the shape of the current–time curves, is very weak, as it neglects the consideration that the dependence of the current on the growing thickness of the insoluble layer and on its charge may vary in different cases.

The object of the present study is to investigate the existence of an insoluble layer at the electrode surface by solubilization experiments. If the current is impeded by an insoluble layer, it should be possible to restore the theoretical diffusion current by solubilizing this layer. In principle, a subsequent reaction is being considered. A preceding reaction, $CrO_4^{2-} \rightarrow HCrO_4^-$, postulated by GREENS AND WALKLEY[6] may exist, but should contribute only negligibly to the amplitude of the "prewave". The significance of the part played by any preceding reaction, $CrO_4^{2-} \rightarrow HCrO_4^-$, in reducing the current in the pre-wave is considered doubtful for three reasons:

1. Addition of EDTA increases the current amplitude of the prewave even at alkaline pH, where its only action is solubilization of the insoluble chromium layer by complex formation.

2. Polyelectrolytes at minute concentrations that could not possibly affect this reaction have, when adsorbed on the surface, a very marked effect on the measured currents.

3. The peak on the prewave, which never exceeds the value of the theoretical diffusion current, cannot be explained by postulating a preceding reaction without assuming increased reaction rates when the surface active chromate is adsorbed. It is, however, in keeping with the concept of an insoluble layer being displaced from the surface by the chromate ion.

EXPERIMENTAL

The polarographic measurements were carried out using a Shimadzu RP2 polarograph. Large drop-times ($\sim$15 sec) were employed in order to better record the events occurring on the mercury surface.

Sodium chromate, the supporting electrolytes, and EDTA employed in these experiments were of analytical grade. In part of the experiments, the following polyelectrolytes were employed: Calf thymus deoxyribonucleic acid (DNA), was purchased from Worthington Co. and degraded by sonication. The preparation of copolymer of 4-vinylpyridine with methacrylic acid (VPMA) at a monomolar ratio

of 4:6 and of poly-4-vinylethylpyridonium bromide (PVEPB), is described elsewhere[7]. The copolymer of lysine with glutamic acid (LGA), at a monomolar ratio of ~1.5:1 (L to GA) was obtained from the Biophysics Department. The diffusion coefficients determined in a Spinco Model E ultracentrifuge using a synthetic boundary cell[8], were $D_{DNA} = 9.2 \times 10^{-8}$ cm^{2}sec^{-1}; $D_{VPMA} = 3.25 \times 10^{-7}$ cm^{2}sec^{-1}; $D_{PVEPB} = 10^{-7}$ cm^{2}sec^{-1}; $D_{LGA} = 4.9 \times 10^{-7}$ cm^{2}sec^{-1}. The diffusion coefficient determinations were carried out in neutral medium for DNA, and in alkaline media for the other polyelectrolytes.

RESULTS

Polarography of chromate at neutral pH in unbuffered solution

The half-wave potential of the prewave was found to be independent of the concentration of $NaNO_3$ which served as supporting electrolyte (Fig. 1). The peak decreased as a function of ionic strength, until at 0.5 *N* $NaNO_3$ it vanished. It seems that even the weakly surface-active NO_3^- at high concentration interferes with the

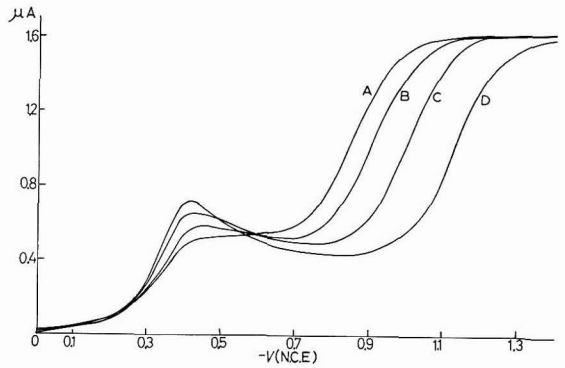

Fig. 1. Polarograms of chromate in unbuffered soln. at pH 6.5 for different concns. of supporting electrolyte. (A) 0.6, (B) 0.3, (C) 0.1, (D) 0.03 *N* $NaNO_3$.

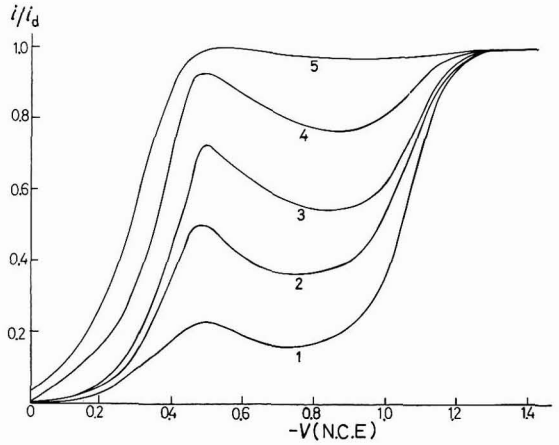

Fig. 2. The ratio of the current to the theoretical diffusion current (i/i_d) against potential in neutral non-buffered soln. Concn. of chromate: (1), $2 \cdot 10^{-3}$; (2) $5 \cdot 10^{-4}$; (3), $2 \cdot 10^{-4}$; (4), $5 \cdot 10^{-5}$; (5), 10^{-5} *M*.

specific adsorption of chromate. The salt concentration has, at most, only a negligible effect on the amplitude of the prewave, in contradistinction to the behavior at alkaline pH. If there is an insoluble or adsorbed layer of the products of the electrode process, it does not carry sufficient charge at neutral pH to affect appreciably the transport of ions. There is, however, a shift with salt concentration in the half-wave potential of the principal wave. It is about 30% smaller than that which occurs at pH 12, indicating a lower charge density on the surface layer at neutral pH. It is difficult to decide conclusively whether the half-wave potential shift is ascribable only to the effect of salt on the potential of the diffused double layer or also to screening of the charges of the chromate ion. The marked specific effect of the cations suggests, however, that the second mechanism may be of importance.

The ratio, i/i_d, (Fig. 2) decreases with increasing chromate concentration, the effect being most pronounced in the minimum current region of the "prewave". At chromate concentrations lower than $2 \cdot 10^{-5}$ M, the "prewave" merges with the prin-

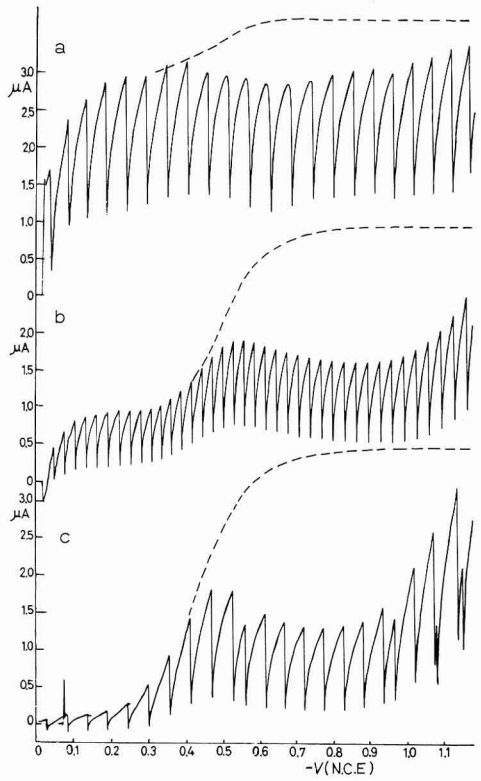

Fig. 3. Effect of EDTA on the polarograms of $5 \cdot 10^{-4}$ M chromate in non-buffered 0.1 N $NaNO_3$. Concn. of added EDTA (at pH 6.4): (a), 0; (b), $5 \cdot 10^{-4}$ M; (c), $3 \cdot 10^{-3}$ M.

cipal wave, the peak disappears, and the polarogram levels off. The addition of EDTA, which forms complexes with Cr^{3+} and has its maximal buffering capacity at pH 6.2,[9] may cause solubilization of the insoluble film of chromium hydroxide if any has formed. Solubilization may be achieved by lowering the pH in the surface as

well as by direct binding of Cr^{3+} by EDTA. The rise of current in the "prewave" until the diffusion current values of the principal wave are reached (as shown in Fig. 3) can be brought about by this solubilization process.

At a chromate concentration of $5 \cdot 10^{-4}$ *M* or higher, Cr–EDTA, which is the product of the surface reaction, tends to become adsorbed at the surface and hence affect the shape of the current–time curves. Cr–EDTA is not adsorbed on a pure mercury surface at these polarization and concentrations either at neutral or alkaline pH. At alkaline pH, no adsorption phenomena are observed even when the electroreduction of chromate is carried out in the presence of much higher chromate concentrations. The conclusion is inevitable, therefore, that Cr–EDTA is adsorbed on a surface which differs in its properties from the pure mercury surface and that the $[OH^-]$ ions, which are a product of the electrode process:

$$HCrO_4^- = 3\ H_2O + 3\ e \rightarrow Cr(OH)_3 + 4\ OH^- \qquad (2)$$

are not responsible for the enhancement of adsorption of Cr–EDTA at higher concentrations of chromate.

Another effect of addition of EDTA on the polarographic behavior of chromate is observed in the potential region between 0 and -0.3 V relative to NCE. A new wave appears in this region, evidently caused by a preceding reaction.

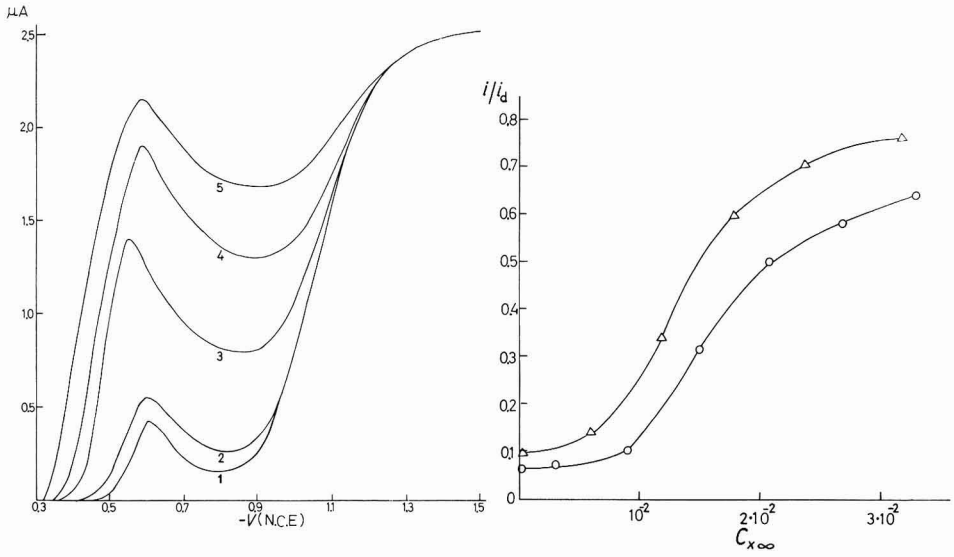

Fig. 4. Effect of EDTA on the polarogram of $5 \cdot 10^{-4}$ *M* chromate at pH 11 and 0.1 *N* $NaNO_3$: (1), no EDTA; (2), $9 \cdot 10^{-3}$; (3), 1.5×10^{-2}; (5), 3.3×10^{-2} *M* EDTA.

Fig. 5. i/i_d for $5 \cdot 10^{-4}$ *M* chromate at -0.85 V relative to NCE against concn. of added EDTA. Supporting electrolytes: (○), 0.1 *N* $NaNO_3$; (△), 1 *N* $NaNO_3$.

At alkaline pH, EDTA does not have a buffering effect and can influence the polarographic current only *via* its effect on the adsorbed layer on the mercury surface. Figure 4 shows the augmentation of the polarographic current on addition of EDTA at pH 11.5. Also, EDTA causes a shift in the half-wave potential of the prewave toward more positive values, presumably by lowering the equilibrium concentration

of free Cr^{3+} near the surface. The concentration of EDTA required to bring about the same increase in current is considerably larger in alkaline than in neutral solutions. EDTA is also more effective at higher ionic strength (Fig. 5) which is in accordance with the concept of interaction between a negatively charged molecule and a negatively charged surface. This interaction results in the removal of negatively charged substance from the surface. In any other situation, *e.g.*, adsorption of EDTA, further reduction rather than an augmentation of the polarographic current should be expected. It can be seen in Fig. 5 that the plots of (i/i_d) *vs.* concentration of added EDTA are of sigmoidal shape. The augmentation of the current due to the addition of EDTA is weak below a certain concentration and increases more rapidly with EDTA from EDTA concentrations of about 1.2×10^{-2} and 1.5×10^{-2} M for 1 and 0.1 N $NaNO_3$, respectively. Probably the EDTA does not cause any appreciable increase in the current until it reduces the surface charge by solubilization to a significant extent.

It should be noted that at alkaline pH values the addition of EDTA does not cause the appearance of the wave at -0.05 V as might be expected (Fig. 4).

Effect of added polyelectrolytes on the "prewave"

The polyelectrolytes used in these experiments are surface active to a varied degree. They affect the polarographic currents only if adsorbed. Native DNA is very weakly surface active, but its adsorption on the surface is considerably enhanced by denaturation. At neutral pH, native DNA affects the amplitude of the prewave as well as the current–time relation only at chromate concentrations above 10^{-4} M. At high chromate concentrations, it affects the current even in the presence of excess EDTA, which has a buffering activity at neutral pH. This excludes the possibility that the $(OH)^-$ ions evolved in the electrode process cause denaturation of DNA prior to its adsorption. The adsorbability of all the negatively charged polyelectrolytes employed in these experiments increased with ionic strength; at ionic strength lower than $I = 0.01$, no effect of the negatively charged polyelectrolytes on the polarographic current could be detected.

In Fig. 6, the relation between the adsorption of denatured DNA at neutral pH and its effect on the instantaneous current, is demonstrated in the current–time curves. At brief times corresponding to small surface concentrations, the adsorbed DNA augments the instantaneous current, which reaches its maximum value when about two-thirds of the surface is covered by DNA, as estimated from the amount adsorbed, Γ, calculated by the relation[10]

$$\Gamma = 0.743\, D^{1/2} t^{1/2} C_{DNA} \qquad (3)$$

After the maximum value is attained, the impeding effect of the adsorbed DNA becomes noticeable. Only after full saturation, when polymolecular adsorption may be reached[11], does the instantaneous current in the presence of DNA assume values that are lower than in the presence of the same concentration of chromate without any additives. However, if the current is raised by adding EDTA at any pH, or buffer at pH values below pH 7, the subsequent addition of DNA always reduced the current. We suggest, as the most plausible interpretation of these results, that the adsorbed DNA molecules bind the chromium ions in their domain, leaving the depleted holes of low resistance in the chromium hydroxide layer. It should be borne in mind that DNA has a very low buffering capacity below pH 8.5 and cannot

cause an increase in the diffusion current by neutralization of the $(OH)^-$ evolved in the electrode process. Moreover, the evolved $(OH)^-$ is about fifty times the equivalent of the adsorbed DNA. Thus unlike EDTA, DNA does not affect the current by a precedent reaction at potentials positive relative to the prewave.

The effect of the adsorbed polyelectrolytes is even more pronounced at alkaline pH. It seems surprising that adsorption of negatively charged polyelectrolytes greatly enhances transport of the depolarizer across the surface layer (Fig. 7). It is difficult

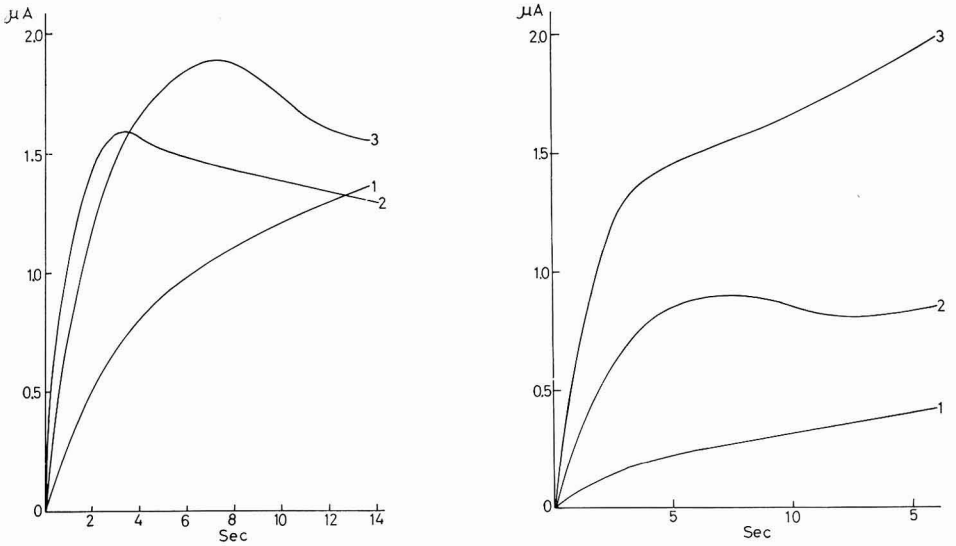

Fig. 6. Current–time curves for $5 \cdot 10^{-4}$ M chromate in the presence of non-buffered 0.1 N KNO_3 soln. and various concns. of added DNA: (1), no DNA; (2) 1.53×10^{-4} mequiv./ml; (3), 0.76×10^{-4} mequiv./ml.

Fig. 7. Current–time curves for $5 \cdot 10^{-4}$ M chromate at -0.9 V relative to NCE in the presence of 0.03 N Na_2CO_3 and different negatively charged polyelectrolytes: (1), no polyelectrolyte; (2), 0.3 mg/ml LGA; (3), 0.25 mg/ml VPMA.

to determine whether the adsorbed polyanion acts here by binding the chromium or by locally increasing the ionic strength near the surface. From the full polarograms it seems, however, that the first mechanism is the more likely, as the adsorbed polyanions do not shift the principal wave as would be expected from the variation in ionic strength[3].

Polycations increase the amplitude of the prewave at even lower surface concentrations than do polyanions. In the case of PVEPB, the full diffusion current at drop-times greater than 10 sec is only recovered at about half-saturation of the surface, while at shorter drop-times, the smaller surface concentrations of PVPEB attained[10] suffice for full current recovery (Fig. 8). In this case, inversion by the adsorbed cation of the surface charge on the surface layer, which is composed to a large extent of CrO_2^-, seems to play a predominant role in the enhancement of the chromate transport to the electrode. However, the possibility of binding of CrO_2^- by the polycation and hence hole formation in the surface layer cannot be excluded.

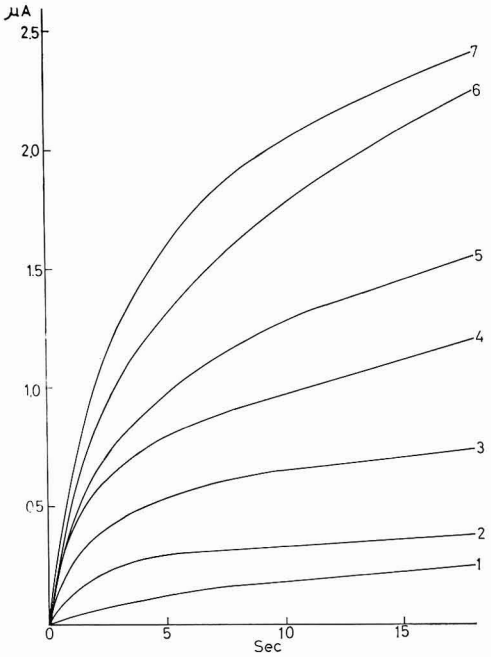

Fig. 8. Current–time curves at −0.9 V relative to NCE for $5 \cdot 10^{-4}$ *M* chromate in the presence of 0.1 *N* Na_2CO_3 and various concns. of quaternized poly-4-vinylpyridine (PVEPB). (1), no PVEPB; (2), 2.5×10^{-5}; (3), $5 \cdot 10^{-5}$; (4), 7.5×10^{-5}; (5), 10^{-4}; (6), 1.75×10^{-4}; (7), $3 \cdot 10^{-4}$ eq/l PVEPB.

DISCUSSION

1. *Dependence of the amplitude on the prewave in neutral solutions*

The effect on the diffusion current of a thin layer of constant thickness near the surface has been discussed previously[12]. The concentration ratio of the depolarizer on each side of the boundary between the thin layer and the bulk was given by the distribution coefficient, κ, and the diffusion coefficients in the thin layer and in the bulk were D_{II} and D_I, respectively. In the present case, we introduce the additional boundary condition that the thickness of the layer is not constant, but increases with the amount of reduction product deposited on the electrode, namely:

$$\frac{d\delta}{dt} = \frac{\bar{v}}{A_t}\frac{dN}{dt} = -\frac{\bar{v} i_t}{A_t n F} \tag{4}$$

where δ is the thickness of the layer at time t, N is the number of moles of depolarizer crossing the surface and $\bar{v}$ is the partial molar volume of the product in the layer. A_t is the surface area at time t. Equation (13) of ref. 12 assumes, with this boundary condition, the following form:

$$i_t = 7.08 \times 10^4 n m^{2/3} t^{1/6} D_I^{1/2} B_I = n F \sigma B_I \tag{5}$$

where m is the rate of flow of mercury in g/sec, n is the number of electrons participating in the reduction process, F is a Faraday unit.

$$B_I = C_\infty / [1 + \{(\delta - \delta_0)/\kappa D_{II}\} (D_I/\pi t)^{1/2}] \tag{6}$$

where C_∞ is the concentration of the depolarizer in the bulk of the solution and δ_0 is the thickness of a part of the surface layer which is fully permeable to the depolarizer. Introducing the value of δ in eqn. (6) from eqn. (4) and inserting into eqn. (5), we obtain for the instantaneous current:

$$i_t = nF\sigma C_\infty / [1 + (D_I^{1/2}/\pi^{1/2}t^{1/2}\kappa D_{II})\{(\bar{v}/nFA_t)\int_0^t i\mathrm{d}t - \delta_0\}] \tag{7}$$

However, the numerator in eqn. (7) is the ideal diffusion current, i_t^0, without any impending barrier. Hence:

$$(i_d/i_t) = 1 + (\beta/nFA)\int_0^t i\mathrm{d}t - \delta_0/\bar{v}] \tag{8}$$

where

$$\beta = (D_I/\pi t)^{1/2}(\bar{v}/\kappa D_{II})$$

Fig. 9, (i_d/i_t) is plotted against $\int_0^t i\mathrm{d}t/nFA$. A straight line is obtained at values of (i_d/i_t) above 1.5. The value of $\int_0^t i\mathrm{d}t/nFA$ at the intercept of the straight line with the line $(i_d/i_t) = 1$, corresponds to $(\delta_0/\bar{v})$. From here $(\delta_0/\bar{v}) = 2 \cdot 10^{-9}$, which means that for crystalline chrome oxide where $\bar{v}$ per chromium atom is 15 cm^3, $\delta_0 = 3$ Å, whereas for a highly hydrated chromium hydroxide when $\bar{v} = 100$, δ_0 would be 20 Å.

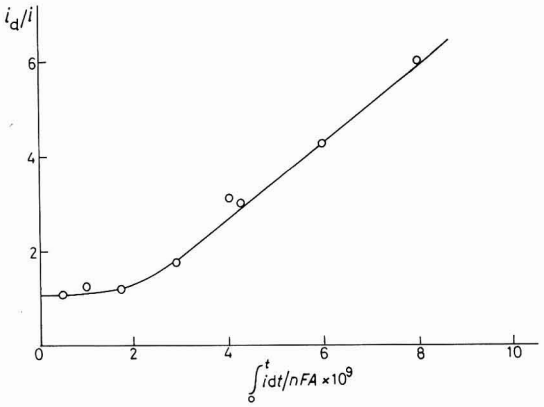

Fig. 9. The ratio of the theoretical instantaneous diffusion current to the measured current (i_d/i) against $\int_0^t i\mathrm{d}t/nFA$.

The value of β obtained from the slope of the straight line is $8 \cdot 10^8$ from which the value obtained for the product $(\bar{v}/\kappa D_{II})$ is about $2 \cdot 10^{12}$. It is impossible to separate the parameters of their product.

In this treatment, the effect of the surface charge of the thin layer on the current has not been considered. However, the values of κ, and therefore also of β, depend on the electrical potential, which is likely to increase with the thickness of the layer formed due to increased alkalinity near the surface brought about by the electrode process (eqn. 2). As κ is expected to decrease with increasing negative

potential of the surface layer, the lower values of β obtained at the higher concentrations of chromate are qualitatively reasonable.

2. *Solubilization of the insoluble film by a complexing agent buffering*

Consider first the solubilizing effect due to buffering action alone. In this model, we assume that the equilibria (eqns. 9 and 10) near the surface are instantaneously established and that the diffusion of the reactants to the surface and away from it are rate-determining in the dissolution process.

$$[Cr^{3+}][OH^-]^3 = K_1 \tag{9}$$

$$\frac{[OH^-][\text{Buf H}]}{[\text{Buf}^-]} = K_2 \tag{10}$$

An insoluble film is formed if the rate of film formation is larger than its dissolution.

If the rates are diffusion-controlled, assuming equal diffusion coefficients for chromate and chromium hydroxide, an insoluble film is formed when $(C_\infty - C_\delta) > [Cr^{3+}]_\delta$.

For $K_1 = 0.5 \times 10^{-30}$ [13], insoluble films should thus be formed in well-buffered 10^{-3} M chromate solutions above pH 5. In fact, formation of insoluble films is not observed up to pH 7. In carbonate[6] or phosphate buffer, and at a chromate concentration of $5 \cdot 10^{-4}$ M, (i/i_d) in the "prewave" is less than 1 at pH-values above 7. It is possible, however, that even below this pH an insoluble film is formed which is swollen or leaky enough to be permeable to ions. The higher negative charge on the insoluble film at the higher pH values may also contribute to its lower permeability to chromate. Under these circumstances, no simple model is likely to explain quantitatively the solubilizing action of buffering substances. Solubilization by complexation alone will occur if the complexing agent has no buffering activity, or a buffering activity only in the pH region in which the film is in any event insoluble. The rate of formation of the film under these conditions is

$$\frac{A_t}{\bar{v}_t}\frac{d\delta}{dt} = [i_t/nF - kC_{y,\delta}] \tag{11}$$

where k is the complexation rate near the surface and the index, y, indicates the complexing agent. The complexing agent diffuses to the surface, forms a complex at a rate $kC_{y,\delta}$ and the complex formed then diffuses back into the solution. This is equivalent to a totally irreversible polarographic process which has been dealt with by many authors. According to DELAHAY[14]

$$C_{y,\delta} = C_y{}^0 \exp(k^2 t/D_y)\ \text{erfc}(kT^{1/2}/D_y{}^{1/2}) \tag{12}$$

where D_y is the diffusion coefficient of the complexing agent and $C_y{}^0$ is its concentration in bulk. For $kT^{1/2}/D_y{}^{1/2} \ll 1$, eqn. (14) gives $C_{y,\delta} \to C_y{}^0$.

For additional boundary conditions, the value of B_1 in eqn. (5) becomes

$$B_1 = C_0/[1 + \beta\left(\frac{\int_0^t i\,dt}{nFA} - \frac{\delta_0}{\bar{v}} - \frac{kC_y{}^0 I_t}{A}\right) \tag{13}$$

where

$$I_t = \int_0^t \exp(k^2 t/D_y)\ \text{erfc}(kT^{1/2}/D_y{}^{1/2})\,dt \tag{14}$$

The third term in the denominator on the right-hand side of eqn. (13), which stands for the dissolution of the insoluble layer, may never exceed the second term which stands for its formation. However, EDTA in non-buffered solution solubilizes not only by its complexing action but also as a result of its buffering capacity, and the calculated $C_{y\delta}$ is not proportional to $C_y{}^0$ as is required by eqn. (12).

3. *Evolution of the reduction wave of H_2CrO_4 in the presence of excess buffering agent*

The most likely precedent reaction is:

$$HCrO_4^- + H^+ \underset{k_2}{\overset{k_1}{\rightleftharpoons}} H_2CrO_4 \tag{15}$$

The rate constants of the precedent reaction in the presence of excess buffer can be obtained from the reduction in the instantaneous current:

$$i/i_d = F(\chi) \tag{16}$$

According to KOUTECKÝ[15,16], for a large ratio of dissociation constant K, to $[H^+]$, $(K/[H^+] \gg 1)$

$$k_2 = (K^2\chi^2/[H]^2)\ (7/12\ t) \tag{17}$$

The values of χ are tabulated by KOUTECKÝ as function of $F(\chi)$. At pH-values between 7 and 8.2, in the presence of 0.04 N phosphate buffer and 0.1 N KNO_3 and with $t = 10$ sec, we obtained for $\chi/[H^+]$ the value $(7 \pm 3) \cdot 10^{10}$ cm^3mol^{-1}. For reaction (15) ($K \simeq 3 \cdot 10^{-4}$ mole cm^{-3})[13], the rate constant of dissociation calculated from eqn. (17) is about $3 \cdot 10^{13}$ cm sec^{-1} and $k_1 \simeq 10^{10}$ cm^3sec^{-1}.

If the buffer concentration is of the order of that of the depolarizer, as in the case illustrated in Fig. 2, the rate constant of the precedent reaction can be obtained from the equations derived by ČIŽEK *et al.*[17]. The reaction in this case is:

$$\begin{array}{lll} HCrO_4^- + XH_2^{2-} \underset{k_2}{\overset{k_1}{\rightleftharpoons}} XH^{3-} + H_2CrO_4 & & \text{(a)} \\ \qquad\qquad\qquad\qquad\qquad\qquad \Big\downarrow 3e + 2H_2O & & \\ \qquad\qquad\qquad\qquad\qquad\qquad Cr(OH)_3 + 3\ OH^- & & \\ 2\ XH_2^{2-} + 3\ (OH)^- \underset{k_4}{\overset{k_3}{\rightleftharpoons}} 3\ XH^{3-} + 3\ H_2O & & \text{(b)} \end{array} \tag{18}$$

and as can be seen, it includes a precedent reaction (a) and a parallel reaction (b).

Significance of the principal wave

According to our conclusions, CrO_4^{4-} may be reduced in the whole potential region starting at about -0.3 V relative to NCE. The principal wave (according to the term coined by GIERST *et al.*[2,3]) which is very sensitive to salt concentration, cannot be simply the reduction of CrO_4^{2-} as suggested by these authors. An alternative possibility is that the difference between the "prewave" and the "principle wave" is not related to the form of the depolarizer but to the location of the reduction process. While in the "prewave", CrO_4^{2-} and $HCrO_4^-$ are reduced at the mercury surface after penetration through the adsorbed layer, the reduction process of the principle wave takes place on the boundary between the adsorbed layer and the bulk solution. The reduction rate at this boundary is a function of the potential on the site of the

depolarizer. This potential is a sum of the contributions of the surface layer and the charges of the depolarizer itself. The ionic strength has an effect on both components of the potential.

The potential of the boundary is a function of pH. The conductance of the surface layer as well as its porosity and surface potential can be modified by incorporation of organic surfactants and polyelectrolytes.

It is possible that the penetration of $HCrO_4^-$ through the layer to the surface is faster than that of CrO_4^{2-}. In this case the preceding reaction, $CrO_4^{2-} \rightarrow HCrO_4^-$ may be of importance.

ACKNOWLEDGEMENTS

The help of Miss D. BACH and Mr. H. GRAET in carrying out this work is gratefully acknowledged.

SUMMARY

The mechanism of electroreduction of chromate was investigated by applying complexing agents and polyelectrolytes that bind trivalent chromium (the electroreduction product) thus affecting the current in the polarographic prewave. It was found that amounts of adsorbed polyelectrolytes so minute as to be insufficient to affect any preceding reactions, caused an increase in the polarographic current, until, under suitable conditions, the theoretical diffusion current could be recovered. Similar augmentation of the current was observed when agents that could solubilize the barely soluble layer possibly formed by the products of the electrode process, were added. It was concluded that the thin layer formed near the surface is responsible for reducing the polarographic current in the prewave. Its impeding effect is a function of its structure, thickness and charge.

REFERENCES

1 J. J. LINGANE AND I. M. KOLTHOFF, *J. Am. Chem. Soc.*, 62 (1960) 852.
2 L. GIERST, *Electrochemical Society Symposium on Electrode Processes, 1959*, Abstr. No. 176.
3 J. J. TONDEUR, A. DOMBERT AND L. GIERST, *J. Electroanal. Chem.*, 3 (1962) 225.
4 A. N. FRUMKIN, *Z. Elektrochem.*, 59 (1955) 807.
5 A. N. FRUMKIN, *J. Electrochem. Soc.*, 107 (1960) 461.
6 J. H. GREENS AND A. WALKLEY, *Australian J. Chem.*, 8 (1955) 51.
7 D. BACH AND I. R. MILLER, *Biochim. Biophys. Acta*, 114 (1966) 311.
8 E. DANIEL AND Z. ALEXANDROWICZ, *Biopolymers*, 1 (1963) 473.
9 A. I. VOGEL, *A Textbook of Quantitative Inorganic Analysis*, Longmans Green, London, 3rd ed., 1961.
10 J. KORYTA, *Collection Czech. Chem. Commun.*, 18 (1953) 597.
11 I. R. MILLER AND D. BACH, *Biopolymers*, 4 (1966) 705.
12 I. R. MILLER, *J. Phys. Chem.*, 69 (1965) 2740.
13 *Gmelins Handbuch*, 8th ed., Part B, 52 (1962) 145.
14 P. DELAHAY, *New Instrumental Methods in Electrochemistry*, Interscience Publishers Inc., New York, 1954.
15 J. KOUTECKÝ, *Collection Czech. Chem. Commun.*, 18 (1953) 597.
16 J. KOUTECKÝ AND J. KORYTA, *Electrochim. Acta*, 3 (1961) 318.
17 J. ČIŽEK, J. KORYTA AND J. KOUTECKÝ, *Collection Czech. Chem. Commun.*, 24 (1959) 3944.

ELECTROANALYTICAL CHEMISTRY AND INTERFACIAL ELECTROCHEMISTRY
Elsevier Publishing Company, Amsterdam – Printed in The Netherlands

THE POLAROGRAPHY OF AQUEOUS PERTECHNETATE ION

CHARLES L. RULFS, RICHARD PACER AND ALFRED ANDERSON
Department of Chemistry, University of Michigan, Ann Arbor, Michigan (U.S.A.)
(Received November 10th, 1966)

The electrochemical and polarographic behavior of aqueous pertechnetate media is rather complex[1-3], yet it is probably not as anomalous as has been suggested[4,5]. Macro-electrolysis from non-complexing acidic media leads to partial electrodeposition of technetium metal with some separation of technetium dioxide[6,7]. The polarographic and coulometric behavior of pertechnetate in sulfuric acid is compatible with this, and hydrochloric acid is only slightly more "complexing" in character[1,8]. In complexing or non-complexing, acidic to neutral media, the expected three- or four-electron first stage of pertechnetate reduction occurs at relatively positive potentials and this fact has been established coulometrically[1,2,8-10]. The rapidity of the chemical reduction of acidic pertechnetate in contact with mercury has been noted[1,8,10], but does not appear to have been recognized in many of the polarographic papers[3,4,14].

COLTON *et al.*[4] have calculated apparent polarographic n-values for pertechnetate reductions in KCl, perchloric acid and other media, which include the following approximations (with generalizations on their validity):

(a) Use of the classical Ilkovič equation (leads to *ca.* 10% error in n)[3].

(b) Use of infinite-dilution D°-values (actual D may be $\pm 20\%$ different).

(c) Use of an obsolete value of D^0 for ReO_4^-, 1.37×10^{-5} cm^2 sec^{-1}, used for TcO_4^- by analogy (1.46 preferable since 1948, but 1.48 has now been measured for TcO_4^-)[11,12].

(d) Use of a "constant" value of $(m^{\frac{2}{3}}t^{\frac{1}{6}})$ for waves at potentials of $E_{\frac{1}{2}}$ -0.5 to -1.8 V (typically, there is about 7% variation over this range).

The conclusions based on this early work have been restated[5] with little attention to subsequent coulometric evidence. Another author[13] notes the disagreement in the literature and cites the conflicting results. This degree of confusion appears to be unwarranted, since several sets of authors[1,2,8,9] have explored and defined the conditions for useful polarographic and coulometric measurements of technetium. The claim[4,5] that, while perrhenate in 4 M perchloric acid is reduced by three electrons at -0.4 V (and pertechnetate should undergo a similar reduction at more positive potential) pertechnetate showed no reduction prior to the supporting electrolyte discharge (about -1.0 V), is surprising. Claimed reductions[4,5] of (VII $\rightarrow$ VI) and (VI $\rightarrow$ IV) in 4 M HCl at -0.52 and -0.68 V, appear to be incompatible with coulometric evidence[1,8] for a four-electron reduction at much more positive potentials.

Pertechnetate reductions in hydrochloric and in sulfuric acids have been studied and reported in some detail[1,8]. A re-examination of the system in perchloric

acid media seemed to be desirable. The nature of technetium "amalgam" has also been examined briefly.

EXPERIMENTAL

A conventional dropping mercury electrode assembly was used with a manual polarograph, the Fisher Elecdropode. All potentials measured are relative to the saturated calomel electrode, using agar-salt bridges to lessen the contamination of test solutions by Cl^-. A hydrogen–oxygen gas coulometer was used with a large mercury pool coulometric cell. The effluent from purging acidic solutions with purified N_2, contains a little $HTcO_4$ which is trapped in alkali. Details of the equipment and of the requisite precautions for coulometry have already been given[1,8,10].

Ammonium pertechnetate solutions of good purity were obtained from Oak Ridge National Laboratory. Concentrations were checked by ultraviolet spectrophotometry at the 246 mμ doublet and at 287.5 mμ (ε=6,160 and 2,316).

A small decade scaler and thin-wall Geiger tube sufficed for the simple relative-counting of ^{99}Tc.

A size 2 International Centrifuge was used. The accessories and the loading employed, gave an estimated angular velocity of 314 rad./sec and an effective arm length of 23 cm.

The dropping technetium "amalgam" electrode was freshly prepared *in situ*. Acidic aqueous pertechnetate was electrolysed, at 5–6 V with stirring, into a pool of mercury in the reservoir. After 30–40 min and without removal of the aqueous layer or breaking of the current, about 25 ml of mercury was discarded from a side tube located just above the D.M.E. capillary. This brought fresh amalgam immediately down to the active electrode region for the polarographic testing. The arrangement was tested with cadmium amalgam and behaved as expected. The amalgam flow eventually slows and tends to plug the capillary, but not before meaningful tests can be run.

RESULTS AND DISCUSSION

The average n-value of 8.54 obtained by COLTON *et al.*[4] for pertechnetate reduction in 2 M KCl is close to 7 (6.8), if the latest value of $D_{TcO_4^-}^0$ is used. Probably no great importance should be placed on this fact in view of the remaining uncertainties in such a calculation, and of the discordant results reported by ASTHEIMER AND SCHWOCHAU[3] for similar media. In neutral LiCl for example, these authors claim an earlier step for the (VII $\rightarrow$V) reduction and the n=7 level does not lie on a plateau.

It appears to be well established by coulometry[1,8] that a four-electron reduction of acidic pertechnetate occurs at positive potentials, although in 4 M HCl the potential only represents that which is permitted by the anodic calomel discharge at the D.M.E. A subsequent reduction to metal is found at -0.9 V. The contrary report[4,5] of ill-defined (VII) $\rightarrow$(VI) and (VI) $\rightarrow$(IV) waves at -0.5 and -0.7 V apparently results from two factors:

(1) Prior chemical reduction of most of the (VII) by mercury to form intermediate-state species.

(2) Failure to examine the region of positive potential for remaining (VII).

The use of 0.25 *M* K_2SO_4 or 0.5 *M* KCl *with* 0.1 *M* KOH, gave a (VII) $\rightarrow$ (IV) wave at -0.8 V and a (IV) $\rightarrow$ (III) step at -1.0 V. This interpretation[1,8] of the steps is supported by coulometric work and should probably, but not necessarily, replace the alternative interpretation[4,5] (based on *D* and the Ilkovič) given for 0.1 *M* KOH alone. The latter reports (VII) $\rightarrow$ (V) and (V) $\rightarrow$ (IV) processes at -0.85 and -1.15 V, respectively. The first group did *not* find the second wave to be pure diffusion-limited which would invalidate the calculation of *n via* the Ilkovič equation.

Pertechnetate solution (0.5–0.1 m*M*) in a series of 4–0.01 *M* (the latter, with *ca.* 0.1 *M* $NaClO_4$) perchloric acid media were de-aerated *in the absence of mercury*. Polarography at the dropping mercury electrode was then conducted as expeditiously as possible. After a polarographic run, the solution and accumulated mercury were shaken intermittently for 5 min in a weighing bottle, returned to the cell and de-aerated together for 5 min more, and then re-examined polarographically.

Two successive stages of reduction are observed. The position of Wave I shifts from an apparent $E_{\frac{1}{2}}$ of *ca.* $+0.05$ V to -0.17 V, as a function of pH. Its slope indicates irreversibility, and its magnitude (*in the absence* of significant pre-reduction by mercury) is greater than that of the less reproducible, second wave. The smaller, more negative Wave II is found at -0.58 to -0.73 V. Its position seems to drift to more negative values with increase in pH. This wave is less well-defined, however, tending to merge with the subsequent discharge of hydrogen ion. Moreover, we suspect that its position is partly defined by the extent to which *a priori* intermediate technetium-states have been formed from chemical reduction with the mercury. Its slope is irreversible for a more than one-electron process.

With solutions more concentrated than 0.1 *M* in $HClO_4$, contact with mercury before polarography can result in an extensive decrease in Wave I. With 4 *M* $HClO_4$,

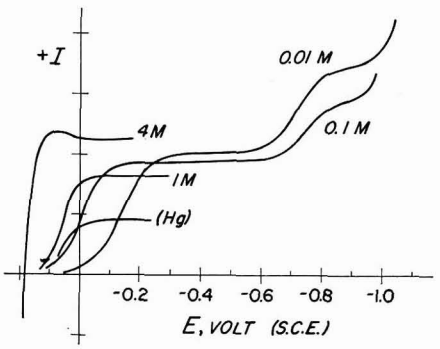

Fig. 1. Polarographic behavior of pertechnetate ion in various concns. of $HClO_4$ (0.01 *M* includes 0.10 *M* $NaClO_4$). The effect of pre-contact with Hg is shown for the 1 *M* medium.

however, the solubility of the mercury salts resulting from this prereduction yields an extensive cathodic current, extending from the most positive potential permitted by the anodic mercury discharge. The general appearance of the waves is shown in Fig. 1.

Coulometry in 0.5 *M* $HClO_4$ with 0.3 mmoles of TcO_4^- present at -0.2 V

S.C.E. gives n-values of 3.92, 3.95 for Wave I. No doubt, in driving a coulometric run at a large mercury pool, the gross faradaic result involves a mixed process. However, the total requirement for the combination of processes,

$$\mathrm{Tc(VII)} + 4\,e^- \rightarrow \mathrm{Tc(III)} \tag{1}$$

and,

$$\mathrm{Tc(VII)} + \mathrm{Hg(O)} \rightarrow \mathrm{Tc(III)} + \mathrm{Hg(I)} \tag{2a}$$

followed by,

$$\mathrm{Hg(I)} \rightarrow \mathrm{Hg(O)} \tag{2b}$$

is probably correct for Wave I. Moreover, the final black precipitate that forms seems to be TcO_2, not Tc_2O_3, the product being partially reoxidized by hydrogen ion, as was true in sulphuric acid[10]. In hydrochloric acid or in phosphate media, moderately stable green solutions of Tc(III) complexes are obtained[1,2,8,9].

The shift in $E_{\frac{1}{2}}$ of Wave I with pH, conforms with the equation,

$$E_{\frac{1}{2}} = 0.06 - 0.106\ \mathrm{pH}.$$

If the four-electron status of the wave is accepted, this agrees closely with an eighth-power dependence on the activity of hydrogen ion. This implies complete stripping of the four pertechnetate oxygens in the primary electrochemical reduction process,

$$\mathrm{TcO_4^-} + 8\ \mathrm{H^+} + 4\,e^- \rightarrow \mathrm{Tc^{3+}} + 4\ \mathrm{H_2O} \tag{3}$$

This is also true in other media[1], although the irreversibility of the wave (slope, criterion) does not allow positive assertions on this point.

The occurrence of technetium electrodeposition on to or into a mercury cathode is evident from polarographic studies, but the status of the product is not clear.

Technetium metal powder digested with mercury at 300° gives no evidence of dissolution. Since the metal powder undoubtedly carries some oxide film and because the melting point of technetium is 2,150°, this result is not surprising. Acidic solutions of pertechnetate are slowly reduced, ultimately to the metallic state, by simple contact with a pool of mercury. Some of the technetium is contained within the mercury, but an exterior film is also evident. An 0.006 M solution of TcO_4^- in 1 M H_2SO_4 was electrolysed at nearly 10 V, applied, into a mercury cathode. An interior portion of the mercury was thieve-sampled, dissolved in nitric acid and counted. Molalities of technetium in mercury up to 0.005 are not difficult to obtain in this manner. The question remains of whether this product is a true amalgam or merely a finely divided suspension of technetium.

Centrifugation provides a simple experimental approach and gives results which can be interpreted within predictable limitations. A measurable centrifugal separation of particulate technetium ($d = 11.5$ g/ml) in liquid mercury would require that the particle size of the technetium exceed a certain value. With the assumptions of Stoke's Law applied to a centrifugal force, the sedimentation equation was solved for the available equipment. With our equipment, we estimate an angular velocity of 314 rad./sec and an effective arm length of 23 cm. Only 10 min would be needed to displace (upward, of course) a technetium particle of 1,000 Å diameter through 1 cm of mercury, and 16.7 h for a 100-Å particle; but 70 days would be required to displace a 10-Å particle this same distance. The measurements would not be sensitive

for particulate sizes below about 20 Å, and negative results would not distinguish a homogeneous solution from such fine particles.

After an electrolysis, a sample withdrawn from within the mercury pool cathode was subjected to 3 h of centrifuging. Small portions were removed from the top and bottom of the centrifuge tube (about 4 cm apart), dissolved in nitric acid, neutralized with ammonia, and counted. In an earlier run, results comparable with those reported were obtained, but the background constituted a larger portion of the total activity. The following data were obtained, after correction for a blank, for three samples from a second run:

Top of tube	*Bottom of tube*	*Ratio*
231 counts/10 min, g Hg	40 counts/10 min, g Hg	5.8
248	80	3.1
215	55	3.9
		Av. 4.3

From the approximately four-fold concentration of technetium under these conditions, one may estimate the particle size of the dispersed technetium metal as lying within the range 10^{-6}–10^{-5} cm. This technique does not eliminate the possible existence of a mercury-insoluble Tc–Hg compound, and refers to the status of the mixture approximately 4 h after formation.

Provision was made for the preparation of a technetium-in-mercury deposit in the upper mercury reservoir of a conventional D.M.E. assembly. Without the dangers of re-solution or air-contact, freshly made "amalgam" could then be brought immediately down to the D.M.E. by simply removing the "dead-space" volume of mercury (contained in the stand-tube) *via* a side cock mounted above the capillary. In three such experiments it was confirmed (radiochemically) that technetium was actually present *within* the mercury exiting from the capillary. The system was operated into freshly de-aerated 0.1 *M* HCl and polarographically scanned for the existence of anodic waves. The available potential region amounted to approximately +0.05 V (where anodic calomel discharge occurs) to −0.85 V S.C.E. where the toe of the cathodic hydrogen wave begins (this is more positive for technetium in mercury than with pure mercury).

Only the usual shape of residual current curve, with currents of less than 0.1 μA, was observed in these experiments. There was no evidence of anodic dissolution of technetium. When solutions were examined after more than 30 min, during which time the dropping continued and nitrogen was loosely maintained as a blanket but not recirculated through the solution, less than 0.5 μA of cathodic wave sometimes developed. This wave appeared at potentials more negative than −0.6 V, corresponding to the presence of small amounts of Tc(III), or lower states. Evidently, H_3O^+ and traces of O_2 permit some dissolution.

Neither experiment alone, nor the two in conjunction, completely characterizes the nature of technetium electrodeposited into mercury. The negative results of the anodic dissolution, however, are compatible with the sizeable particles deduced from centrifugation.

ACKNOWLEDGEMENTS

Support by the U.S. Atomic Energy Commission, Contract AT(11-1)-1483, is gratefully acknowledged.

SUMMARY

The polarographic reduction of pertechnetate in 4–0.01 M perchloric acid media takes place in two stages. The $E_{\frac{1}{2}}$ of the more positive wave at +0.10 to −0.17 V S.C.E. is pH-dependent, $E_{\frac{1}{2}} = 0.06 - 0.10_6$ pH. Coulometry indicates a four-electron process, $TcO_4^- + 8\,H^+ + 4\,e^- = Tc^{3+}$. A second wave at −0.73 V appears to involve the three-electron step (III) → (O).

Technetium electrodeposits into mercury in a finely-divided form. Centrifugation of the product indicates particles of 10^{-5}–10^{-6} cm diameter. A freshly-prepared technetium "amalgam" dropping-electrode showed no anodic polarographic activity in 0.1 M HCl from −0.8 to +0.05 V S.C.E., indicating little solubility, or true amalgam character.

REFERENCES

1 G. B. S. SALARIA, C. L. RULFS AND P. J. ELVING, *J. Chem. Soc.*, (1963) 2479.
2 H. H. MILLER, M. T. KELLEY AND P. F. THOMASON, *Advances in Polarography*, edited by I. S. LONGMUIR, Vol. 2, Pergamon Press, London, 1960, pp. 716–26.
3 L. ASTHEIMER AND K. SCHWOCHAU, *J. Electroanal. Chem.*, 8 (1964) 382–89.
4 R. COLTON, J. DALZIEL, W. P. GRIFFITH AND G. WILKINSON, *J. Chem. Soc.*, (1960) 71.
5 R. COLTON, *The Chemistry of Rhenium and Technetium*, John Wiley, London, New York, Sydney, 1965, pp. 150–57.
6 J. D. EAKINS AND D. G. HUMPHRIES, *J. Inorg. & Nucl. Chem.*, 25 (1963) 737.
7 R. E. VOLTZ AND M. L. HOLT, *J. Electrochem. Soc.*, 114 (1967) 128.
8 G. B. S. SALARIA, C. L. RULFS AND P. J. ELVING, *Anal. Chem.*, 35 (1963) 979.
9 A. A. TERRY AND H. E. ZITTEL, *Anal. Chem.*, 35 (1963) 614.
10 C. L. RULFS, R. PACER AND R. HIRSCH, *J. Inorg. & Nucl. Chem.*, 29 (1967) 681.
11 C. L. RULFS AND P. J. ELVING, *J. Am. Chem. Soc.*, 73 (1951) 3284.
12 K. SCHWOCHAU AND L. ASTHEIMER, *Z. Naturforsch.*, 17a (1962) 820.
13 R. D. PEACOCK, *The Chemistry of Technetium and Rhenium*, Elsevier, Amsterdam, London, New York, 1966, p. 35.
14 R. J. MAGEE, I. A. P. SCOTT AND C. L. WILSON, *Talanta*, 2 (1959) 376.

ELECTROANALYTICAL CHEMISTRY AND INTERFACIAL ELECTROCHEMISTRY
Elsevier Publishing Company, Amsterdam – Printed in The Netherlands

POLAROGRAPHIC STUDY OF THE SELENOCYANATE COMPLEXES OF ZINC AND CADMIUM

A. A. HUMFFRAY, A. M. BOND AND J. S. FORREST
Department of Physical Chemistry, University of Melbourne, Melbourne, Victoria (Australia)
(Received November 3rd 1966)

Many polarographic investigations have been made of thiocyanate complexes since the work of HUME *et al.*[1], but the only polarographic study of selenocyanate complexes appears to be that on cadmium selenocyanates by TOROPOVA[2], who found evidence only for $Cd(CNSe)_4^{2-}$. GOLUB AND ANDREICHENKO[3], using the potentiometric method and a wider range of ligand concentrations, demonstrated the existence of five cadmium selenocyanate complexes in aqueous solution. TOROPOVA predicted, on the basis of the crystallographic data of ZHDANOV AND ZVONKOVA[4], that the stabilities of zinc selenocyanates would be lower than those of zinc thiocyanates. This report deals with a polarographic study of the systems zinc–selenocyanate and cadmium–selenocyanate; for comparison purposes, measurements were also made on the system cadmium–thiocyanate.

EXPERIMENTAL

All chemicals used were of reagent-grade purity, except potassium selenocyanate, which was a B.D.H. sample purified by four successive recrystallisations from acetone. The purity of this, and the concentrations of solutions prepared were checked by weighing the selenium precipitated on acidification. All measurements were made at $30 \pm 0.1°$, and at an ionic strength of 2.0, maintained by potassium nitrate. An H-cell was used, in which the saturated calomel electrode was separated from the test solution by a potassium nitrate–agar plug and a sintered-glass disc. No maxima were encountered, and maximum suppressors were not added.

Polarograms were obtained using a Cambridge recording polarograph; the potentials were checked to 0.1 mV using a Doran pH–mV meter or a Tinsley Vernier Potentiometer, and a correction applied for the iR drop. The D.M.E. had the following characteristics: $m^{2/3}t^{1/6} = 4.40$ and $t = 3.1$ sec (in 2.0 M KNO_3 at zero applied potential *vs.* S.C.E.). Oxygen-free nitrogen was used to de-aerate the solutions.

The half-wave potentials were mainly estimated using the simple method of FRANK AND HUME[5], but reversibility was verified by the linearity of plots of $E_{d.e.}$ *vs.* $\log i/(i_d - i)$, with slopes of 30 ± 2 mV. $E_{\frac{1}{2}}$-values obtained from these plots agreed well with those obtained by the simpler method.

The concentrations of Cd^{2+} and Zn^{2+} were approximately 0.2 mM; the ligand concentrations are shown in the Tables.

RESULTS AND DISCUSSION

(a) Cd^{2+}–CNS^- system

The overall stability constants for the complex species $CdCNS^+$, $Cd(CNS)_2$, $Cd(CNS)_3^-$ and $Cd(CNS)_4^{2-}$ were found to be 10, 55, 7 and 44, respectively, in excellent agreement with the values (11, 56, 6, 60) of HUME *et al.*[1]. The method of calculation was that used by these workers, and the results are summarised in Table 1.

TABLE 1

ANALYSIS OF $F_j(X)$ FUNCTION FOR Cd–CNS SYSTEM

Cx (*M*)	$-E_{\frac{1}{2}}$ (*V vs. S.C.E.*)	i_d (*divs.*)	$F_0(X)$	$F_1(X)$	$F_2(X)$	$F_3(X)$	$F_4(X)$
0.0	0.5726	62.4	1.00				
0.2	0.5921	60.6	4.58	17.9			
0.4	0.6111	58.8	20.2	48.0	95.0		
0.6	0.6195	55.2	40.9	66.5	94.2		
0.8	0.6272	54.6	74.6	92.0	102.5	59.4	
1.0	0.6343	54.6	128.2	127.2	117.2	62.2	
1.2	0.6398	54.6	195.4	162.0	126.7	59.8	44.0
1.4	0.6456	53.4	311.6	221.9	151.4	68.9	44.2
1.6	0.6511	52.8	479.9	299.3	180.8	78.6	44.8
1.8	0.6560	52.8	697.3	386.8	209.3	85.7	43.7

$\beta_1 = 10, \beta_2 = 55, \beta_3 = 7, \beta_4 = 44$

TABLE 2

ANALYSIS OF $F_j(X)$ FUNCTION FOR Cd–CNSe SYSTEM

Cx (*M*)	$E_{\frac{1}{2}}$ (*V vs. S.C.E.*)	i_d (*divs.*)	$F_0(X)$	$F_1(X)$	$F_2(X)$	$F_3(X)$	$F_4(X)$
0.0	0.5726	62.4	1				
0.067	0.5868	61.2	3.024	30.21			
0.133	0.5961	60.0	6.279	39.69	148.1		
0.2	0.6065	57.6	14.49	67.45	237.3	686.3	
0.4	0.6269	57.0	69.79	172.0	379.9	699.8	
0.6	0.6440	53.4	275.7	457.8	729.7	1050	1016
0.8	0.6563	52.8	714.3	891.6	1090	1237	996.1
1.0	0.6667	52.8	1583	1582	1562	1462	1022
1.2	0.6749	52.2	2997	2497	2057	1631	988.4

$\beta_1 = 20 \pm 2, \beta_2 = 100 \pm 5, \beta_3 = 440 \pm 10, \beta_4 = 1000 \pm 20$

(b) Cd^{2+}–$CNSe^-$ system

Because of the small change in $E_{\frac{1}{2}}$ with increasing concentration of selenocyanate above 1 *M*, the maximum concentration of the latter employed was 1.2 *M*. The overall stability constants for the species $CdCNSe^+$, $Cd(CNSe)_2$, $Cd(CNSe)_3^-$ and $Cd(CNSe)_4^{2-}$ were found to be $\beta_1 = 20 \pm 2$, $\beta_2 = 100 \pm 5$, $\beta_3 = 440 \pm 10$ and $\beta_4 = 1000 \pm 20$, respectively. Details of the calculations are listed in Table 2, and the graphical method of evaluation is shown in Fig. 1. GOLUB AND ANDREICHENKO[2], at 20° and ionic strength 1.5, obtained the following values; $\beta_1 = 22$, $\beta_2 = 180$, $\beta_3 = 10{,}000$, $\beta_4 = 1750$. In view of the difference in temperature and in ionic strength, the agreement for β_1, β_2 and β_4 is satisfactory, but the exceptionally high stability of

$Cd(CNSe)_3^-$ suggested by their β_3-value is not easily explained. Our results indicate that the complex $Cd(CNSe)_4^{2-}$ is more stable than is $Cd(CNSe)_3^-$, a trend also shown by the thiocyanates of cadmium (and of zinc and mercury). At the intermediate temperature of 25°, TOROPOVA's β_4-value of 4000 seems to be inconsistent both with ours and with that of GOLUB AND ANDREICHENKO, but this large β_4-value may result from the neglect of the other species present. At an ionic strength of 2.0, and maximum ligand concentration of 1.2 M, our results gave no indication of higher complexes. Figure 2 indicates the percentage distribution of cadmium present in the form of each species as a function of selenocyanate concentration.

(c) Zn–CNSe system

At ionic strength 2.0 and up to a maximum ligand concentration of 1.4 M,

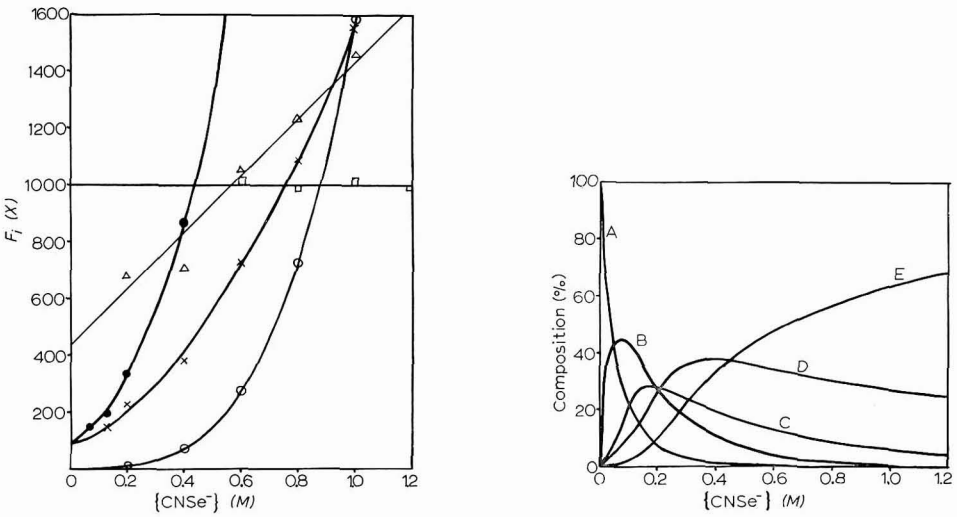

Fig. 1. $F_j(X)$ plots for Cd–CNSe system: (○), $F_0(X)$; (●), $F_1(X)$; (×), $F_2(X)$; (△), $F_3(X)$; (□), $F_4(X)$. (Ordinate scale divided by five for F_1.)

Fig. 2. Percentage distribution of various species present in Cd–CNSe system. (A), Cd^{2+}; (B), $CdCNSe^+$; (C), $Cd(CNSe)_2$; (D), $Cd(CNSe)_3^-$; (E), $Cd(CNSe)_4^{2-}$.

TABLE 3

ANALYSIS OF $F_j(X)$ FUNCTION FOR Zn–CNSe SYSTEM

Cx (M)	$-E_{\frac{1}{2}}$ (V vs. S.C.E.)	i_d (divs.)	$F_0(X)$	$F_1(X)$	$F_2(X)$
0.0	0.9938	51.0	1		
0.2	1.0055	50.4	2.477	7.385	
0.4	1.0145	50.4	4.933	9.833	10.1
0.6	1.0203	49.8	7.768	11.28	9.13
0.8	1.0251	49.8	12.13	13.91	10.1
1.0	1.0294	49.8	16.85	15.85	10.1
1.4	1.0384	49.2	31.47	21.76	11.4

$\beta_1 = 5.8 \pm 0.5, \beta_2 = 10 \pm 1$

only two complexes appear to exist in solution, *i.e.*, $ZnCNSe^+$ and $Zn(CNSe)_2$. The formation constants for these species were evaluated as before; the results are $\beta_1 = 5.8 \pm 0.5$, $\beta_2 = 10 \pm 1$. Details are listed in Table 3, and Fig. 3 shows the graphical treatment. The percentage distribution of zinc in the form of each species as a function of selenocyanate concentration is shown in Fig. 4. Comparison with the stability constants for zinc thiocyanates[5], namely $\beta_1 = 3$, $\beta_2 = 7$, $\beta_3 = 1$, $\beta_4 = 20$, shows

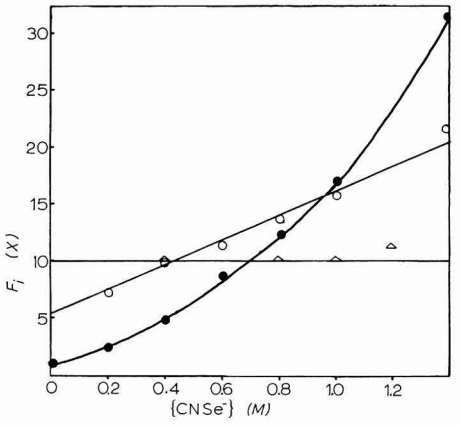

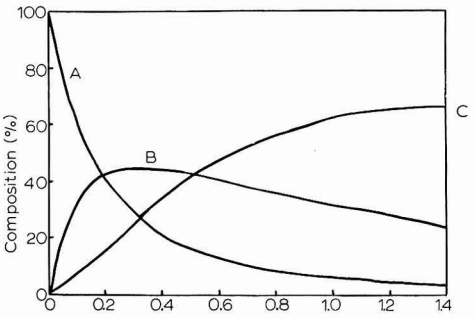

Fig. 3. $F_j(X)$ plots for Zn–CNSe system: (●), $F_0(X)$; (○), $F_1(X)$; (△), $F_2(X)$.

Fig. 4. Percentage distribution of various species present in Zn–CNSe system. (A), Zn^{2+}; (B), $ZnCNSe^+$; (C), $Zn(CNSe)_2$.

that the two selenocyanate complexes are slightly more stable than the two corresponding thiocyanate complexes. This would be understandable if the bonding occurred through selenium in the former, as the latter are really isothiocyanates[4]. The differences in stability are however not very great. Perhaps of greater significance is the absence of any definite indication of higher complexes at a selenocyanate concentration of 1.4 *M*. In the zinc thiocyanate system, 60% of the zinc present exists as $Zn(CNS)_4^{2-}$ at a thiocyanate concentration of 1.0 *M*. Thus, although the first two zinc selenocyanate complexes have stabilities comparable to those of the corresponding thiocyanates, the higher thiocyanate complexes are more stable than the selenium analogues, as predicted by TOROPOVA. The manner of co-ordination of the selenocyanate ion in the zinc complexes could presumably be determined by X-ray crystallographic[4] or infra-red[6] studies.

SUMMARY

Polarographic measurements on aqueous solutions containing cadmium and selenocyanate ions have shown the existence of the species $CdCNSe^+$, $Cd(CNSe)_2$, $Cd(CNSe)_3^-$ and $Cd(CNSe)_4^{2-}$, with stability constants (at ionic strength 2.0) of 20, 100, 440 and 1000, respectively. Under similar conditions for mixtures of zinc and selenocyanate ions, only two species, $ZnCNSe^+$ and $Zn(CNSe)_2$, are found, with stability constants (at ionic strength 2.0) of 5.8 and 10, respectively.

REFERENCES

1 D. N. HUME, D. D. DEFORD AND G. C. B. CAVE, *J. Am. Chem. Soc.*, 73 (1951) 5323.
2 V. F. TOROPOVA, *Zh. Neorgan. Khim.*, 1 (1956) 243.
3 A. M. GOLUB AND O. E. ANDREICHENKO, *Zh. Neorgan. Khim.*, 7 (1962) 549.
4 G. S. ZHDANOV AND Z. V. ZVONKOVA, *Usp. Khim.*, 22 (1953) 3.
5 R. E. FRANK AND D. N. HUME, *J. Am. Chem. Soc.*, 75 (1953) 1736.
6 C. PECILE, A. TURCO AND G. PIZZOLOTTO, *Ric. Sci.*, 31 (2A) (1961) 247;
A. TURCO, C. PECILE AND M. NICCOLINI, *J. Chem. Soc.*, (1962) 3008.

ELECTROANALYTICAL CHEMISTRY AND INTERFACIAL ELECTROCHEMISTRY
Elsevier Publishing Company, Amsterdam – Printed in The Netherlands

TETRAALKYLIERTE AMMONIUMVERBINDUNGEN ALS LEITELEKTROLYTE ZUR POLAROGRAPHISCHEN BESTIMMUNG ALIPHATISCHER KETONE

W. WIESENER UND K. SCHWABE
Zentralinstitut für Kernforschung Rossendorf, Bereich Radiochemie, 8051 Dresden
(Eingegangen am 11. November, 1966)

EINLEITUNG

Bei der polarographischen Bestimmung einiger organischer Verbindungen, besonders aliphatischer gesättigter Ketone ist das Hauptproblem, einen Leitelektrolyten zu finden, der ein genügend negatives Abscheidungspotential besitzt. Die Reduktionspotentiale der aliphatischen Ketone liegen grösstenteils negativer als -2.5 V. Das Potential des Endanstiegs der herkömmlichen Leitelektrolyte, wie Tetramethyl-, Tetraäthyl- und Tetrabutylammoniumsalze weisen einen sehr negativen Wert auf, er reicht aber für viele Bestimmungen noch nicht aus. Wir haben uns deshalb zur Aufgabe gestellt, das Potential des Endanstiegs der quarternären Ammoniumverbindungen in Abhängigkeit von der Anzahl der C-Atome (C_2–C_8), den Einfluss von Methanol und des Anions auf das Potential des Endanstiegs dieser Verbindungen zu untersuchen. Weiterhin haben wir die Halbstufenpotentiale (HSP bzw. $E_{\frac{1}{2}}$) und die Stufenhöhen (h) aliphatischer Ketone in diesen Leitsalzen ermittelt und ihre Konzentrationsproportionalität geprüft. Alle Messungen wurden in Kompensation gegen eine Bezugselektrode durchgeführt. Die Messgenauigkeit der Potentiale liegt bei $\pm$ 3 mV.

MESSTECHNIK

In Fig. 1 ist die verwendete Messzelle abgebildet. Als Anode diente Bodenquecksilber, als Kathode die Quecksilbertropfelektrode, deren Potential in Kompensation gegen eine gesättigte Kalomelektrode (SCE) gemessen wurde. Die Bezugselektrode steckte in einem seitlichen Schenkel des Messgefässes, der mit der gleichen Lösung gefüllt war wie die Messzelle. Die verwendeten Depolarisatoren waren analysenreine Substanzen. Die tetraalkylierten Ammoniumverbindungen wurden weitgehendst selbst hergestellt.

MESSERGEBNISSE UND DISKUSSION

a) Die Abhängigkeit des Potentials des Endanstiegs (PE) von der Anzahl der C-Atome

Die bisher verwendeten Leitsalze sind Tetramethyl (TMA)-, Tetraäthyl (TAeA)-, Tetrabutyl (TnBA)-Ammoniumverbindungen mit einem Abscheidungspotential bis -2.8 V, wobei das PE in der Reihenfolge TMA-, TAeA-, TnBA-Kation

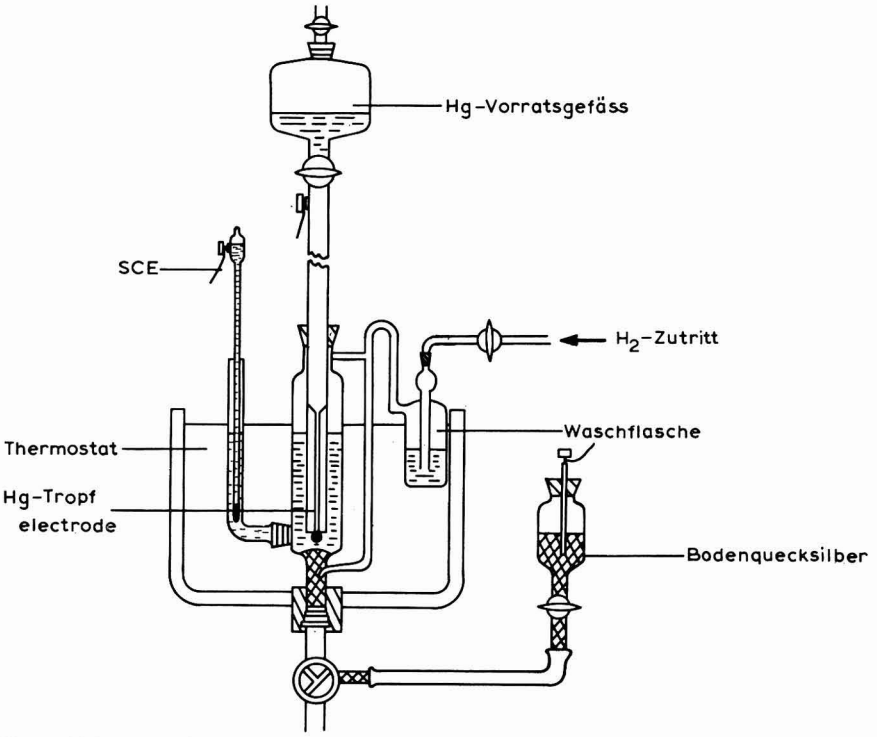

Fig. 1. Polarographische Messzelle.

negativer wird. Wir haben die PE der Tetraalkylammoniumjodide und -hydroxyde in Abhängigkeit von der Anzahl der C-Atome (C_2–C_8) in Wasser und Wasser–Methanol-Gemischen bei 25° gemessen. Die Konzentration der Lösungen war 0.1 *M*.

Die gemessenen PE (in mV), bezogen auf die ges. Kalomelelektrode, sind in Tabelle 1 zusammengefasst.

Die PE der Tetraalkylammoniumjodide konnten in Wasser bei einer Konzentration von 0.1 *M* mit Ausnahme von TAeAJ nicht bestimmt werden, da sie schwer löslich sind. Das PE des TnAAJ lässt sich in keiner Lösung angeben, da es auch nach mehrmaliger Reinigung keinen brauchbaren Kurvenverlauf zeigte.

Betrachtet man die PE der Jodide in Abhängigkeit von der Anzahl der C-Atome in Methanol–Wasser-Gemischen, so findet man mit zunehmender Kettenlänge eine Verschiebung der PE nach negativeren Werten, mit Ausnahme des TnHAJ. Analoges Verhalten beobachtet man bei den Tetraalkylammoniumhydroxiden. Die für TnHAOH und TnOAOH fehlenden PE konnten nicht bestimmt werden, da die Verbindungen in diesen Lösungsmittelgemischen nicht ausreichend löslich waren. Die auftretende Negativierung des PE mit steigender Anzahl der C-Atome kann auf den sogenannten (+, −)-Induktionseffekt zurückgeführt werden. In den Tetraalkylammoniumverbindungen sind die Alkylgruppen die negativen Substituenten, der Stickstoff bildet das positive Ende des Dipols. Negative Substituenten ziehen positive Ladung an, dies entspricht einer Elektronenabgabe des Substituenten und damit einem starken (+)-Induktionseffekt. Dieser steigt in der Reihenfolge Methyl-,

n-Alkyl-, iso-Alkylgruppe an. Infolgedessen nimmt die Reduzierbarkeit mit steigender Kettenlänge ab. Der Induktionseffekt klingt aber mit der Entfernung ab, deshalb wird ab C_4 der Unterschied zwischen den PE geringer. Die besonders negativen PE der Tetra-iso-amylammoniumverbindungen ergeben sich möglicherweise durch die verstärkte Wirkung des Induktionseffektes auf Grund der grösseren Zahl der Methylgruppen. Auch ist es naheliegend, dass die Amalgambildung einen Einfluss auf die Verschiebung des PE ausübt[1].

$$R_4N^+ + e^- \xrightarrow{Hg} R_4N(Hg)_x$$

Da die Amalgambildung mit wachsender Kettenlänge des neutralen Radikals, das durch Aufnahme eines Elektrons entsteht, abnimmt, behindern die neutralen Reaktionsprodukte die weitere Abscheidung der Tetraalkylammoniumkationen an dem Quecksilbertropfen, was sich in einer Negativierung des Reduktionspotentials auswirkt. Bei den Tetra-iso-ammylammoniumverbindungen ist die Amalgambildung besonders gering, weil sich hier die Molekülreste offenbar sterisch behindern.

b) Abhängigkeit des PE von der Methanolkonzentration

Aus Tabelle 1 geht der Einfluss des Methanols auf das PE hervor. Vergleicht man die PE des TAeAJ in Wasser, 60 Vol-% und 90 Vol-% Methanol miteinander, so findet man beträchtliche Unterschiede. Das PE in 60 Vol-% Methanol ist negativer (70 mV) als das in Wasser, das PE in 90 Vol-% Methanol ist positiver (250 mV) als das in Wasser. Bei den übrigen Tetraalkylammoniumjodiden ist ein Vergleich der PE in Wasser–Methanol-Gemischen mit denen in Wasser auf Grund der Schwerlöslichkeit nicht möglich. Bei allen untersuchten Verbindungen liegt bis C_6 das PE in 90 Vol-% Methanol positiver als in 60 Vol.% Methanol. Die Qualität der polarographischen Kurve fällt mit steigendem Methanolgehalt in der Lösung.

Zweifellos spielt für die Negativierung des PE das Adsorptionsverhalten der Lösungsmittelmoleküle eine entscheidende Rolle. Diese werden mit wachsendem Gehalt in der Lösung in zunehmendem Masse selbst an der Quecksilberoberfläche adsorbiert und verdrängen damit die Tetraalkylammoniumionen aus der Grenzschicht. Die Entladung der organischen Ionen wird erschwert und das PE mit steigenden Volumenprozenten (60 Vol-%) nach negativeren Werten verschoben.

Die positivierende Wirkung des Methanols, die bei 90 Vol-% Methanol den negativierenden Einfluss offenbar so stark überkompensiert, dass bereits ein positiveres Potential als in Wasser vorliegt, kann auf die Solvatationstendenz des Lösungsmittels zurückgeführt werden. Je grösser die Solvatationstendenz eines Lösungsmittels ist, umso mehr wird der Übergang $R_4N^+ \rightarrow R_4N(Hg)$ gehemmt. Da die Solvatationsenergie des Wassers am grössten ist, bewirkt ein Zusatz von Methanol zur wässrigen Lösung eine Verschiebung des PE in positiver Richtung.

c) Das PE in Abhängigkeit vom Anion

Die Abhängigkeit des PE vom Anion ist nur am TAeA-ion untersucht worden. Die Tabelle 2 zeigt die PE von 0.1 *M* TAeA-chlorid, -jodid, -bromid und -hydroxid. Es ist keine eindeutige Abhängigkeit vom Anion festzustellen. Die geringen Abweichungen untereinander liegen innerhalb der Fehlergrenze.

Zusammenfassend kann folgendes gesagt werden: Besonders die Tetraalkylammoniumhydroxide und speziell die Tetra-iso-amylammoniumverbindungen

TABELLE 1

POTENTIALE DES ENDANSTIEGS (mV) DER TETRAALKYLAMMONIUMVERBINDUNGEN IN WASSER–METHANOL-GEMISCHEN

	Jodid in			*Hydroxyd in*				
	Wasser	*60% CH_3OH*	*90% CH_3OH*	*Wasser*	*20% CH_3OH*	*60% CH_3OH*	*90% CH_3OH*	*CH_3OH*
$(C_2H_5)_4N^+$	−2750	−2820	−2500	−2745	−2770	−2815	−2629	[b]
$(n\text{-}C_3H_7)_4N^+$	—	−2960	−2710	−2860	−2890	−2952	−2780	[b]
$(n\text{-}C_4H_9)_4N^+$	—	−3020	−2750	−2910	−2920	−3015	−2765	[b]
$(n\text{-}C_5H_{11})_4N^+$	—	—	—	—	−2890	−3002	−2890	[b]
$(i\text{-}C_5H_{11})_4N^+$	—	−3115	−2954	−2943	−2947	−3050	−2880	[b]
$(n\text{-}C_6H_{13})_4N^+$	—	−2932	−1854	[a]	[a]	−2903	−2900	[b]
$(n\text{-}C_8H_{17})_4N^+$	—	—	−3050	[a]	[a]	[a]	[a]	−3067

[a] Trübung. [b] Schleichender Endanstieg.
TnPAJ = Tetra-n-propylammoniumjodid
TiAAJ = Tetra-iso-amylammoniumjodid
TnAAJ = Tetra-n-amylammoniumjodid
TnHAJ = Tetra-n-hexylammoniumjodid
TnOAJ = Tetra-n-octylammoniumjodid
−OH = entspechende Hydroxid

TABELLE 2

POTENTIALE DES ENDANSTIEGS IN mV GEGEN SCE

TAeACl	*TAeABr*	*TAeAI*	*TAeAOH*
−2742	−2749	−2751	−2745

sind wertvolle und brauchbare Leitelektrolyte zur polarographischen Bestimmung schwer reduzierbarer organischer und anorganischer Stoffe. Durch Verwendung von TiAAJ als Leitelektrolyt wird der Spannungsbereich auf −3.11 V gegen ges. Kalomelelektrode erweitert, wenn ein Lösungsmittelgemisch, bestehend aus 60 Vol-% Methanol und 40 Vol-% H_2O verwendet wird. Einen grossen Vorteil besitzen die Tetraalkylammoniumverbindungen insofern gegenüber anorganischen Leitsalzen, als sie bis zu hohen Konzentrationen in reinen organischen Lösungsmitteln löslich sind.

Der Kurvenverlauf einiger Tetraalkylammoniumverbindungen in unterschiedlichen Lösungsmittelgemischen wird in den Polarogrammen 1–3 wiedergegeben. Die Werte für die PE können aus den Polarogrammen nicht entnommen werden, weil hier als Anode Bodenquecksilber verwendet wurde und dieses je nach der Zusammensetzung der Lösung sein Potential ändert.

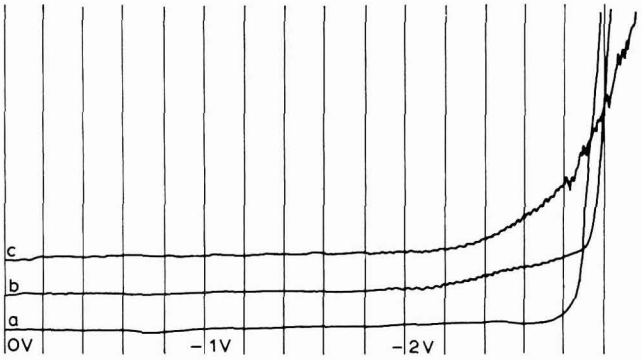

Polarogramm 1. Tetra-n-amylammoniumhydroxyd.
a) in 20 Vol-% Methanol; PE, −2890 mV. b) in 60 Vol-% Methanol; PE, −3002 mV. c) in 90 Vol-% Methanol; PE, −2890 mV.

d) Das Halbstufenpotential aliphatischer Ketone in Abhängigkeit vom Leitelektrolyten und der Methanolkonzentration

Es wurden die Halbstufenpotentiale von Aceton, n-Pentanon, 3-Methylpentanon-2, 3-Isopropylpentanon-2 und n-Heptanon-2 bestimmt und ihre Abhängigkeit vom Leitelektrolyten (Tetraalkylammoniumverbindungen) und der Methanolkonzentration untersucht. Ausserdem wurde die Stufenhöhe dieser Ketone ermittelt und ihre Konzentrationsproportionalität geprüft. Da die Ketone im Prinzip in den einzelnen Leitelektrolyten ähnliches Verhalten zeigten, wird nur auf das n-Heptanon und Aceton näher eingegangen.

In den Tabellen 3 und 4 sind die Messergebnisse zusammengestellt.

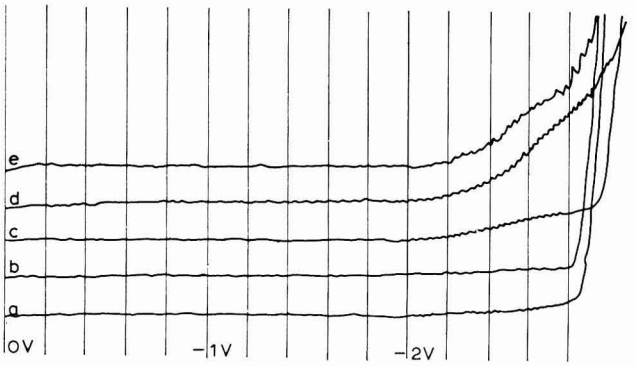

Polarogramm 2. Tetra-iso-amylammoniumhydroxyd.
a) in Wasser; PE, −2943 mV. b) in 20 Vol-% Methanol; PE, −2947 mV. c) in 60 Vol-% Methanol; PE, −3050 mV. d) in 90 Vol-% Methanol; PE, −2880 mV. e) in 100% Methanol.

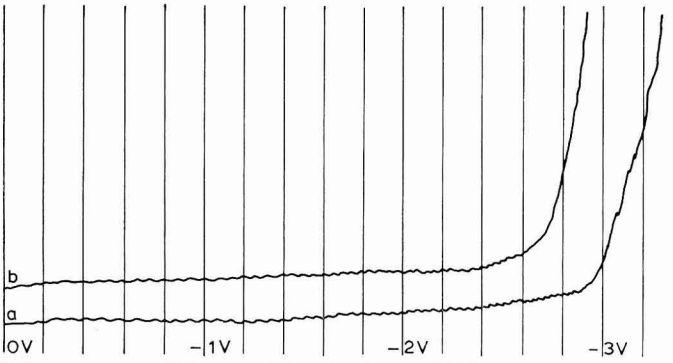

Polarogramm 3. Tetra-n-octylammoniumverbindungen.
a) TnOAOH in 100% Methanol; PE, −3067 mV. b) TnOAI in 90 Vol-% Methanol; PE, −3050 mV.

TABELLE 3

HSP DES n-HEPTANONS (c, $4.76 \cdot 10^{-3}$ M) UND PE DES LEITELEKTROLYTEN (c, 0.1 M) IN WASSER–METHANOL-GEMISCHEN IN mV

Leitelektrolyt	*Hydroxyd in*						*Jodid in*	
	Wasser		*20% CH_3OH*		*60% CH_3OH*		*60% CH_3OH*	
	$E_{\frac{1}{2}}$	*PE*	$E_{\frac{1}{2}}$	*PE*	$E_{\frac{1}{2}}$	*PE*	$E_{\frac{1}{2}}$	*PE*
$(C_2H_5)_4N^+$	−2511	−2745	−2540	−2770	—	—	−2640	−2820
$(n\text{-}C_3H_7)_4N^+$	−2678	−2860	−2645	−2890	−2620	−2952		
$(n\text{-}C_4H_9)_4N^+$	−2537	−2910	−2526	−2920	−2523	−3015	−2635	−3020
$(n\text{-}C_5H_{11})_4N^+$			−2282	−2890	−2422	−3002		
$(i\text{-}C_5H_{11})_4N^+$			−2497	−2497	−2560	−3050	−2644	−3115
$(n\text{-}C_6H_{13})_4N^+$					−2418	−2903		

TABELLE 4

HSP DES ACETONS (c, $6.98 \cdot 10^{-3}$ M) UND PE DES LEITELEKTROLYTEN (c, 0.1 M)

Leitelektrolyt	$E_{\frac{1}{2}}$ *(mV)*	*PE (mV)*
TnBAOH in H_2O	−2682	−2910
TnAAOH in 60 Vol-% CH_3OH	−2564	−3002
TnOAOH in 100 Vol-% CH_3OH	−2650	−3067

Die Ergebnisse aus Tabelle 3 zeigen, dass das HSP von n-Heptanon in den verschiedenen Alkylammoniumjodiden bei einem nahezu konstanten Wert liegt, obwohl sich die PE der Leitsalze erheblich voneinander unterscheiden. Das HSP ist demnach von dem Tetraalkylammoniumkation unabhängig. Dagegen findet man in den verschiedenen Tetraalkylammoniumhydroxidlösungen einen komplexen Einfluss des Leitelektrolyten auf das HSP und eine Abhängigkeit des HSP von der Konzentration des organischen Lösungsmittels.

In Tabelle 4 wird das HSP des Acetons in verschiedenen Lösungen wiedergegeben. Der Unterschied zwischen den Werten lässt sich schwer erklären. Zweifellos ist nicht nur der Leitelektrolyt- und Lösungsmitteleinfluss entscheidend, sondern auch die spezifischen Wirkungen des Depolarisators selbst. Der Potentialbereich, in dem die Reduktion des jeweiligen Depolarisators stattfindet, spielt wegen der spezifischen Adsorption der Leitelektrolytkationen an der Hg-Elektrode eine wichtige Rolle, weil die spezifische Adsorption selbst potentialabhängig ist. Eingehende Untersuchungen über die Adsorption von Tetraalkylammoniumverbindungen an der Hg-Elektrode sind von DAMASKIN[2] gemacht worden.

Mit Hilfe dieser Erkenntnisse kann der Einfluss des Leitelektrolyten und des Lösungsmittels auf das HSP der untersuchten Ketone wie folgt gedeutet werden:

1. Die geringen Unterschiede und die ausgesprochen negativen HSP des n-Heptanons in den verschiedenen Tetraalkylammoniumjodidlösungen in 60 Vol-% Methanol lassen sich auf die zusätzliche Adsorption der stark oberflächenaktiven Jodidionen bei sehr negativen Potentialen zurückführen. Der Einfluss der Anionen ist so stark, dass er die Wirkung der Kationen überkompensiert.

2. Bei den Hydroxiden dagegen wirkt sich nur die Kapillaraktivität der Kationen auf die Lage des HSP aus. Die in den wässrigen und alkoholischen Lösungen auftretende Positivierung mit zunehmender Kohlenstoffzahl lässt sich mit der wachsenden Adsorption der Tetraalkylammoniumkationen an der Hg-Elektrode erklären. Die Kationen besetzen die innere Helmholtzschicht und erleichtern damit den Ketondipolen das Eindringen in die Doppelschicht und die Reduktion.

3. Die Negativierung des HSP in TnAAOH und TiAAOH mit zunehmendem Methanolgehalt kann auf die gleichen Ursachen zurückgeführt werden wie bei der Verschiebung des PE. Durch das Bestreben der Lösungsmittelmoleküle selbst an der Elektrodenoberfläche adsorbiert zu werden, verdrängen sie die Ketonmoleküle aus der Grenzschicht. Der geringfügige Einfluss des Methanols auf das HSP in TnPAOH und TnBAOH beruht möglicherweise auf der geringeren Adsorption des Methanols bei den hier sehr negativen HSP (-2.5 V).

e) Ermittlung der Stufenhöhe und ihre Konzentrationsproportionalität

Es wurde die Konzentrationsproportionalität der Stufenhöhe von n-Heptanon und Aceton in verschiedenen Leitsalzen geprüft. Die Stufenhöhe ergibt sich aus den Polarogrammen, die manuell mit Hilfe der Kompensationsschaltung gegen die SCE erhalten wurden (1 mm entspricht 0.66 μA).

Die Wirkung des organischen Leitelektrolyten und Lösungsmittels auf die Stufenhöhe des Ketons soll hier kurz erörtert werden. In Tabelle 9 werden zu diesem Zweck die Stufenhöhen konstanter Konzentration, in verschiedenen Leitelektrolytlösungen mit unterschiedlicher Methanolkonzentration angegeben.

Die Höhe des Diffusionsstromes ändert sich mit dem Leitelektrolyten und mit

TABELLE 5

POLAROGRAMM 4. STUFENHÖHE UND HALBSTUFENPOTENTIAL VON n-HEPTANON IN TiAAI IN 60 VOL-% CH_3OH (PE, −3115 mV)

Depol. Konz. *(10⁻³ M)*	*h* *(mm)*	$E_{\frac{1}{2}}$ *(mV)*
a) Leere Lösung		
b) 2.44	13.0	−2660
c) 4.76	18.5	−2640
d) 5.88	21.0	−2630
e) 6.97	23.5	−2640
8.04	26.4	−2640

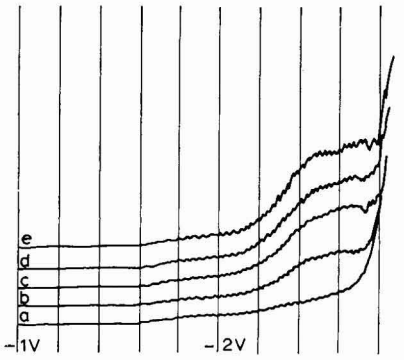

TABELLE 6

POLAROGRAMM 5. STUFENHÖHE UND HALBSTUFENPOTENTIAL VON n-HEPTANON IN TnAAOH IN 25 VOL-% CH_3OH (PE, −2890 mV)

Depol. Konz. *(10⁻³ M)*	*h* *(mm)*	$E_{\frac{1}{2}}$ *(mV)*
a) Leere Lösung		
b) 2.44	13.3	−2290
c) 4.76	19.4	−2265
d) 6.97	25.0	−2285
e) 9.09	29.5	−2280
f) 11.10	35.0	−2280
g) 13.00	40.0	−2290

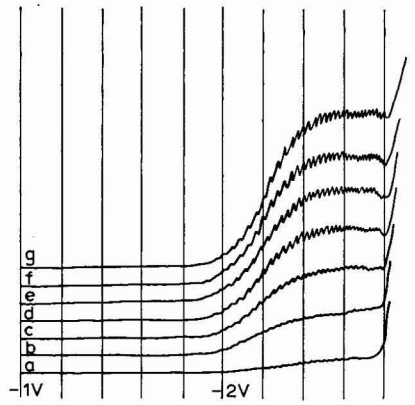

TABELLE 7

POLAROGRAMM 6. STUFENHÖHE UND HALBSTUFENPOTENTIAL VON n-HEPTANON IN TiAAOH IN 20 VOL-% CH_3OH (PE, −2947 mV)

Depol. Konz. *(10⁻³ M)*	*h* *(mm)*	$E_{\frac{1}{2}}$ *(mV)*
a) Leere Lösung		
b) 4.76	15.7	−2500
c) 5.88	19.7	−2518
d) 8.04	—	—
e) 10.10	29.8	−2520
f) 12.10	34.0	−2490

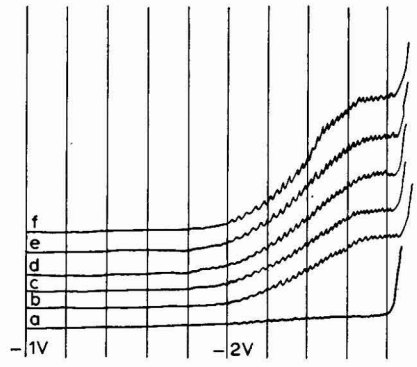

TABELLE 8

POLAROGRAMM 7. STUFENHÖHE UND HALBSTUFENPOTENTIAL VON ACETON IN TnAAOH IN 60 VOL-% CH_3OH (PE, −3002 mV)

Depol. Konz. *(10^{-3} M)*	*h* *(mm)*	$E_{\frac{1}{2}}$ *(mV)*
a) Leere Lösung		
b) 2.44	16.3	−2545
c) 4.76	23.3	−2555
d) 6.97	30.3	−2555
e) 9.09	37.2	−2565
f) 11.10	43.3	−2580
g) 13.00	49.5	−2585

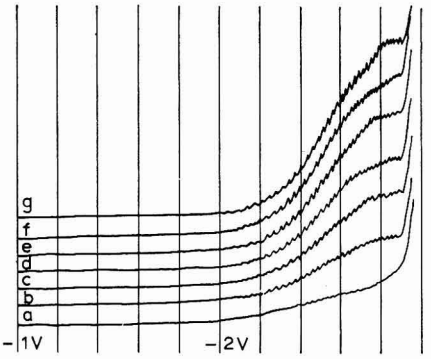

TABELLE 9

DIE STUFENHÖHE IN ABHÄNGIGKEIT VOM LEITELEKTROLYTEN UND DER METHANOLKONZENTRATION

n-Heptanonkonzentration $4.76 \cdot 10^{-3}$ *M*

Leitelektrolyt	*h (mm) in Lösungsmittel:*			
	Wasser	*20 Vol-% CH_3OH*	*30 Vol-% CH_3OH*	*60 Vol-% CH_3OH*
TAeAI				53.2
TnBAI				22.5
TiAAI				18.5
TAeAOH	15.5	15.0		
TPAOH		12.3		20.2
TnBAOH	14.0	12.0	11.0	19.0
TnAAOH		19.4		22.4
TiAAOH		15.7		21.0
TnHAOH				29.0

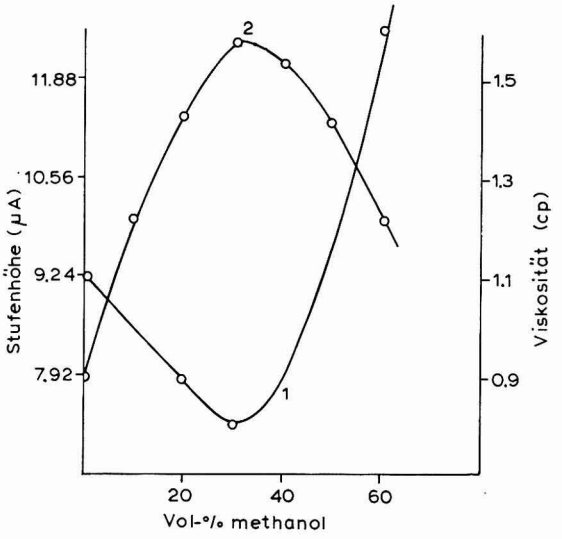

Fig. 2. Abhängigkeit der Stufenhöhe (1) und der Viskosität der Lösung (2) von der Methanolkonzentration.

der Methanolkonzentration. Offenbar wird der Diffusionsstrom im wesentlichen von der Viskosität der Aufnahmelösung beeinflusst.

In Fig. 2 ist die Stufenhöhe des n-Heptanons in TnBAOH in Abhängigkeit von der Methanolkonzentration aufgetragen (Kurve 1). Die Kurve durchläuft ein Minimum.

Bei dem gleichen Methanolgehalt (30%), wo die Stufenhöhe ein Minimum aufweist, besitzt die Viskosität ein Maximum (Kurve 2). Bei den angegebenen Viskositäten handelt es sich allerdings um reine Methanol–Wasser-Gemische.

Eine systematische Abhängigkeit zwischen der Stufenhöhe und der Art der Tetraalkylammoniumverbindung besteht nicht, man muss daher bei der Bestimmung eines Ketons in verschiedenen Leitsalzlösungen für jede Lösung eine getrennte Eichkurve aufnehmen.

ZUSAMMENFASSUNG

Es werden die polarographischen Potentiale des Endanstiegs (PE) der Tetraalkylammoniumjodide und -hydroxide von C_2H_5 bis C_8H_{17} in Wasser und Methanol–Wasser-Gemischen bestimmt. Die PE werden mit zunehmender Länge des Alkylrestes nach negativeren Werten verschoben, so dass Werte von -3.1 V gegen die SCE (25°) erreicht werden. Die Verbindungen eignen sich als Leitelektrolyte für die Bestimmung von Depolarisatoren mit sehr negativem Halbstufenpotential. Dies wurde durch die polarographische Reduktion einer Anzahl aliphatischer Ketone (insbesondere Aceton und n-Heptanon) nachgewiesen. Die Stufenhöhen sind konzentrationsproportional. Sie werden durch die Viskosität des Lösungsmittels in der üblichen Weise beeinflusst.

SUMMARY

The polarographic potential of the final rise (PE) was determined in water and in methanol–water mixtures for tetra-alkylammonium iodides and hydroxides from C_2H_5 to C_8H_{17}. With increasing alkyl chain length the PE was shifted to more negative values so that a value of -3.1 V *vs.* SCE at 25° was reached. The compounds are suitable as conducting electrolytes for the determination of depolarizers with very negative half-wave potentials. This was shown by the polarographic reduction of a number of aliphatic ketones (in particular, acetone and n-heptanone). The wave heights are proportional to the concentration and are affected by the viscosity of the solvent in the usual way.

LITERATUR

1 H. N. McCoy und W. C. Moore, *J. Am. Chem. Soc.*, 33 (1911) 273.
2 B. B. Damaskin und N. V. Nikolajeva-Federovic, *Zh. Fiz. Khim.*, 6 (1961) 1279.

ELECTROANALYTICAL CHEMISTRY AND INTERFACIAL ELECTROCHEMISTRY
Elsevier Publishing Company, Amsterdam – Printed in The Netherlands

DIE KATALYTISCHE WIRKUNG VON N,N-DIMETHYL-*p*-PHENYLENDIAMIN AUF DIE WASSERSTOFFABSCHEIDUNG AUS ORGANISCHEN SÄUREN UND AUF DIE POLAROGRAPHISCHE REDUKTION VON NITROVERBINDUNGEN IN METHANOLISCHEN LÖSUNGEN

D. JANNAKOUDAKIS, A. WILDENAU UND L. HOLLECK
Chemisches Institut der Hochschule, Bamberg (Deutschland)
(Eingegangen am 12 Dezember, 1966)

Bei der polarographischen Reduktion von *p*-Dimethylamino-substituierten Azo- und Nitroverbindungen in methanolischen Lösungen wurde bei Anwesenheit organischer Säuren gefunden, dass eine katalytische Abscheidung von Wasserstoff auftrat, die bei beiden Verbindungen auf die Wirkung des gleichen Reduktionsproduktes N,N-Dimethyl-*p*-phenylendiamin zurückzuführen war[1,2].

Katalytische Wasserstoffwellen wurden bereits von HEYROVSKÝ UND BABIČKA bei Proteinen beschrieben[3]. Positivierende Wirkungen auf Wasserstoffstufen starker Säuren in wässrigen Lösungen werden vor allem bei Anwesenheit von Stickstoffbasen, wie z.B. Chinin, beobachtet[4,5]. Die katalytische Wasserstoffentwicklung durch diese Substanzen erfuhr verschiedene Deutungen durch eine Reihe von Autoren[5–11].

In der vorliegenden Arbeit wird der Einfluss des N,N-Dimethyl-*p*-phenylendiamins auf die polarographische Wasserstoffabscheidung aus verhältnismässig schwachen organischen Säuren, wie z.B. Benzoesäure oder Chlorphenole, sowie auf die polarographische Reduktionsstufe von Nitroverbindungen in wasserfreiem Methanol beschrieben.

EXPERIMENTELLES

Die polarographischen Untersuchungen wurden unter Verwendung der von HOLLECK UND BECHER[12] beschriebenen Messzelle durchgeführt, bei der die Messlösung über zwei Glasfritten und dazwischengeschaltete nichtwässrige Elektrolytlösung mit einer wässrigen gesättigten Kalomelelektrode (GKE) in Verbindung steht; auf diese sind die Potentialangaben bezogen. Auch mit einer normalen polarographischen Zelle wurden jedoch zufriedenstellende Ergebnisse erzielt. Die Zelle wurde auf 20° thermostatiert. Als Leitsalz diente wegen seiner guten Löslichkeit in Methanol 0.1 *N* Lithiumchlorid. Wegen der leichten Oxidierbarkeit des N,N-Dimethyl-*p*-phenylendiamins wurde diese Substanz in vorher entlüftetem Methanol gelöst und im Dunkeln aufbewahrt.

ERGEBNISSE

In Abb. 1. sind polarographische Strom–Spannungs-Kurven von Benzoesäurelösungen wiedergegeben. Ohne Katalysatorzusatz ist die Säurestufe schlecht ausgeprägt (Kurve 1). Mit N,N-Dimethyl-*p*-phenylendiamin als Katalysator bildet sich die Stufe unter Vorverlagerung und Auftreten eines Maximums aus (Kurve 2). Das Maximum lässt sich durch Inhibitoren, wie z.B. Triphenylphosphin oder Triphenylphosphinoxid, unterdrücken (Kurve 3). Ähnlich wie das N,N-Dimethyl-*p*-phenylendiamin, aber wesentlich schwächer, zeigt sich auch N,N-Dimethylanilin katalytisch wirksam (Kurve 4).

Der Grenzstrom in Anwesenheit von N,N-Dimethyl-*p*-phenylendiamin ist gut ausgebildet, besonders in Gegenwart von Maximadämpfern wie Triphenylphosphin, und durch die Diffusion der Säuremoleküle bestimmt. Die Stufenhöhe ist proportional der Säurekonzentration im untersuchten Bereich von 10^{-4} *M* bis 10^{-2} *M*; sie bleibt bei Variation der Katalysatorkonzentration von äquimolarer Menge bis zu einem Hundertstel der Säuremenge erhalten. Mit abnehmender Katalysatorkonzentration verringert sich nur die Höhe des Maximums. Diese Stufe erweist sich somit in Gegenwart von N,N-Dimethyl-*p*-phenylendiamin zur polarographischen Bestimmung von Säuren in Methanol geeignet.

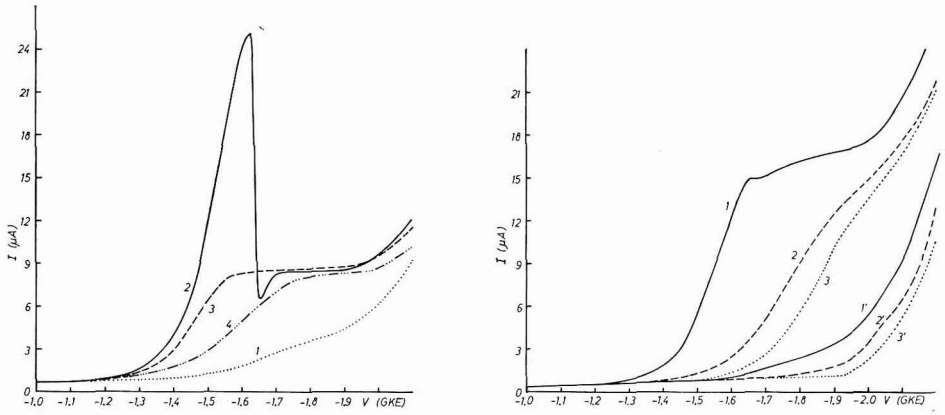

Abb. 1. Strom–Spannungs-Kurven von 0.002 *M* Benzoesäure in Methanol (0.1 *N* LiCl). (1) ohne Zusatz; (2) mit 0.001 *M* N,N-Dimethyl-*p*-phenylendiamin; (3) mit 0.001 *M* N,N-Dimethyl-*p*-phenylendiamin und 0.1% Triphenylphosphin; (4) mit 0.001 *M* N,N-Dimethylanilin.

Abb. 2. Strom–Spannungs-Kurven von 0.004 *M* Chlorphenolen in Methanol (0.1 *N* LiCl) bei Zusatz von 0.001 *M* N,N-Dimethyl-*p*-phenylendiamin. (1) 2,4,6-Trichlorphenol; (2) 2,4-Dichlorphenol; (3) 2-Chlorphenol; (1′–3′): dazugehörige Polarogramme ohne Katalysator.

Bei Chlorphenolen, die ohne Katalysator keine deutliche Wasserstoffstufe ergeben, erscheint in Anwesenheit des N,N-Dimethyl-*p*-phenylendiamins—besonders ausgeprägt bei Trichlorphenol—eine auswertbare polarographische Stufe (Abb. 2).

Die katalytische Wirkung des N,N-Dimethyl-*p*-phenylendiamins in Methanol worin die genannten Säuren nur in ganz geringer Menge dissoziiert sind, lässt sich durch einen Katalysemechanismus nach MAJRANOVSKII[5] wie folgt beschreiben:

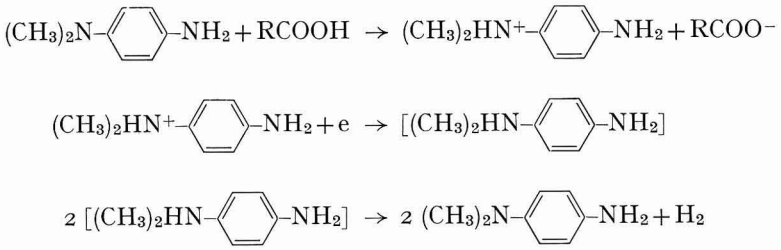

Da der Grenzstrom durch die Diffusion der Säuremoleküle bedingt ist und keine Abhängigkeit von der Katalysatorkonzentration zeigt, kann auf eine Reaktion mit dem Katalysator an der Elektrodenoberfläche geschlossen werden.

Diese Wirkung zeigt sich auch in wässrigen Lösungen, wo ohne Pufferung ebenfalls die Benzoesäurestufe positiviert wird und in gepufferten Lösungen ein früherer Grenzanstieg zu beobachten ist.

Bemerkenswerte Resultate werden erhalten, wenn der katalytische Einfluss des N,N-Dimethyl-p-phenylendiamins auf die Protonenübertragung bei der Reduktion aromatischer Nitroverbindungen in Methanol in Gegenwart schwacher organischer Säuren, wie Benzoesäure oder Chlorphenole, untersucht wird. In einer früheren Arbeit über die polarographische Reduktion aromatischer Nitroverbindungen in methanolischen Lösungen wurde gefunden, dass bei Zusatz organischer Säuren, deren pK_a-Wert in wässrigen Lösungen grösser als 7 ist, keine Vorstufe auftrat[13]. Während

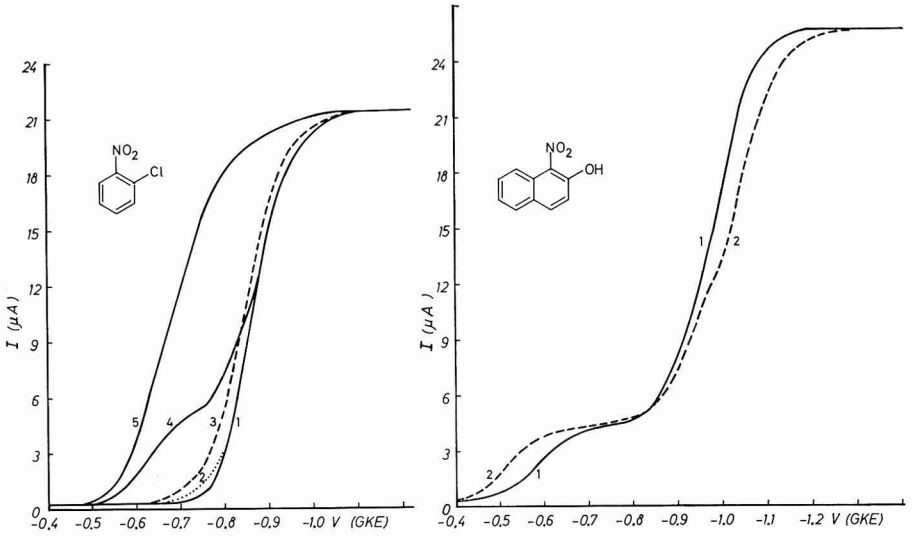

Abb. 3. Strom–Spannungs-Kurven von 0.001 M o-Nitrochlorbenzol in Methanol (0.1 N LiCl). (1) ohne Zusatz; (2) mit 0,001 M 2,4-Dichlorphenol; (3) mit 0.004 M Dichlorphenol; (4) mit 0.001 M Dichlorphenol und 0.001 M N,N-Dimethyl-p-phenylendiamin; (5) mit 0.004 M Dichlorphenol und 0.001 M N,N-Dimethyl-p-phenylendiamin.

Abb. 4. Strom–Spannungs-Kurven von 0.001 M 1-Nitro-2-naphthol in Methanol (0.1 N LiCl). (1) ohne Zusatz; (2) mit 0.001 M N,N-Dimethyl-p-phenylendiamin.

mit 2,4,6-Trichlorphenol eine Vorstufe erschien, wurde bei 2,4-Dichlorphenol im allgemeinen keine Wirkung gefunden. Da N,N-Dimethyl-*p*-phenylendiamin auch bei Dichlorphenol eine katalytische Wirkung auf die Wasserstoffabscheidung zeigt, lag es nahe, zu untersuchen, ob eine derartige Protonenübertragung auch zum Auftreten einer Vorstufe mit kleinen Mengen von 2,4-Dichlorphenol bei der Reduktion von Nitroverbindungen führt. In Abb. 3 wird als Beispiel die Wirkung von Dichlorphenol auf die Reduktionsstufe von *o*-Nitrochlorbenzol mit und ohne Zusatz von N,N-Dimethyl-*p*-phenylendiamin gezeigt.

Eine äquimolare Menge Dichlorphenol bewirkt ohne Katalysator praktisch keine Vorstufe (Kurve 2) und eine vierfache Menge nur eine geringe Positivierung der Gesamtstufe (Kurve 3). In Gegenwart von N,N-Dimethyl-*p*-phenylendiamin dagegen tritt bei den gleichen Dichlorphenolkonzentrationen eine gut ausgebildete Vorstufe (Kurve 4) bzw. eine starke Vorverlagerung der Gesamtstufe (Kurve 5) auf, wie dies ohne Katalysator bei wesentlich stärkeren Säuren der Fall ist.

Diese Reduktionserleichterung kann durch eine Protonenübertragung ähnlich der vorher beschriebenen katalytischen Wasserstoffabscheidung erklärt werden:

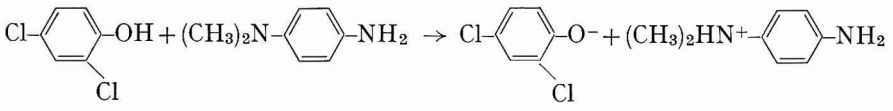

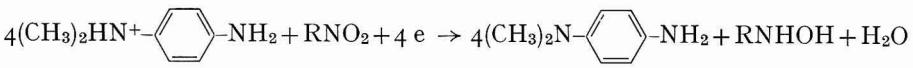

Bei stärkeren Säuren als Dichlorphenol, die in äquimolarer Menge eine Vorstufe erzeugen, wie z.B. Benzoesäure oder Trichlorphenole, wird entsprechend eine weitere Positivierung dieser Vorstufe durch N,N-Dimethyl-*p*-phenylendiamin beobachtet.

Der katalytische Einfluss des N,N-Dimethyl-*p*-phenylendiamins bleibt erhalten, wenn die Nitroverbindung selbst als schwacher Protonendonator zu fungieren vermag, wie es bei Nitrophenolen oder Nitronaphtholen der Fall ist. Bei der polarographischen Reduktion dieser Verbindungen in Methanol treten infolge erleichterter Reduktion durch die Eigenprotonisierung auch ohne Katalysator Vorstufen auf, die ein Sechstel der Gesamtstufenhöhe betragen, da es sich hier um eine sechselektronige Reduktion bis zum Amin handelt (Abb. 4, Kurve 1). Diese Vorstufen lassen sich ebenfalls durch N,N-Dimethyl-*p*-phenylendiamin vorverlagern (Abb. 4, Kurve 2).

Bei Nitroverbindungen, die selbst starke Protonendonatoren sind, wie z.B. Nitrobenzoesäuren, ist keine weitere Reduktionserleichterung durch den Katalysator festzustellen. Die zweite Stufe bei Nitrophenolen oder Nitronaphtholen, die der Reduktion der verbleibenden Anionen ohne Beteiligung von Protonen entspricht, zeigt in allen Fällen einen Inhibitionseffekt durch N,N-Dimethyl-*p*-phenylendiamin mit einer angedeuteten Zweiteilung (Abb. 4, Kurve 2), welche auf der erschwerten Weiterreduktion des primär gebildeten Radikals beruht[14].

Der Alexander von Humboldt-Stiftung danken wir bestens für ein dem einen von uns (D.J.) gewährtes Stipendium, dem Bundesministerium für Wirtschaft und der Gesellschaft Deutscher Chemiker für Unterstützung durch Bereitstellung von Mitteln.

ZUSAMMENFASSUNG

In Gegenwart organischer Säuren—auch schwacher, wie z.B. Chlorphenole—zeigt N,N-Dimethyl-p-phenylendiamin in methanolischen Lösungen eine katalytische Wirkung auf die Wasserstoffabscheidung, die zu gut auswertbaren polarographischen Stufen führt. Eine weitere katalytische Wirkung dieser Verbindung auf den infolge Protonenübertragung vorverlagerten Stufenanteil bei der polarographischen Reduktion aromatischer Nitroverbindungen in Gegenwart von Protonendonatoren wird beschrieben. Durch schwache organische Säuren, die in kleinen Mengen keine positivierende Wirkung zeigen, wird eine solche bei Zusatz von N,N-Dimethyl-p-phenylendiamin erzielt.

SUMMARY

In methanolic solutions of organic acids, N,N-dimethyl-p-phenylenediamine catalyses the hydrogen evolution reaction at the DME, and a well-defined polarographic wave is recorded. A similar catalytic effect is also observed in the reduction of aromatic nitro compounds in presence of acids. N,N-dimethyl-p-phenylenediamine causes either the development of a pre-wave or its shift to more positive potentials when it is originally present. The height of this pre-wave is proportional to the acid content of the solution.

LITERATUR

1 L. Holleck, D. Jannakoudakis und A. Wildenau, *Electrochim. Acta*, im Druck.
2 D. Jannakoudakis und A. Wildenau, *Z. Naturforsch.*, im Druck.
3 J. Heyrovský und J. Babička, *Collection Czech. Chem. Commun.*, 2 (1930) 370.
4 W. Hans und W. Jentsch, *Z. Elektrochem.*, 56 (1952) 648.
5 S. G. Majranovskii, *Izv. Akad. Nauk SSSR, Otd. Khim. Nauk*, (1953) 615, 805.
6 J. Heyrovský, *Chem. Listy*, 31 (1937) 440; *Collection Czech. Chem. Commun.*, 9 (1937) 273, 345.
7 J. Heyrovský, *Polarographie*, Springer, Wien, 1941, p. 135.
8 A. N. Frumkin und E. P. Andrejewa, *Dokl. Akad. Nauk SSSR*, 114 (1957) 1272.
9 M. von Stackelberg und H. Fassbender, *Z. Elektrochem.*, 62 (1958) 834.
10 M. von Stackelberg, W. Hans und W. Jentsch, *Z. Elektrochem.*, 62 (1958) 839.
11 H. W. Nürnberg, in I. S. Longmuir (Ed.), *Advances in Polarography*, Vol. II, Pergamon, Oxford 1960, p. 694.
12 L. Holleck und D. Becher, *J. Electroanal. Chem.*, 4 (1962) 321.
13 D. Jannakoudakis und A. Wildenau, *Z. Naturforsch.*, im Druck.
14 B. Kastening, *Naturwissenschaften*, 49 (1962) 130.

Elsevier Publishing Company, Amsterdam – Printed in The Netherlands

SHORT COMMUNICATIONS

Bibliography on the uses of propylene carbonate in high energy, density batteries

Papers on the electrochemistry of propylene carbonate are now being published, *e.g.*, ref. 1–6. In a recent article on the subject[1], it was stated that "the use of propylene carbonate in electrochemistry has been limited to studies of conductivities and some polarographic and impedance measurements". A good deal of information on this solvent is to be found, however, in reports to various U.S. Government agencies on the development of batteries employing aprotic, organic solvents and inorganic solutes as the electrolytes. Lithium is generally used as the negative plate, and considerable emphasis is placed on propylene carbonate as the electrolyte solvent.

These reports describe work in progress and may thus be incomplete. Nevertheless, a good deal of information is given regarding the purity of these solvents, analytical procedures, precautions in handling and the development of satisfactory reference electrodes.

It should be noted that propylene carbonate is supplied commercially as a relatively impure material and is difficult to purify to a level suitable for electrode studies.

A list of the government reports available to the general public, on the subject of aprotic organic solvents for batteries is given below. It includes the report title, principal author, corporate author, funding agency, date and acquisition number. When possible, only the final report to a given contract is listed; otherwise the available quarterly progress reports are tabulated. Successive contracts are designated by the letters (a) and (b) *e.g.*, 1, 1a.

These reports can be ordered from *Clearinghouse for Federal Scientific and Technical Information*, Springfield, Virginia, 22151.

Tyco Laboratories, Inc.,
Waltham, Mass. (U.S.A.)

RAYMOND JASINSKI

1 R. NELSON AND R. ADAMS, *J. Electroanal. Chem.*, 13 (1967) 184.
2 R. MEREDITH AND C. TOBIAS, *J. Electrochem. Soc.*, 108 (1961) 286.
3 L. MARCOUX, K. PRATER, B. PRATER AND R. ADAMS, *Anal. Chem.*, 37 (1965) 1446.
4 P. KRONICK AND R. FUOSS, *J. Am. Chem. Soc.*, 77 (1955) 6114.
5 L. CHOW AND R. FUOSS, *J. Am. Chem. Soc.*, 80 (1958) 1095.
6 R. FUOSS AND E. HIRSCH, *J. Am. Chem. Soc.*, 82 (1960) 1013.

Received January 16th, 1967

Title		Principal author	Agency	Report	Date	Acquisition no.
1.	*Research and Development of a High Capacity Non-Aqueous Secondary Battery*	R. SELIM, P. R. Mallory & Co., Burlington, Mass.	NASA	Final	Sept. 1964	N66-22942
1a.				Final	Dec. 1965	N66-35218
2.	*Development of High Energy, Density Primary Batteries*	W. MEYERS, Livingston Electronics, Montgomeryville, Pa.	NASA	4th Q	June 1966	N66-37685
				3rd Q	Mar. 1966	N66-31223
				2nd Q	Dec. 1965	N66-23463
2a.				1st Q	Oct. 1965	N66-15342
				Final	June 1965	N66-29446
2b.				Final	March 1964	N64-31454
3.	*A Program to Develop a High Energy, Density Primary Battery*	W. ELLIOTT, Globe Union, Inc., Milwaukee, Wisc.	NASA	8th Q	June 1966	N66-37038
				7th Q	Mar. 1966	N66-25063
				6th Q	Dec. 1965	N66-16139
				5th Q	Sept. 1965	N66-11247
				4th Q	Mar. 1965	N65-29824
				3rd Q	Dec. 1964	N65-23703
				2nd Q	Sept. 1964	N65-11518
4.	*Investigation of Electrochemistry of High Energy Compounds in Organic Electrolytes*	R. FOLEY, The American Univ., Washington, D.C.	NASA	3rd(suppl.)	April 1966	N66-37304
				3rd Q	April 1966	N66-35664
				2nd Q	Oct. 1965	N66-14600
				1st Q	April 1965	N65-27831
5.	*Electrochemical Characterization of Systems for Secondary Battery Applications*	M. SHAW, Whittaker Corp., Narmco R &D Div., San Diego, Calif.	NASA	1st Q	July 1966	N66-37286
6.	*Properties of Non-Aqueous Electrolytes*	R. KELLER, Rocketdyne Canoga Park, Calif.	NASA	1st Q	Sept. 1966	NASA-CR72106
7.	*High Energy Electrochemical Battery System Using Organic Electrolytes*	H. KNAPP	USA/ECOM		Oct. 1965	AD627215
8.	*High Energy System*	D. BODEN, Electric Storage Battery Co., Yardley, Pa.	USA/ECOM	Final	Sept. 1966	AD639709
				3rd Q	March 1966	AD634491
				2nd Q	Jan. 1966	AD630691
				1st Q	Sept. 1965	AD628961

9. *High Energy Battery System Study*	J. FARRAR, Rocketdyne, Canoga Park, Calif.	USA/ECOM	Final 7th Q 6th Q 5th Q 4th Q 3rd Q 2nd Q 1st Q	June 1965 Mar. 1965 Dec. 1964 Sept 1964 June 1964 Mar. 1964 Dec. 1963 Sept. 1963	AD622818 AD617714 AD616385 AD458472 AD450559 AD452714 AD435627 AD429290
10. *New Cathode–Anode Couples Using Non-Aqueous Electrolytes* 10a.	J. CHILTON, Lockheed Missile & Space Agcy., Sunnyvale, Calif.	AFAPL	Summary Summary	Oct. 1963 Apr. 1962	AD425876 AD277171
11. *Limited Cycle Secondary Battery Using Lithium Anodes*	M. BAUMAN, see 10	AFAPL	Summary	May 1964	AD601128
12. *Lithium–Silver Chloride Secondary Battery Investigation*	J. CHILTON, see 10	AFAPL	Summary	Feb. 1965	AD612189
13. *Lithium–Nickel Halide Secondary Battery Investigation*	A. LYALL, Gulton Industries, Metuchen, N.J.	AFAPL	Summary	Jan. 1965	AD612492
14. *Lithium–Moist Air Battery*	W. ELLIOTT, Globe-Union Inc., Milwaukee, Wisc.	USA ERDL	1st Q	Oct. 1966	AD642248
15. *Evaluation of Rechargeable Lithium–Copper Chloride Organic Electrolyte Battery*	M. RAO, P.R. Mallory & Co., Burlington, Mass.	USA/ERDL	1st Q	Sept. 1966	AD643378
16. *Electrochemical Studies in Cyclic Esters*	W. HARRIS, Univ. of Calif., Berkeley, Calif.	AEC	Thesis	July 1958	UCRL8381

Note sur l'activation anodique de la surface du métal support de l'électrode à hydrogène

Pour étudier l'influence d'un certain paramètre sur le processus électrochimique de l'électrode à hydrogène, il faut que la surface du métal support ait toujours les mêmes propriétés.

Parmi les méthodes proposées pour la préparation de la surface métallique (l'activation de la surface) l'anodisation est la plus utilisée.

La manière d'appliquer l'anodisation est dictée par la nature du métal, car les métaux nobles une fois activés maintiennent cette activité, contrairement aux autres métaux pour lesquels l'activité change en fonction du temps; de telle sorte que l'on utilise l'anodisation soit au début de chaque expérience effectuée avec l'électrode à hydrogène par une ou plusieurs impulsions anodiques[1,2], soit même au cours de l'expérience en employant le courant électrique onde rectangulaire[3].

On a signalé dans plusieurs travaux l'amélioration de la réproductibilité des résultats expérimentaux due au remplacement du courant électrique continu par le courant onde rectangulaire[3], mais à notre connaissance, d'autres conséquences de ce remplacement, n'ont pas été communiquées.

Dans cette Note on présente les résultats d'une comparaison courant continu (c.c.)–courant onde rectangulaire (c.o.r.) du point de vue de la valeur du facteur de séparation isotopique H–D par électrolyse α.

$$\alpha = N/n$$

où N = la concentration isotopique de la solution;

n = la concentration isotopique de l'hydrogène dégagé (pour N, $n \ll 1$)

ainsi qu'une étude de la valeur du facteur de séparation α, en fonction des caractéristiques du c.o.r.: de la durée de l'alternance positive (c'est à dire la durée de l'anodisation) et de la période (la fréquence de l'anodisation).

On a employé du nickel dans des solutions aqueuses deutérées de NaOH.

Matériels et méthodes

La cellule d'électrolyse est représentée dans la Fig. 1. Elle permet la délimitation de la surface de la plaquette de nickel, exposée au courant électrique (1 cm^2) et le remplacement facile des plaquettes et de la solution.

Les seuls matériaux en contact avec la solution sont Ni, Pt, plexiglas et polyéthylène. La cellule a été thermostatée par plongement dans un bain d'eau maintenu à la température $T = 25 \pm 0.15°$. La solution a été agitée seulement par les gaz dégagés.

Au début de chaque série d'expériences la cellule et les électrodes ont été soigneusement nettoyées, rincées maintes fois à l'eau bidistillée et séchées par un courant d'air chaud. Au cours des expériences effectuées avec la même plaquette, pendant les pauses, la cellule est restée tantôt remplie soit avec la solution utilisée soit avec de l'eau bidistillée, tantôt vidée et séchée. Le remplacement de la solution a été précédé seulement du rinçage et du séchage de la cellule et des électrodes.

Pour éviter des erreurs relatives on a découpé les plaquettes de nickel d'une seule plaque et toutes les solutions électrolytiques ont été préparées en partant d'une seule eau deutérée (2.6% D_2O), bidistillée et d'une même boîte à NaOH p.a. Merck. La concentration, N, de la solution, a été calculée en négligeant le deutérium contenu

dans NaOH (supposé concentration naturelle) par rapport à celui contenu dans l'eau deutérée (concentration 2.6%).

L'analyse spectroscopique a mis en évidence de très faibles traces de Fe, Mn et Si dans la plaque de nickel utilisée. Les expériences ont été effectuées en employant

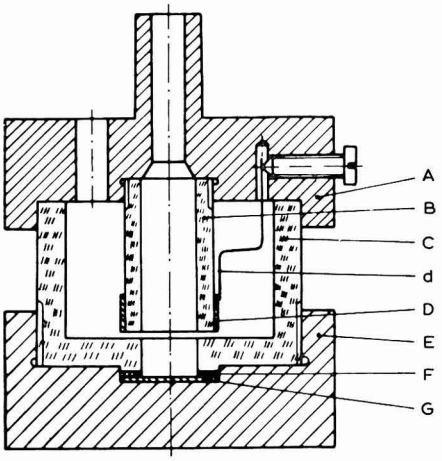

Fig. 1. Cellule d'électrolyse (A, E), couvercles détachables; (B), cylindre séparateur des compartiments à gaz; (C), corps de la cellule; (D), anode (Pt) attachée au couvercle A par le fil métallique (d) (Pt); (F), garniture en polyéthylène; (G), plaquette de Ni; (///), cuivre nickelé; (''' '''), plexiglas.

des plaquettes exposées préalablement au c.o.r. jusqu'à la stabilisation de la valeur du facteur de séparation, cette valeur étant commune pour toutes les plaquettes, indépendamment de l'état initial de la surface (mate ou lisse, uniforme ou présentant des raies accidentelles)[4].

On a employé du c.o.r. aux alternances inégales en ce qui concerne la durée, l'alternance positive étant très courte par rapport à la période du courant (0.1–0.6 sec par rapport au minimum 28 sec) pour assurer le débit continu d'hydrogène nécessaire à l'analyse par chromatographie gazeuse. L'amplitude du c.o.r. à été toujours 1 A.

Chaque détermination du facteur de séparation a été effectuée avec de la solution fraîche (1 cm^3). Durant les 25 premières min d'électrolyse, on a analysé 5 fois l'hydrogène dégagé (toutes les 5 min) ce qui a permis le calcul d'une valeur moyenne de la concentration isotopique, n*. Le facteur de séparation a été calculé avec cette valeur moyenne, n.

Résultats

On a porté dans la Fig. 2 les valeurs des facteurs de séparation déterminées successivement avec la même plaquette, en utilisant tantôt le c.o.r. (période 28 sec, alternance positive 0.1 sec) tantôt le c.c. Sur l'abscisse on a porté le nombre de l'expérience en ordre chronologique. Entre les deux cas (c.c.–c.o.r.) on remarque une

* *Note.* On a obtenu n = const. durant les premières 30 min d'électrolyse bien que l'augmentation de la concentration isotopique de la solution, à cause du fractionnement isotopique, devait provoquer la croissance de la concentration isotopique de l'hydrogène dégagé; on suppose que l'effet du fractionnement est compensé par la modification du facteur de séparation à cause de l'augmentation de la concentration de NaOH, chose prouvée par des travaux en cours.

différence évidente autant en ce qui concerne la valeur du facteur de séparation, que la durée de l'établissement d'une valeur constante.

La modification de la valeur du facteur de séparation sous l'action du c.o.r., par rapport au c.c., indique peut être soit une amélioration de l'échange isotopique

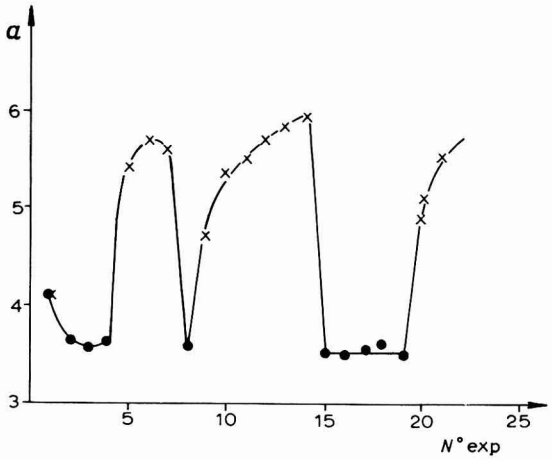

Fig. 2. Comparaison c.c.–c.o.r. Le facteur de séparation en fonction du nombre d'expériences effectuées avec la plaquette: (●), c.o.r. (période 28 sec, amplitude positive 0.1 sec); (×), c.c.

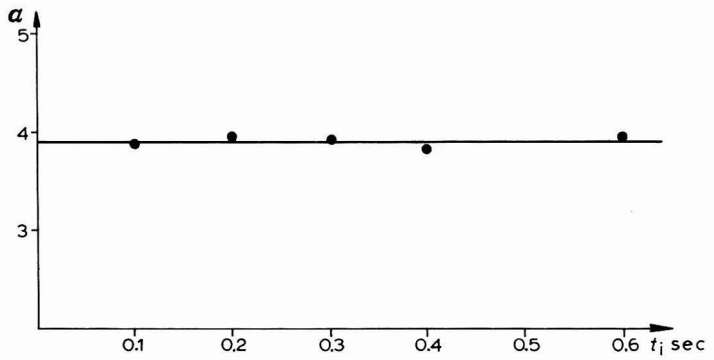

Fig. 3. Le facteur de séparation en fonction de la durée de l'alternance positive du c.o.r. (période, 29 sec.).

entre l'hydrogène dégagé et l'eau, catalysé par la surface de nickel[5], soit une différence de mécanisme d'électrode à cause de la présence de l'oxygène.

La valeur du facteur de séparation a été constante par rapport à la durée de l'alternance positive du c.o.r. (Fig. 3). Par contre, le prolongement de la période a été suivi aussitôt par un changement de la valeur du facteur de séparation (Fig. 4). Ici, les numéros accompagnant les points représentent l'ordre chronologique des expériences. Chaque point porté dans les Figs. 3 et 4 représente la moyenne de 3–5 valeurs individuelles des facteurs de séparation.

En particulier, on doit remarquer que le nombre d'impulses anodiques pendant les 5 min d'accumulation d'un échantillon de gaz n'est pas constant; il décroît de 15 à 1, quand la période augmente de 20 à 300 sec.

La durée d'établissement d'une valeur constante du facteur de séparation à la suite d'une modification de la période du c.o.r. a été toujours au-dessous de 5 min, ainsi que le procédé utilisé n'a pas rendu possible sa mise en évidence.

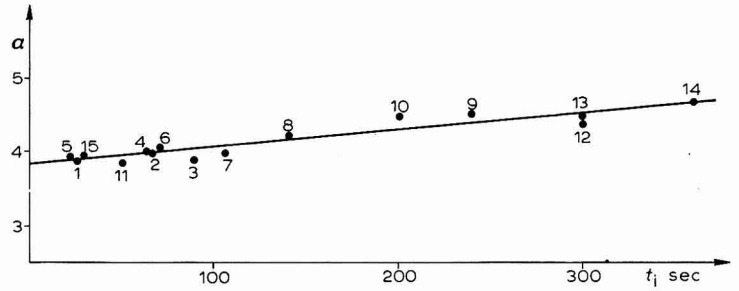

Fig. 4. Le facteur de séparation en fonction de la durée de la période du c.o.r. (alternance positive, 0.1 sec).

Conclusions

En employant le c.o.r. pour maintenir une activité constante de la surface de la cathode (nickel) au cours du processus d'électrolyse, on modifie la valeur du facteur de séparation isotopique H–D, par rapport à l'électrolyse en c.c. Cette modification est déterminée par la période du c.o.r. et diminue quand on augmente la période. La durée de l'alternance positive (0.1–0.6 sec) n' a aucune influence sur la valeur du facteur de séparation.

Institut de Physique Atomique EVELINA PALIBRODA
Cluj (Roumanie)

1 J. O'M. BOCKRIS, I. A. AMMAR ET A. K. M. S. HUQ, *J. Phys. Chem.*, 61 (1957) 879.
2 J. O'M. BOCKRIS ET B. E. CONWAY, *Record Chem. Progr.*, 25 (1964) 31.
3 H. VAN BUTTLAR, *Ber. Bunsenges, Physik. Chem.*, 67 (1963) 650.
4 E. PALIBRODA, en cours de parution dans *Rev. Chim. Bucharest.*
5 P. RÜETSCHI ET G. P. LEWIS, *J. Phys. Chem.*, 8 (1966) 1487.

Reçu le 22 novembre, 1966

J. Electroanal. Chem., 15 (1967) 92–95

Comments on a recent paper, "Experimental and theoretical examination of methods of obtaining double-layer parameters" by J. O'M. Bockris *et al.*[1]

In a recent paper BOCKRIS and co-workers[1] have suggested that the differential capacity of the electrical double layer at the mercury–solution interface as measured by the a.c. impedance method is not identical with the thermodynamic capacity obtained by differentiation of the Lippman equation. This unusual suggestion appears to be based in large part on a comparison of measured capacities for aqueous HCl

solutions with values calculated from the corresponding electrocapillary curves by numerical double differentiation. The results of this computation fail to show the well-known minimum in the diffuse-layer capacity close to the potential of zero charge for dilute solutions, an observation which apparently has led BOCKRIS *et al.* to the conclusion that the measured capacity in the vicinity of the p.z.c. is too low. The supposed error in the capacity is attributed not to experimental error but rather to a fundamental breakdown in the thermodynamic relationship between the differential capacity and the interfacial tension. This viewpoint, however, cannot be accepted for several reasons. Firstly, the failure of the electrocapillary measurements to show the fine detail of the capacity–potential curve after two numerical differentiations of the experimental data is hardly surprising; on the contrary it is surprising that the general agreement found is so good. Secondly, the arguments advanced to explain why the capacity measured by the a.c. method should differ from the differentiated electrocapillary measurements are less than reasonable. Thus it is not possible, as is assumed by BOCKRIS *et al.*, to redistribute or to reorient charged or dipolar species without causing a compensating change in the composition of the double layer, provided of course that the system remains in equilibrium. This is particularly clear in the process mentioned in ref. 1 whereby an ion is translated from the diffuse layer into the inner layer where it becomes specifically adsorbed. Such a process could not occur without redistribution of the coulombically held charge in the diffuse layer and a consequent change in the ionic surface excesses. The potential excursion producing such a change would certainly affect the interfacial tension except under conditions where the rate of the potential variation were comparable with the rate of relaxation of the ions and dipoles in the double layer, *i.e.*, under non-equilibrium conditions. There is no evidence to suggest that relaxation effects of this kind would be found at frequencies below 1 Mc in this type of system. Furthermore, the reorientation of adsorbed dipoles by the applied field would lead to a *larger* capacity since the potential generated by the dipoles would oppose the applied potential, resulting in a smaller change of the potential difference across the double layer for a given variation of the electrode charge. The analogy between such effects and the phenomenon of faradaic rectification seems somewhat obscure. Although it is true that the non-linearity of the capacity–potential curve can lead to errors in the measured capacity, it can easily be shown that the tendency is to smooth out rather than to accentuate the curvature. Such errors have nothing to do with the detailed structure of the double layer but depend only on the form of the potential dependence of the capacity. In any case, errors of this kind can be reduced to a negligible level by restricting the amplitude of the applied a.c. signal[2]. There is no reason to suppose, therefore, that the measured capacity will be in serious error providing the frequency and the amplitude of the applied a.c. are kept sufficiently small. This view is reinforced by the fact that the anomalous results of BOCKRIS *et al.* can easily be shown to be due to experimental errors.

The unreliability of the electrocapillary data in ref. 1 at the lower concentrations is suggested by the plots in Fig. 1 where the interfacial tension (γ) is plotted against the potential measured with respect to the anion-reversible reference electrode (E^-). According to Fig. 1 the 0.01 N and 0.03 N curves cut the 0.1 N and 0.3 N curves in several places. It is clear, therefore, that the observed variation of γ with concentration at constant E^- is complex. This is confirmed by interpolating γ at constant E^- and

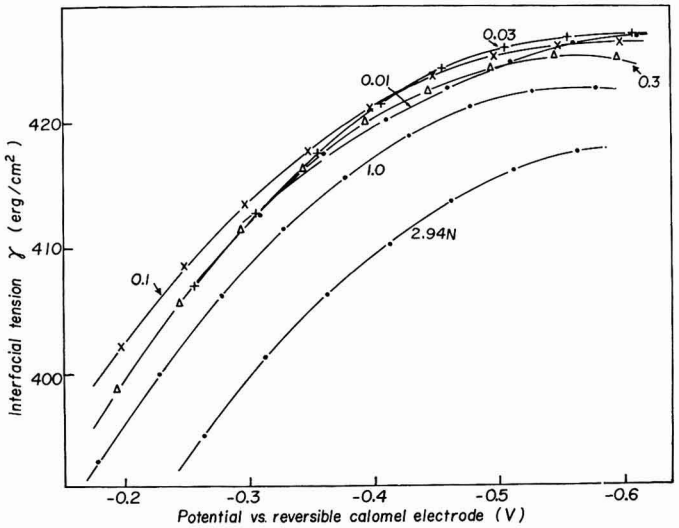

Fig. 1. Electrocapillary data of BOCKRIS *et al.*[1] for aq. HCl solns. at 25°. The interfacial tension is plotted against the potential measured with respect to a calomel electrode in the same soln.

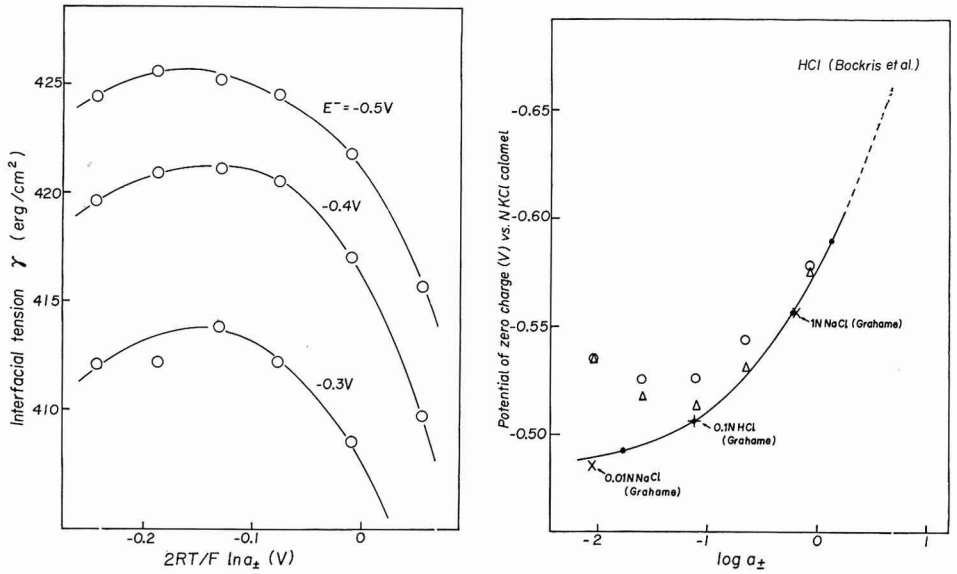

Fig. 2. Values of the interfacial tension interpolated at constant E^- from the plots in Fig. 1 and plotted against the chemical potential of HCl in soln.

Fig. 3. Comparison of zero charge potentials given by BOCKRIS *et al.*[1] for aq. HCl solns. (○, electrocapillary; △, streaming electrode) with published data of GRAHAME AND PARSONS for KCl[4], NaCl[5] and HCl[5] solns. at 25°. All potentials are referred to the N KCl calomel scale. The curve is drawn through the KCl points.

plotting the resulting values of γ against $2RT/F \cdot \ln a_{\pm}$ (Fig. 2). According to Fig. 2, the interfacial tension *increases* with the HCl concentration at the low concentration end and passes through a maximum value close to 0.1 N. The slope of this plot is

related to the surface excess of cations (Γ^+) by the well-known thermodynamic relationship[3]

$$-(\partial\gamma/\partial\mu)_{E^-} = \Gamma^+$$

It therefore appears according to Fig. 2, that the cation is repelled from the electrode in 0.01 N HCl by an amount several times larger than the *limiting* value (0.59 μC/cm^2) predicted by diffuse-layer theory for a *non-specifically adsorbed* electrolyte. Such behavior is quite unknown in previously studied systems. In KCl solutions in particular, the cation is positively adsorbed at all concentrations and at all potentials according to the results of GRAHAME AND PARSONS[4]. The anomalous curvature in Fig. 2 would seem to be due to systematically low values of the measured interfacial tension for the most dilute solutions. Similar errors appear also at negative polarizations where the analogous plots of γ *vs.* $2RT/F \cdot \ln a_\pm$ at constant E^+ lead to impossibly large repulsion of anions at low HCl concentrations. The discrepancies are consistent with a systematic experimental error in γ of 2–3 erg/cm^2 for the 0.01 N solution and 1–2 erg/cm^2 for the 0.03 N solution.

In addition to the error in the electrocapillary measurements it is evident that the zero charge potentials given by BOCKRIS *et al.* are also in serious error, again at the lower concentrations. The zero charge potentials recalculated for a N KCl calomel scale are compared in Fig. 3 with values given by GRAHAME AND PARSONS[4] for KCl solutions. Values also measured by GRAHAME[5] for 0.1 N HCl and 0.1 N NaCl are virtually indistinguishable from the curve drawn through the KCl points; additional points for 0.01 and 1 N NaCl are within 3 mV of the line. The HCl values of BOCKRIS *et al.* obtained both from the electrocapillary curves and by streaming electrode measurements, however, lie systematically above the KCl values especially at the lower concentrations where the p.z.c. apparently shifts in the *positive* direction with increasing concentration. This is obviously an impossible result. Comparison with the KCl curve shows that the reported value of the p.z.c. for the 0.01 N solution is too negative by 45 mV. The same is true also for the data given elsewhere by WROBLOWA, BOCKRIS AND KOVAC[6] for LiCl, RbCl and CsCl which are shown in Fig. 4*. The worst discrepancy here is found for 0.01 M LiCl for which the reported p.z.c. lies 75 mV above the KCl curve. The sign and magnitude of this discrepancy suggests strongly that the electrocapillary curve is depressed on the anodic side, an effect that has been observed previously[7,8]. The discrepancies in the HCl data which were also obtained from streaming electrode measurements are more difficult to understand. Although no effort was apparently made to vary the mercury flow rate during these measurements, a flow rate which is too low usually results in a p.z.c. which is too positive, whereas the observed discrepancy is in the opposite direction**.

* The surface charge data for these systems given in ref. 6. are reported for potentials measured against a saturated calomel electrode but denoted E^- *vs.* S.C.E. which is self-contradictory. On the assumption that the S.C.E. scale is correct, the p.z.c. for 0.01 N LiCl is too negative by $\sim$230 mV by comparison with the KCl data. If on the other hand the reference electrode is assumed to be a calomel electrode in the same solution, the error is reduced to the comparatively modest level of 75 mV. The values of the p.z.c. given in Fig. 4 have been calculated on this assumption.

** The practice of shunting the cell with a condenser during streaming electrode measurements does not seem a good one since the capacitance will presumably load the circuit. Under conditions where the shunt capacitance and the circuit resistance are high, a slow approach to the equilibrium potential might be anticipated. It should be pointed out, however, that this also would lead to positive errors in the measured p.z.c.

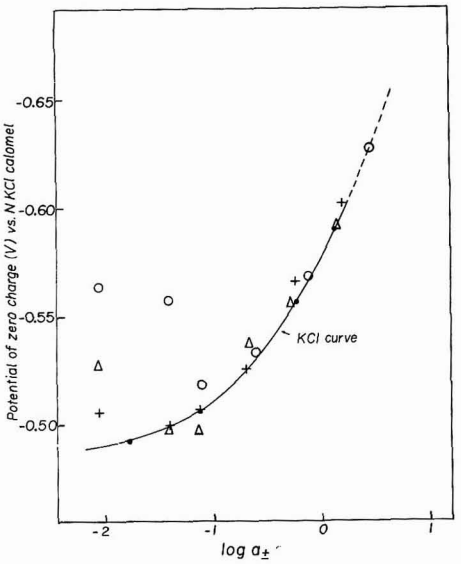

Fig. 4. Comparison of zero charge potentials given by WROBLOWA *et al.*[6] for aq. LiCl (○), RbCl (+) and CsCl (△) solutions with published data of GRAHAME AND PARSONS[4] for KCl solns. at 25°. The curve is drawn through the KCl points.

Recalculation of the interfacial tension for the 0.01 *N* HCl solution by integrating the capacity data given in ref. 1 using a zero charge potential of −0.597 V (*vs.* R.C.E.) calculated from the KCl data reduces the discrepancy with the electrocapillary data reported by BOCKRIS *et al.* from a maximum of ~7 erg/cm² to ~3 erg/cm² at the far cathodic end and increases the discrepancy from ~1 erg/cm² to ~3 erg/cm² at the far anodic end. The residual discrepancy can be accounted for by the error of 2–3 erg/cm² in the electrocapillary data noted earlier. The large discrepancies found by BOCKRIS *et al.* on the cathodic side are evidently due to the additive effects of experimental errors in γ and the p.z.c. in this region, whereas the errors are of opposite sign and tend to cancel on the anodic side. In Fig. 5, the differences between interfacial tension values calculated by double integration of capacity data and directly measured electrocapillary data are shown for a 0.0271 *M* solution of $HClO_4$[8] obtained with the apparatus described previously[9,10]. The large discrepancies reported by BOCKRIS *et al.* are absent from these measurements*. The discrepancy on the cathodic side is no more than 0.2 erg/cm² up to the hydrogen evolution potential (~ −0.8 V) although a difference of up to 1.2 erg/cm² is observed on the anodic side. This is believed due to the effects of a sticking meniscus. Similar effects have been noticed in other systems, notably NaF solutions[8] where errors of up to 30 mV in the electrocapillary maximum determined from isotension potentials can occur apparently due to depression of the interfacial tension on the anodic branch of the curve. It is

* The discrepancy on the cathodic side is also within 0.5 erg/cm² for 0.00847 *M* sodium benzenedisulfonate solution reported by PARRY AND PARSONS[11] and 0.01 *M* sodium dihydrogen phosphate described by PARSONS AND ZOBEL[7]. The latter authors also report negative deviations of up to ~25 mV in the p.z.c. determined from the electrocapillary curve as compared with the streaming electrode value and conclude for the reasons described here that the electrocapillary values are incorrect.

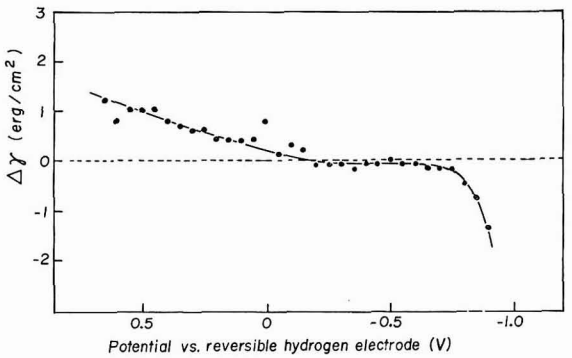

Fig. 5. Plot of the difference between the interfacial tension calcd. by double integration of the capacity and directly measured electrocapillary values for a 0.0271 *M* aq. $HClO_4$ soln. at 25°[8]. Potentials are measured with respect to a hydrogen electrode in the same soln.

evidently necessary to treat electrocapillary measurements in this region of polarization with some reserve.

It is clear from the foregoing that the accuracy of the measurements described in ref. 1 leaves something to be desired. It would appear that the subsequent discussion and far reaching conclusions are not only questionable on theoretical grounds but also cannot be sustained by the experimental measurements. BOCKRIS *et al.* have suggested (ref. 1, p. 432) "that less care need be exercised in the capacity measurements but more effort be expended on repeated determinations of the potential of zero charge...". This seems to be the most obvious conclusion to be drawn from this work.

Air Force Cambridge Research Laboratories, RICHARD PAYNE
L.G. Hanscom Field, Bedford, Mass. (U.S.A.)

1 J. O'M. BOCKRIS, K. MÜLLER, H. WROBLOWA AND Z. KOVAC, *J. Electroanal. Chem.*, 10 (1965) 416.
2 D. C. GRAHAME, ONR Report No. 14, Feb., 1954.
3 D. C. GRAHAME, *Chem. Rev.*, 41 (1947) 441.
4 D. C. GRAHAME AND R. PARSONS, *J. Am. Chem. Soc.*, 83 (1961) 1291.
5 D. C. GRAHAME, in *Electrochemical Data*, B. E. CONWAY (Ed.), Elsevier Publishing Company, Amsterdam, 1952.
6 H. WROBLOWA, J. O'M. BOCKRIS AND Z. KOVAC, *Trans. Faraday Soc.*, 61 (1965) 1523.
7 R. PARSONS AND F. G. R. ZOBEL, *J. Electroanal. Chem.*, 9 (1965) 333.
8 R. PAYNE, unpublished data.
9 G. J. HILLS AND R. PAYNE, *Trans. Faraday Soc.*, 61 (1965) 316.
10 K. M. JOSHI AND R. PARSONS, *Electrochim. Acta*, 4 (1961) 129.
11 J. M. PARRY AND R. PARSONS, *Trans. Faraday Soc.*, 59 (1963) 241.

Received March 25th, 1966

Is there a fundamental difference between stationary and non-stationary double-layer measurements? (Comments on a paper by R. Payne[1])

1. Introduction

The present authors have evaluated previously[2] double-layer parameters referring to similar polarisable electrodes, both from electrocapillary and capacity data. *The general agreement was very good,* as expected. Certain discrepancies were observed, however, in a restricted concentration and potential region. These were outside the experimental error, essentially insensitive to the values of integration constants used, and systematic. They were largest in the most dilute solution, 0.01 N.

The discrepancies disappeared when the charge density was used as the electric variable in comparing measured (electrocapillary method: γ_m) and calculated (double integration of capacity data: γ_c) interfacial tension. A speculative model was proposed to rationalise this new fact.

PAYNE's contention[1] is that the discrepancies arose from experimental errors.

A misapprehension at the basis of PAYNE's remarks must first be corrected. The error analysis upon which our conclusion was based will then be published to indicate the necessity of a modelistic interpretation; and sticking of the meniscus will be considered in more detail, to test whether a hypothesis involving it, such as Payne's, could be tenable.

It will also be examined whether, on the basis of capacity data alone, any discrepancies may arise, in order to have an independent check of the results of the comparison between directly-measured and capacity-derived surface tensions.

2. The misapprehension

At the beginning of PAYNE's paper, it is stated that the present authors based their conclusions largely on the failure to reproduce the experimental differential capacity (C_m) curves in dilute solutions by double differentiation of electrocapillary data ($\partial^2\gamma_m/\partial E^2 = -C_c$). This statement misrepresents the position. We based our conclusions on the failure to be able to reproduce the directly-measured γ_m by the γ_c obtained by double integration of C_m. Figure 1 shows such a plot (see also Figs. 2, 3 and 5 of our previous paper[2]) of $\Delta\gamma$ against $E(\Delta\gamma = \gamma_c - \gamma_m)$. In the integration procedure[2], errors are not magnified as they are in the converse differentiation procedure.

Had PAYNE concentrated upon the reported discrepancies in surface tension from the two experimental methods, and their potential dependence, it may be that he would not have come to the conclusion that experimental difficulties suffice to cover the differences observed from the solutions under a.c. and static conditions.

3. Error analysis for the measured quantities

3.1. Interfacial tension. We detail our previous statements (Ref. 2, Section Results) as follows:[3]

(*i*) Error in reading the heights, H_1 and H_2, of the mercury in the two limbs of the manometer: $2 \times (\pm 0.1$ mm);

(*ii*) Error in reading the height of the mercury in the reservoir (H_3) above the capillary tip (H_4): $2 \times (\pm 0.1$ mm);

(*iii*) Error in adjusting the position, ΔH_4, of the meniscus of the mercury above the capillary tip: less than ± 0.04 mm;

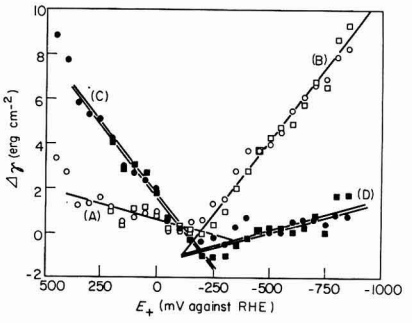

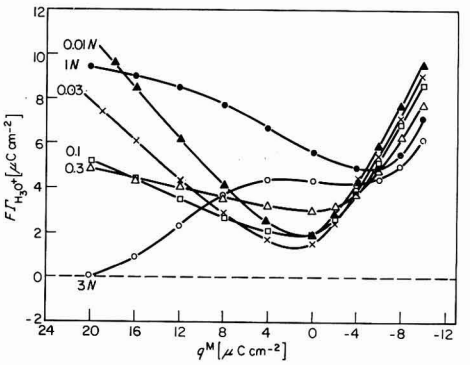

Fig. 1. Effect of the choice of the potential of zero charge upon discrepancies in the system Hg/0.01 *N* HCl. (○), (□), $E_+^{zc} = -133$ mV ($E_-^{zc} = -642$ mV); (●), (■), $E_+^{zc} = -83$ mV ($E_-^{zc} = -592$mV); circles: DEVANATHAN's values[6], squares: our values[2,3], as compared to values calculated by integration of the measured differential capacities, using either of the E^{zc} given. The difference in slopes between the lines on the anodic and cathodic sides is equivalent in either case to 1.6 μC cm^{-2}, or a discrepancy of $\Delta C = -10$ μF cm^{-2} over a region of 160 mV near E^{zc}.

Fig. 2. Excess of cations at the interface Hg/HCl aq., evaluated from differential capacity data with the aid of integration constants obtained from diffuse layer theory (ref. 2, method D). Concentrations as given in the figure.

(*iv*) Error, ∂H_5, due to the uncertainty in potential (± 1 mV), for the lower part of the electrocapillary curve only: ± 0.1 erg cm^{-2}, equivalent to ± 0.1 mm;

(*v*) Error, ∂H_6, due to a change in temperature ($\pm 0.5°$) during the measurements, on the basis of HANSEN AND WILLIAMS' data[4]: ± 0.1 erg cm^{-2}, equivalent to ± 0.1 mm;

(*vi*) Error due to the uncertainty in the absolute value of the interfacial tension[5] at E^{zc}, γ_{max}: ± 0.2 erg cm^{-2}, equivalent to ± 0.2 mm.

The i-th value of the interfacial tension was calculated as $\gamma_i = (\gamma_{max}/H_{max})\ H_i$ where H_i is the sum (taking appropriate signs) of all relevant readings. Error (v_i) affects only the absolute values of the measured interfacial tension. For the purpose of the present analysis, (γ_{max}/H_{max}) can be taken as a constant (its order of magnitude is unity), any uncertainty in it affects γ_m and γ_c in precisely the same way because γ_m^{zc} was taken as integration constant to obtain absolute values of γ_c. All other errors are linear with respect to H_i, the random error in the values of γ_m relevant here is therefore ± 0.2 erg cm^{-2}, as given previously (this is the square root of the sum of the squares of all individual errors). The individual errors reported above for various readings were checked by observations through two or more different people; the compounded error estimate receives support from Fig. 1 where the data of DEVANATHAN[6] have also been plotted. The measure of agreement was the same with two or more curves measured separately against hydrogen and calomel electrodes[3]. At extreme anodic and cathodic potentials, a figure of ± 0.8 erg cm^{-2} for

the random error was found experimentally; this is probably connected with those phenomena which lead to the complete instability of the meniscus immediately beyond such potentials.

Sources of systematic error are impurities and sticking of the meniscus. Sticking is discussed in detail below.

Conditions of high purity were maintained throughout the work, and in identical ways for the two measuring systems[3,7]. It must be noted that the effect of neutral trace impurities should be most marked near the potential of zero charge, and should be somewhat higher for the electrocapillary results (longer time available for adsorption); but the correction of an error supposed to be introduced by such an impurity, in γ_m, would make the discrepancy in surface tensions from the two methods even larger than that reported. (This is readily seen from the well-known lowering of the capacity by adsorption near E^{zc}; in our electrocapillary data, an increase of C_e in this region, rather than a lowering, is observed.)

The potential dependence of a hypothetical effect of dischargeable impurities would differ in character from that of the discrepancies, as is evident at the cathodic end of the $\Delta\gamma$–E plots (*cf.* Figs. 2, 4 and 5 of our previous work[2], and Fig. 5 of PAYNE[1]). Such an effect would tend to be an exponential, not a linear, function of potential. But $\Delta\gamma$ is found to be a linear function of E, *cf.* Fig. 1.

Further, the effect of errors in a particular region of potentials on the final conclusions is minimised in our method of analysis, *viz.*, we analyse the $\Delta\gamma$–E plot as a whole, but it is magnified when considering, for example, only potentials between -300 and -500 mV (against a calomel electrode in the same solution), see Figs. 1 and 2 of PAYNE[1]. A small decrease of γ_m with decreasing concentration was indeed observed by DEVANATHAN as well[6], but this is restricted to a few potentials and not observed over the entire rest of the potential range. The corresponding surface excesses are discussed below.

In conclusion, errors admissible on the basis of measured interfacial tension are an order of magnitude smaller (*cf.* above analysis and Fig. 2 of ref. 2) than those required to explain the discrepancies, and the tendency of systematic errors is contrary to the trends (potential dependence and location) in our observations.

3.2. Differential capacity. The experimental uncertainties have been reported[2]. The discrepancy, $\Delta C = C_m - C_e = -\partial^2\Delta\gamma/\partial E^2$, as evaluated from $\Delta\gamma$–E plots, is about $-10\,\mu$F cm^{-2} near E^{zc} (*cf.* legend to Fig. 1). If this was to be attributed to an error in the determination of C_m, the measured differential capacity, then this error would have to be of the order to 50% of C_m, hypothetical "true" values being higher.

3.3. Sticking of the meniscus. The experimental precautions taken against an effect of this (wide manometer limbs and producing meniscus oscillations before each reading) have been described[2]. We observed no sticking even in the most dilute solutions of HCl and KCl. PARSONS AND ZOBEL who also mentioned the possibility of sticking of the meniscus in their paper dealing with NaH_2PO_4 solutions[8], have stated that the discrepancies observed do not seem to have a purely-mechanical origin.

If sticking of the meniscus were due to electrodeposited material, it should

increase exponentially with E, because of the exponential dependence of reaction rates on potential. If sticking were due to adsorption of components from the solution, it should be more pronounced in concentrated solutions. It should, at any rate, be accompanied by an increase in scatter of the data which is not observed, except slightly and at all potentials in the more dilute solutions, and within the error limits stated.

To be the origin of the systematic discrepancies of Fig. 1, sticking would have to vary somewhat linearly with potential. An explanation of such a potential dependence has not been offered.

Were such sticking errors important in electrocapillary determinations, then several of the methods used by GRAHAME[9,10] to determine the potential of zero charge, E^{zc}, *i.e.* his methods I–IV, ought to suffer error. If, then, method VII, the back-integration method, leads to agreement with I, as sometimes claimed by GRAHAME, but I is wrong, then VII must be wrong. However, the present authors find that VII leads to disagreement with both I and V (the results due to VII being too positive), while I and V agree within the error limits (which are rather high in dilute solutions, *cf.* ref. 2, p. 422). A similar tendency to disagreement between the values of E^{zc} found by back-integration and others can be seen in GRAHAME's work on KI (ref. 11, Fig. 1). This observation would be consistent with the suggestion that C_m as a function of d.c. potential *measured* may differ significantly in certain concentration and potential regions from the coefficient $-\partial^2\gamma_m/\partial E^2$ near E^{zc} in dilute solutions. (See also below Sections 4.3–4.5.)

3.4. Potential of zero charge from the streaming electrode. PAYNE criticised the use of condensers in the circuit for such measurements. Slow approach to stable values was taken into account; no other adverse effects of the presence of the condensers have been established.

4. Error analysis for the evaluation procedures

The directly-measured quantities have been shown to be sufficiently accurate and reliable for the analysis made. The errors discussed in Section 3 are not of a magnitude or type to explain the $\Delta\gamma$–E relation observed in the work of the present authors and of GRAHAME[2], of PAYNE (ref. 1, Fig. 5) or of PARSONS AND ZOBEL[8]. Therefore, the procedures for evaluating derived quantities will be discussed.

4.1. Capacity calculated from interfacial-tension data. The errors introduced are well known to be large, and the results were only used as incidental evidence, as mentioned above and in ref. 2. By algebraic procedures, the scatter was reduced to less than 10 μF cm^{-2} in C_e even for 0.01 N solutions so that fairly smooth curves could be drawn. Our analysis, however, rests entirely on $\Delta\gamma$, and not upon the intrinsically inaccurate values of C derived from surface tension measurements.

4.2. Interfacial tension calculated from differential-capacity data: Effect of errors in E^{zc}. Experimental errors in E^{zc} (by way of the two integrations) do not affect the existence but only the position (anodic, cathodic, or both sides) of the observed discrepancies (in terms of $\Delta\gamma$); the *difference* in $\partial\Delta\gamma/\partial E$ between anodic and cathodic side and the value of $\Delta C = -\partial^2\Delta\gamma/\partial E^2$ are unaffected. This is evident from Fig. 1 and is illustrated again in Table 1 where GRAHAME's data[12] (the same as used in ref. 2, Fig. 5) have been integrated using three different values of E^{zc}, and are

compared with γ_m from our work[7]. Discrepancies are apparent on the anodic side when using GRAHAME's E^{zc} (value obtained by back-integration), on the cathodic side when using E^{zc} from the electrocapillary data in Table 1, and on both sides when using E^{zc} from the electrocapillary data of DEVANATHAN[13]. The $\Delta\gamma$–E relations are always linear from the branches of the electrocapillary curve (where, hence, $\Delta C = 0$) and exhibit the curvature discussed near E^{zc} (where, hence, $\Delta C \neq 0$). The calculated electrocapillary curves have wider diameters than the measured ones. Use of another

TABLE 1

INTERFACIAL TENSION OF THE SYSTEM Hg/0.01 *N* KCl AQ.

E_- (*mV vs. RCE*)	γ (*erg cm*$^{-2}$)			
		calculated from C using E^{zc} (*mV*)		
	measured	−620	−610[13]	−594[12]
−100	385.00	386.23	387.01	388.35
−150	393.05	394.52	395.22	396.43
−200	399.86	401.73	402.36	403.43
−250	406.14	407.98	408.53	409.47
−300	411.07	413.32	413.79	414.60
−350	415.85	417.73	418.13	418.80
−400	419.06	421.21	421.54	422.07
−450	422.02	423.76	424.02	424.41
−500	424.18	425.45	425.62	425.89
−550	425.76	426.40	426.50	426.63
−600	426.70	426.78	426.80	426.80
−650	426.63	426.74	426.69	426.55
−700	425.71	426.30	426.17	425.90
−750	424.29	425.44	425.23	424.83
−800	422.74	424.13	423.84	432.31
−850	420.61	422.35	421.98	421.32
−900	418.10	420.10	419.66	418.86
−950	415.42	417.39	416.86	415.94
−1000	411.99	414.23	413.63	412.57
−1050	408.18	410.62	409.95	408.75
−1100	403.90	406.60	405.84	404.51
−1150	399.05	402.16	401.33	399.87
−1200	394.08	397.31	396.40	394.81
−1250	388.75	392.06	391.08	389.35
−1300	382.65	386.41	385.36	383.49
−1350	376.55	380.37	379.24	377.24
−1400	369.83	373.93	372.72	370.59
−1450	362.85	367.09	365.81	363.54
−1500	355.73	359.83	358.48	356.08
−1550	347.39	352.18	350.75	348.21
−1600	339.23	344.10	342.60	339.92
−1650	330.95	335.59	334.01	331.20
−1700	322.18	326.64	324.98	322.04
−1750	311.64	317.24	315.51	312.43
−1800	301.59	307.38	305.57	302.36
−1850	291.07	297.05		
−1900	282.41	286.24		

value of E^{zc} in the integrations does not reduce the discrepancies on one branch without increasing them on the other, and hence does not bring them within reach of the errors admissible, contrary to the claim of PAYNE. Only by using different values of E^{zc} for the two branches of one and the same calculated capillary curve could one remove the discrepancies—hardly a valid procedure.

4.3. Potential of zero charge from electrocapillary data. By graphical means, one can show that the sticking which PAYNE suggests as the origin of the discrepancies will affect greatly the values of E^{zc} evaluated from electrocapillary curves, provided it starts at E^{zc}. For example, if due to sticking on the anodic side, $\gamma_m{}^{zc}$ is found 0.2 erg cm^{-2} too low, and any successive value of γ_m 50 mV more to the anodic side by an additional 0.4 erg cm^{-2} too low as compared to the preceding value, then E^{zc} will be determined about 50 mV too negative. Such large errors would throw serious doubt upon the use of the electrocapillary method. In agreement with PARSONS AND ZOBEL[8], we find that irreproducibility and scatter do not increase sufficiently, and neither does the disagreement between various authors, when going to certain dilute solutions (it is only here that any discrepancies between the two methods were observed) to justify the assumption of such sticking.

4.4. Surface excesses from electrocapillary data. PAYNE[1] attempts to judge our electrocapillary data from the limiting values for $\Gamma_{H_3O^+(H_2O)}$ or $\Gamma_{Cl^-(H_2O)}$ for the most dilute solution as evaluated by him from a few of our published results. We have pointed out before[2] that, because of the graphical procedure of evaluating surface excesses from γ, no matter whether this is γ_m or γ_c, larger error limits apply for the extreme concentrations (0.01 and $3N$) than for the others (0.03 to 1.0 N), and we have therefore not based our analysis[2] on surface excesses directly. By using several sets of data for Γ, evaluated from γ_m–μ_{HCl} plots at constant E_+ and E_- *measured*, and by applying the technique of graphical differentiation described[2], we were able to reduce the absolute error in the determination of average values of Γ to ± 1 μC cm^{-2} for 0.03 to 1.0 N solutions, and to ± 2 μC cm^{-2} for the extreme concentrations. These error limits are in accord with the above given experimental error in γ_m. Within these limits, we have also found that $F(z_+\Gamma_+ + z_-\Gamma_-) = -q^M$, the charge on the metal, which was an important check particularly for dilute solutions[3]. The limiting values expected from diffuse layer theory were obtained correctly, they are given in Table 2.

TABLE 2

SURFACE EXCESSES OF THE SYSTEM Hg/HCl AQ. (FROM γ_m)

Concentration	*Limiting value of* $\Gamma_{Cl^-(H_2O)}$, *cathodic end*	*Least positive (or most negative) value of* $\Gamma_{H_3O^+(H_2O)}$
3 N	6.0	10.4
1 N	4.5	8.8
0.3 N	3.3	4.7
0.1 N	1.8	2.2
0.03 N	1.0	−1.6
0.01 N	0.7	−2.0

4.5. Surface excesses from capacity data: A corresponding inconsistence in certain regions. Errors introduced by the evaluation procedures have a similar origin

to those discussed in Section 4.4 since one differentiation is involved. Method D (see below)[2] because of the particular integration constants used[2], offers an independent check of our contention that the capacity data contains a small contribution not directly related to a net change in surface excesses.

In method D, the differential capacity as a function of chemical potential was differentiated graphically, to obtain $(\partial C/\partial\mu)_{E-} = (\partial C_+/\partial E_-)_\mu$ (in one step, not two, as reported by GRAHAME AND SODERBERG[14]). The integration was carried out algebraically after curve fitting (see ref. 2). As integration constants, the values from diffuse-layer theory were used; these should be most reliable in the dilute solutions considered. However, the results for Γ_+ and Γ_- in dilute solutions found thus are consistently and considerably too high on the *anodic* side, to an extent very clearly outside the experimental error. The latter is not affected by the integration procedure; this was shown by algebraic double differentiation of an electrocapillary curve calculated from capacity data—the original data were retrieved precisely. However, if the original data (C_m) carry an inconsistency in some region of potential and the integration is carried out across this region, then data obtained by this integration will deviate systematically on the side far from the potential at which the integration constant was introduced. The integration constants are reliable, on the other hand, because they are based on theory applicable in dilute solution and are, of course, in agreement with the values of Γ from γ_m in Table 2.

Figure 2 shows the results of evaluating Γ from C_m by method D. For example, Γ_- at $q^M = 17$ μC cm^{-2} in 0.01 N HCl amounts to 26 μC cm^{-2}, the *same* value as obtained in 1 N HCl. This is clearly an anomaly, and supports the suggestion that it is in the capacity, not the electrocapillary, data that the discrepancies originate, when the solution is sufficiently dilute.

5. The model

After having redirected the discussion from apparent discrepancies between measured capacity values and the uncertain ones which arise from the double differentiation of electrocapillary curves (as discussed by PAYNE[1]) to the discrepancies which were the central point in our paper (*i.e.* those between directly-measured and capacitance-calculated interfacial tension where the uncertainties are much less) one finds that:

(*i*) The experimental errors in interfacial-tension measurements are about ten times smaller than those needed to explain the discrepancies between directly-measured surface tensions and those which are calculated from capacitance measurements in dilute solutions;

(*ii*) Sticking of the meniscus, as a source of systematic error, was not significantly present, nor could reasonably be expected to cover the type of discrepancy observed;

(*iii*) The evaluation procedure for γ_c does not introduce the systematic deviations found;

(*iv*) Use of different values for E^{zc}, even by several tens of millivolts, will only shift the magnitude of the discrepancies from one potential region to another, so that the discrepancies observed are not eliminated by use of some different value of E^{zc}.

Additional evidence for this are the inconsistencies showing up when surface

excesses are evaluated from capacitance data in conjunction with reliable integration constants from diffuse layer theory.

In these circumstances, it is appropriate to enquire whether the imposition of an alternating current may make a significant difference to the interface in certain ranges of potential and concentration. The surface excesses present (which make up the charge on the solution side of the double-layer capacitor, as quantitatively verified[3]), as well as their changes, are equilibrium values for a given field (and its changes), which in turn are related to the interfacial-charge density. We have suggested that this field is not identical with that which should arise with respect to the corresponding applied d.c. potential difference across the interface. When the (thermodynamically-determined) charge density was substituted for the latter as electric variable in plotting surface excesses (our[2] method E), or in plotting the calculated and measured interfacial tensions (our[2] Fig. 6), the discrepancies disappeared. The view that the discrepancies observed are due to artifacts is not consistent with this central result.

The Electrochemistry Laboratory
The University of Pennsylvania
Philadelphia, Pa. 19104, U.S.A.

J. O'M. BOCKRIS
K. MÜLLER*
H. WROBLOWA
Z. KOVAC**

1 R. PAYNE, *J. Electroanal. Chem.*, 15 (1967) 95.
2 J. O'M. BOCKRIS, K. MÜLLER, H. WROBLOWA AND Z. KOVAC, *J. Electroanal. Chem.*, 10 (1965) 416.
3 Z. KOVAC, *Dissertation*, University of Pennsylvania, Philadelphia, 1964; cf. *Dissertation Abstr.*, 26 (1965) 2496.
4 L. A. HANSEN AND J. W. WILLIAMS, *J. Phys. Chem.*, 39 (1935) 439.
5 S. R. CRAXFORD, *Dissertation*, London, 1936.
6 M. A. V. DEVANATHAN, *Thesis*, University of London, 1951.
7 K. MÜLLER, *Dissertation*, University of Pennsylvania, Philadelphia, 1965; *cf. Dissertation Abstr.*, 26 (1966) 7064.
8 R. PARSONS AND F. G. R. ZOBEL, *J. Electroanal. Chem.*, 9 (1965) 333.
9 D. C. GRAHAME, R. P. LARSEN AND M. A. POTH, *J. Am. Chem. Soc.*, 71 (1949) 2978.
10 D. C. GRAHAME, E. M. COFFIN, J. I. CUMMINGS AND M. A. POTH, *J. Am. Chem. Soc.*, 74 (1952) 1207.
11 D. C. GRAHAME, *J. Am. Chem. Soc.*, 80 (1958) 4201.
12 D. C. GRAHAME, unpublished work.
13 M. A. V. DEVANATHAN AND P. PERIES, *Trans. Faraday Soc.*, 50 (1954) 1236.
14 D. C. GRAHAME AND B. A. SODERBERG, *J. Chem. Phys.*, 22 (1954) 449.

Received March 25th, 1967

* Present address: Research Institute for Catalysis, Hokkaido University, Sapporo, Japan
** Present address: Thomas J. Watson Research Center, International Business Machines Corporation, Yorktown Heights, N.Y. 10598, U.S.A.

VOL. 15 NO. 1 JOURNAL OF ELECTROANALYTICAL CHEMISTRY SEPTEMBER 1967
AND INTERFACIAL ELECTROCHEMISTRY

CONTENTS